The Thesis Committee for Rebecca Suzanne Comeaux
Certifies that this is the approved version of the following thesis:

Black Mangrove (*Avicennia sp.*) Colony Expansion in the Gulf of Mexico with Climate Change: Implications for Wetland Health and Resistance to Rising Sea Levels

APPROVED BY

SUPERVISING COMMITTEE:

Supervisor:

———————————————————
Mead A. Allison

———————————————————
Thomas S. Bianchi

———————————————————
David Mohrig

———————————————————
Clark R. Wilson

Black Mangrove (*Avicennia sp.*) Colony Expansion in the Gulf of Mexico with Climate Change: Implications for Wetland Health and Resistance to Rising Sea Levels

by

Rebecca Suzanne Comeaux, B.S. Geo. Sci.

Thesis

Presented to the Faculty of the Graduate School of

The University of Texas at Austin

in Partial Fulfillment

of the Requirements

for the Degree of

Master of Science in Geological Sciences

The University of Texas at Austin

December 2010

Acknowledgements

I would like to offer my sincerest appreciation towards the people who have guided me through the various components of this study. I would like to thank Mead Allison for accepting me as a graduate student and suggesting this particular study as a thesis project. Mead played an integral part in the completion of field work, conceptual discussion and input, and in teaching me about radioisotope methods and GPS field measurement translation into ArcMap. I would also like to thank Thomas Bianchi (TAMU), David Mohrig, and Clark Wilson for their valuable insight on this study and their willingness to serve on my committee. Thomas Bianchi participated in Galveston field work and results discussion, and Clark Wilson helped me find a solution for elevation data collection. Remaining people who assisted and provided advice in the completion of fieldwork include Edward Buskey and Sally Morehead (UT MSI, Mission-Aransas National Estuarine Research Reserve), who offered useful knowledge and suggestions for mangrove occurrence and field site localities at Port Aransas, TX and Anna Armitage and Eric Madrid (TAMUG) who assisted me in field site selection at Galveston, TX. Eric Madrid also contributed general discussion of the biology and ecology of mangroves. Other field assistants included Michael Ramirez, Richard Smith, and Justin Caulk, all of whom I am thankful for spending hard-worked days collecting and sampling cores and completing elevation surveys.

In addition to field analysis, there are several key people who have helped me learn, execute, and develop lab work practices and technique. I would like to thank Dan

December 3rd, 2010

Abstract

Black Mangrove (*Avicennia sp.*) Colony Expansion in the Gulf of Mexico with Climate Change: Implications for Wetland Health and Resistance to Rising Sea Levels

Rebecca Suzanne Comeaux, M.S. Geo. Sci.

The University of Texas at Austin, 2010

Supervisor: Mead A. Allison

Populations of black mangroves (*Avicennia sp.*) are hypothesized to expand their latitudinal range with global climate change in the 21st century, induced by a reduction in the frequency and severity of coastal freezes, which are known to limit mangrove colony extent and individual tree size, as well as an overall warmer climate. The Gulf of Mexico is located at the northward limit of black mangrove habitat and is therefore a prime candidate for population expansion with global warming. This expansion may come at the expense of existing Gulf coastal saline wetlands that are dominantly *Spartina spp.* marsh grasses. The present study was conducted to focus, not on the extent to date of this

replacement, but to examine the potential implications of a marsh to mangrove transition in Gulf wetlands, specifically 1) resistance to accelerating eustatic sea level rise (ESLR) rates, 2) wetland resistance to wave attack in large storms (increased cyclonic storm frequency/intensity is predicted with future climate warming), and 3) organic carbon sequestration and wetland soil geochemistry.

Field sites of adjacent and intergrown *Avicennia* mangrove and *Spartina* marsh populations in similar geomorphological setting were selected in back-barrier areas near Port Aransas and Galveston, TX (two sites each) as part of a larger-scale planned study of the full latitudinal transition of the western Gulf funded by the National Institute for Climate Change Research (U.S. Department of Energy). The reconnaissance conducted for site surveys show that black mangrove populations in this part of Texas are clustered near inlet areas, suggesting seed transport vectors are a major control on colony establishment, and likely, on the potential rapidity of wetland habitat replacement. Resistance to ESLR was tested by 1) creating high-accuracy (±1 cm) elevation maps over ~5,000 m^2 areas of adjacent mangrove and marsh areas, and 2) measuring mineral and organic matter accumulation rates (Pb/Cs radiotracer geochronology, loss on ignition) from auger cores. Elevation surveys in Port Aransas indicate mangrove vegetated areas are 4 cm higher in elevation than surrounding marsh on an average regional scale, and 1 to 2 cm higher at the individual mangrove scale: at the Galveston sites, any trend is complicated by the area's pre-existing geomorphology and the relative youth of the mangrove colonies. ^{137}Cs accumulation rates and loss on ignition data indicate that mineral trapping is 4.1 times higher and sediment organics are 1.7 times lower in

mangroves at Port Aransas; no such definable trends exist at the Galveston sites or in calculated ^{210}Pb sediment accumulation rates. This additional mineral particle trapping in mangroves does not differ in grain size character from marsh mineral accumulation. Elevation change may also be effected by root volume displacement: live root weight measurements in the rooted horizon (~0 to 20 cm depth) are consistently higher in mangrove cores from Port Aransas and the site at the west end of Galveston Island. Port Aransas porosities are lower in mangrove rooted horizons, with a corresponding increase in sediment strength (measured by shear vane in the cores), suggesting mangrove intervals may be more resistant to wave-induced erosion during storm events. Port Aransas mangroves exhibit higher pore water redox potentials and salinities over entire core depths and depressed pH over rooted intervals, suggesting a distinct diagenetic environment exists relative to marsh sites. Increased salinities and higher redox potentials may be a function of the rooting network, which introduces oxygen into the sediment and focuses evapo-transpiration and salt exclusion within this zone: this may prove advantageous when competing with marsh grasses by elevating salinities to levels that are toxic for *Spartina*. Trends observed in the more mature systems of Port Aransas are generally absent at the Galveston sites, suggesting the youth and physically shorter stature of these systems means they have not yet established a unique sediment signature.

Table of Contents

List of Tables

List of Figures

CHAPTER 1

Introduction

1.1 CLIMATE CHANGE

Within the next century, global climate change is predicted to accelerate rates of sea level rise, increase cyclonic storm frequency/intensity, and enhance climate warming (IPCC, 2007). Climate change at temperate latitudes may be characterized by both rising temperatures and a reduced freeze frequency that could shift the latitudinal limits of flora and fauna. Low-elevation (<1 m above mean sea level) coastal wetland settings are highly susceptible to these changes because they exist at the boundaries of terrestrial and marine environments. The present study is focused on examining the implications of possible expansion of mangroves in coastal wetlands, specifically the pioneer black mangrove, *Avicennia germinans* (referred to as *Avicennia* throughout the rest of this thesis)*, at the expense of salt marsh vegetation which predominates in temperate latitudes globally (Alongi, 1998; Stevens et al., 2006; Stuart et al., 2006; Perry and Mendelssohn, 2009). The Gulf of Mexico, where the present study is focused, is located at the northern limit of black mangrove habitat and is therefore a prime candidate for population expansion with predicted global climate change (Sherrod and McMillan, 1981; 1985; Tomlinson, 1986; Bianchi et al., 1999).

Black mangrove expansion may come at the expense of existing Gulf coastal saline wetlands that are dominantly *Spartina* species salt marsh grasses such as *S.*

alterniflora and *S. patens* (referred to as *Spartina* from this point forward) (Stevens et al., 2006; Perry and Mendelssohn, 2009). This potential change in dominant vegetation may have implications for coastal wetland resistance to future sea level rise by affecting elevation gain rates in the wetland through 1) differences in vertical displacement of the soil surface with root growth, 2) organic deposition rate or re-mineralization efficiency of leaf versus grass litter in the soil, or 3) changes in canopy structure impacting the trapping efficiency of mineral sediment. Rooting may also affect sediment strength and resistance to wave attack. Any change in the preservation of organic matter deposited has major implications for carbon sequestration in wetlands.

Black mangrove expansion in the Gulf of Mexico would have ecological and societal impacts as well (Stevens et al., 2006; Gilman et al., 2008). Mangroves may change the geochemistry of estuaries through interactions with the soil substrate, production rates, supply of nutrients, and gas exchange, which may affect associated wildlife living within them (Scholander et al., 1955; Andersen and Kristensen, 1988; Passioura et al., 1992; Twilley et al., 1992; Alongi, 1998; Bianchi et al., 1999; Marchand et al., 2004; Stevens et al., 2006; Bianchi, 2007). Gulf of Mexico fisheries and estuarine resources and recreation may all change with mangrove replacement of salt marsh vegetation. Coastal saline wetlands also buffer storm surges that impact human population centers along the coast. Land loss rates and the extent of this buffer are associated with the type of coastal vegetation present.

2

1.2 FOCUS AND OBJECTIVES

The present study was conducted to focus, not on the historical extent of this replacement, but to examine the potential implications of a possible marsh to mangrove transition with climate change, specifically 1) resistance to accelerating eustatic sea level rise (ESLR) rates, 2) wetland resistance to wave attack in large storms (increased cyclonic storm frequency/intensity), and 3) organic carbon sequestration and wetland soil geochemistry. Previous studies regarding mangroves and Holocene sea levels suggest that mangroves may be able to keep pace with rising sea level on millennial timescales (Ellison and Farnsworth, 1997; He et al., 2007; McKee et al., 2007). *Rhizophora* (red mangrove) seedlings were shown to have an increased growth rate when exposed to a 16 cm artificial flooding event (Ellison and Farnsworth, 1997), and *Avicennia* appears to have the best flooding tolerance among four different mangrove taxa examined by He et al. (2007). Several studies suggest mangrove forests are able to significantly attenuate wave energy (Brinkman et al., 1997; Mazda et al., 1997; 2006; Massel et al., 1999; Quartel et al., 2007; Tanaka et al., 2007). A study by Ward et al. (2006) demonstrated the ability of mangrove systems to rapidly recover from cyclonic storm events when a colony in southern Florida was able to replace lost biomass from Hurricane Andrew after only a four year period. Concerning carbon sequestration, Chen and Twilley (1999) demonstrated that Gulf mangrove and salt marsh systems may have different organic accumulation rates influenced by separate biomass production methods. Below-ground biomass may significantly change the subsurface geochemistry and affect the degree of soil anoxia, pH, and nutrient and contaminant cycling (Howes et al., 1981; Boto, 1982).

The present study, funded by the Department of Energy's National Institute for Climate Change Research (Coastal Center), is designed to test the impact of a mangrove expansion scenario with climate change by examining areas along the latitudinal range from south Texas to Louisiana where black mangroves are found co-existing with salt marsh habitat, and have periodically experienced freeze-induced diebacks (Sherrod and McMillan, 1985; McMillan and Sherrod, 1986; Everitt and Judd, 1989; Everitt et al., 1996). My thesis work is a subset of this project that examines mixed systems of *Avicennia* (black) mangroves and *Spartina* salt marsh grasses near Port Aransas and Galveston, TX. The overall project will study a wider range of the Gulf of Mexico coastal saline wetland sites, including sites located further north in Mississippi delta inter-distributary wetlands and in south TX. Sites in LA will provide comparable data from a more organic and mud-rich setting, whereas south TX sites are located in warmer settings with less frequent diebacks, that tends to have older mangrove colonies and larger individual tree sizes.

CHAPTER 2

Background

2.1 CHARACTERISTICS OF MANGROVE AND MARSH SYSTEMS

Mangroves and marsh systems are the dominant flora in coastal and estuarine environments and possess traits that allow them to thrive in these settings (Ball, 1988; Day et al., 1989; Alongi, 1998; Bianchi, 2007). Both are highly productive, saline tolerant plants that trap mineral sediment and co-occur at lower latitudes globally: mangroves are limited in the Northern Hemisphere to latitudes lower than about 27-38° N. Relatively low transpiration rates, the process that withdraws water from the sediment and allows plants to fix carbon, are characteristic of mangroves and most halophytes, including salt marsh grasses (Giurgevich and Dunn, 1982; Alongi, 1998). Mangroves and salt marshes fulfill similar ecological niches in different latitudinal ranges (Turner, 1976; Ball, 1988; Twilley et al., 1992; Howes and Goehringer, 1994; Alongi, 1996; Alongi, 1998) and it remains unclear exactly what controls distribution in areas where these wetland types co-occur. It is clear from existing research, however, that in addition to a latitudinal control on mangroves, these flora are characterized by differences in carbon fixation mechanisms and organic matter accumulation rates.

Mangroves are C_3 plants (plants that produce the three-carbon compound phosphoglyceric acid during the dark reactions in photosynthesis) that are generally freeze intolerant (McMillan and Sherrod, 1986; Alongi, 1998; Stuart et al., 2006). This

5

characteristic may allow these plants to be used as ecological indicators of latitudinal climate controls (Sherrod and McMillan, 1981; 1985; McMillan and Sherrod, 1986; Stuart et al., 2006). For example, Stuart et al. (2006) demonstrated that sub-freezing conditions caused a die-back of black mangroves as a result of xylem embolism and loss of hydraulic conductivity. McMillan and Sherrod (1986) found Texas populations of *Avicennia* to be more tolerant to freezing conditions of 2 to 3°C than populations in Louisiana and Florida. Results of this study suggested that a 4 to 5 day period of 2 to 3°C chilling temperatures will damage the majority of a Texas mangrove population, however most will recover and survive. Despite the chilling tolerance of Texas mangroves, occasional periods of subfreezing conditions have drastically eliminated a majority of these populations (Sherrod and McMillan, 1981; McMillan and Sherrod, 1986). Mangroves are more structurally complex than salt marshes, with most above-ground biomass present in the stems and prop roots (*Rhizophora* mangroves) or pneumatophores (*Avicennia*) (Tomlinson, 1986; Alongi, 1998). Leaf litter, woody material, and live roots compose the bulk of mangrove organic matter. The root structure of black mangroves (Fig. 1) consists of pneumatophores (aerial roots) which attach to laterally extensive horizontal cable roots and deeper anchoring roots (Tomlinson, 1986; Marchand et al., 2004). Wells and Coleman (1981) demonstrated mangrove root volumes may dramatically increase surrounding soil elevations by vertical displacement as they grow. Mangroves also have longer life spans than seasonal salt marsh grasses, but their ultimate size and biomass is usually governed by latitude, with the greatest age and size found close to the equator (Boto, 1982; Alongi, 1998). Below-ground biomass

Figure 1:   Idealized cross-section of a black mangrove root system. Roots consist of laterally extensive horizontal cable roots, aerial roots (pneumatophores), and finer rootlets and anchoring roots (from Marchand et al. 2004).

7
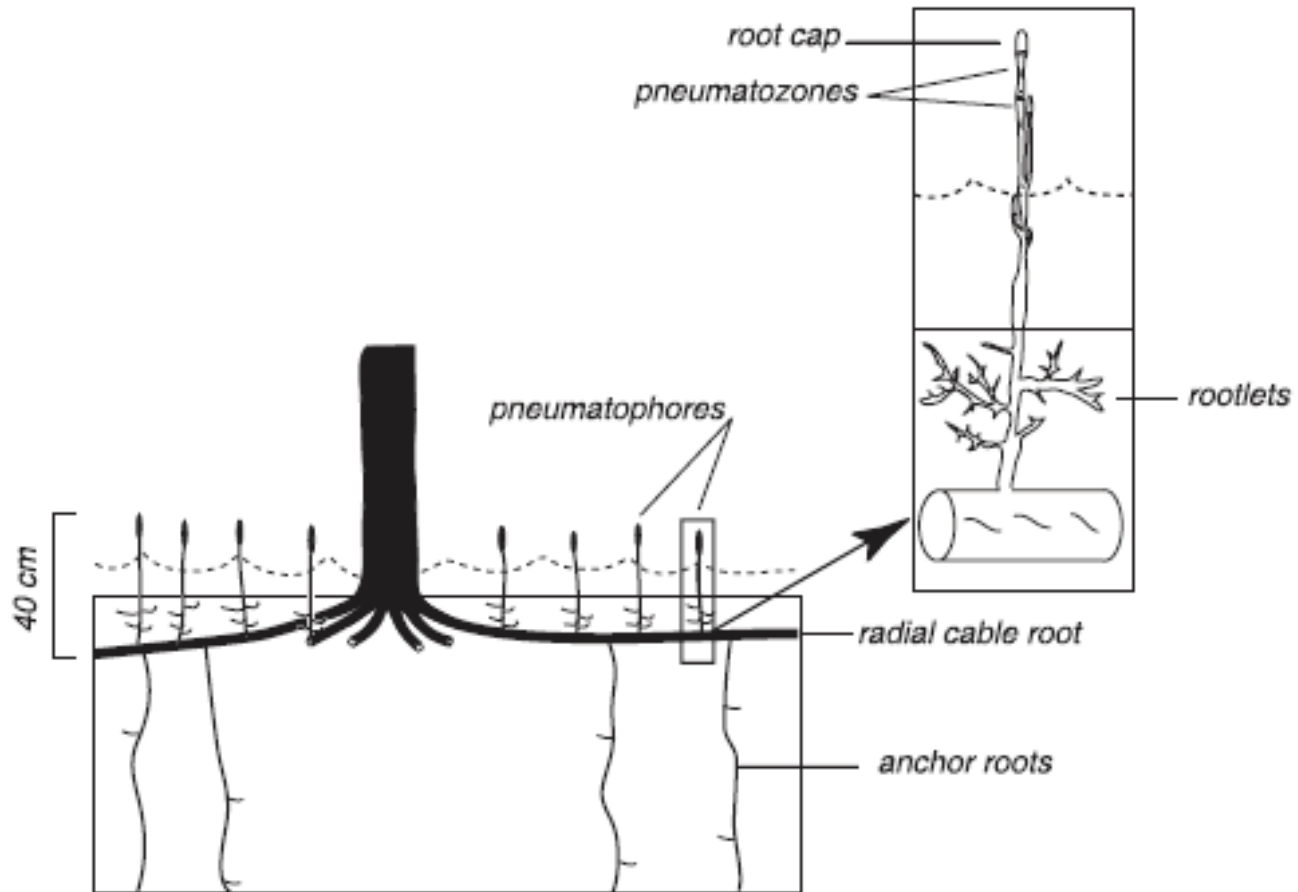
composes approximately 50 percent of total forest biomass, while wood production makes up about 60 percent of net primary production. Smaller forest area and stunted individual tree size can occur in arid conditions and/or other types of environmental stress (Alongi, 1998).

$Spartina$ salt marsh grass is a C_4 plant (where the four-carbon compound oxaloacetic acid is produced during the dark reactions in photosynthesis) which predominates in higher salinity wetlands, but is found in many subtropical and temperate latitudinal settings (Pezeshki, 1997; Alongi, 1998; Stevens et al., 2006). $Spartina$ is characterized by winter periods of stem dieback that lead to seasonal changes in above-ground biomass. Two to four times more biomass exists in subsurface roots and rhizomes than above-ground blades (Alongi, 1998). Fibrous roots extend to approximately 10 cm depth (Ravit et al., 2006). Lacking a woody stem, $Spartina$ is smaller and simpler in structural form than black mangroves. Grass blades, roots and rhizomes compose the organic matter of salt marshes (Alongi, 1998). The lack of woody tissues in $Spartina$ is just one of the many important differences between grass and mangrove wetlands (Alongi, 1998; Bianchi, 2007).

2.2 STUDY AREA

Study sites for the present investigation are located in lagoonal settings behind barrier islands in the Gulf of Mexico near Port Aransas and Galveston, Texas (Fig. 2-5). Holocene and Pleistocene depositional processes created the current Texas coastline, which consists of a series of fluvial-deltaic systems that empty into the Gulf of Mexico.

Figure 2: Field locations in Port Aransas and Galveston, TX.
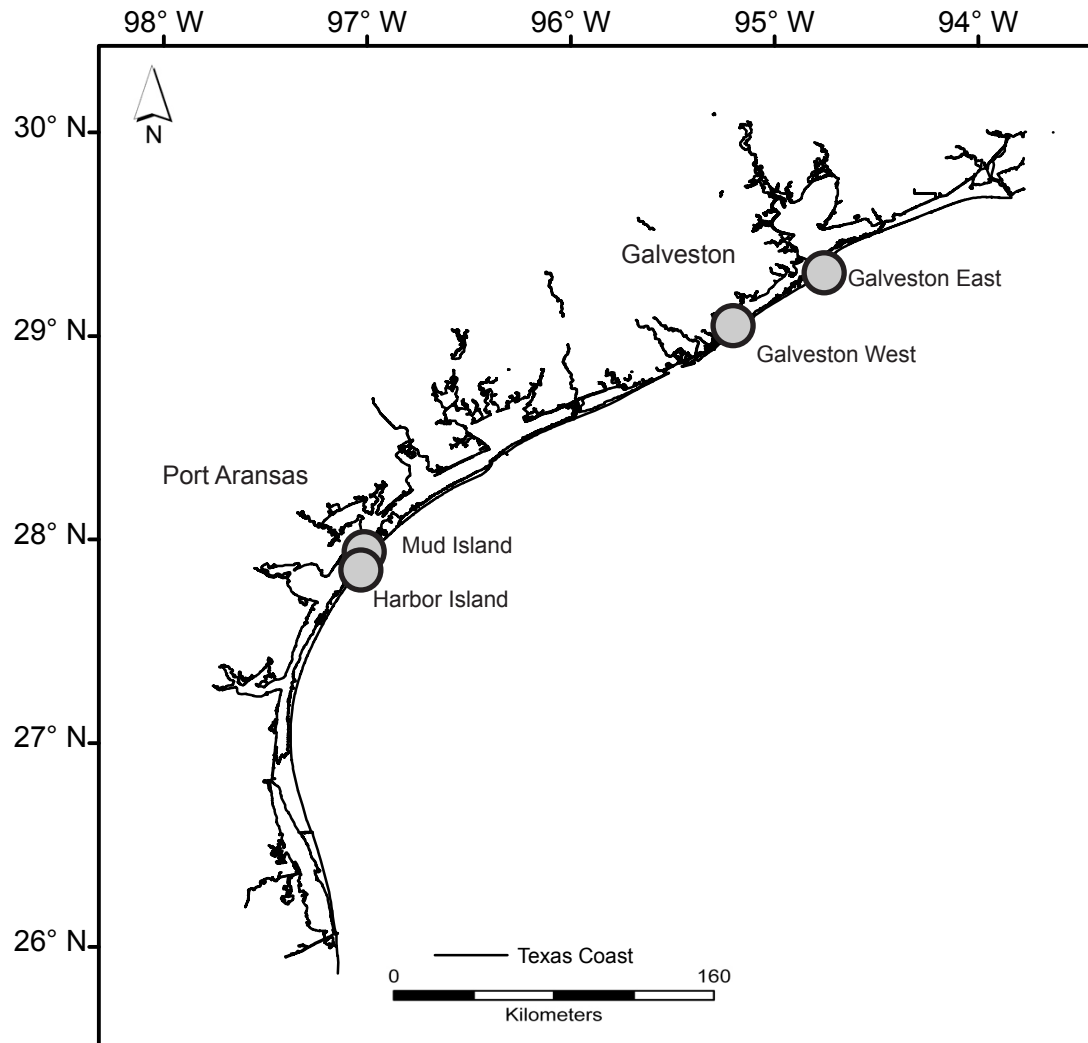
Flooded river valley and back-barrier lagoonal estuaries are sheltered from the open Gulf by barrier islands that, in the case of Galveston and Corpus Christi Bay (Port Aransas), rest on post-glacial flooded valleys formed during lowstand conditions (LeBlanc and Hodgson, 1959; Bianchi et al., 1999). The major river systems that provide freshwater and much of the sediment flux to these two estuarine systems are the San Jacinto and Trinity Rivers (Galveston Bay; White and Tremblay, 2002), and the Nueces River (Corpus Christi Bay). Brackish marshes (salinity range between 0 to ~25) exist along the Trinity River system and salt (salinity >25) to brackish marshes are contained within the Nueces River system (Bianchi et al., 1999; White et al., 2002). The present-day Galveston, Matagorda, and Lavaca estuary complexes were established around 7,700 to 6,700 years before present, as flooding shifted bayhead deltas landward, creating modern-day Matagorda Bay and increasing the Galveston estuary area by 30 percent. This occurred during a climatic shift which decreased forest vegetation and increased grassland area (Anderson et al., 2008; Maddox et al., 2008).

Past sea levels were 90 to 130 m lower during the last ice age (approximately 20,000 years ago) and the present TX coastline would have extended 60 to 80 km seaward during this period. Since then regional sea levels have risen at an average rate of 0.25 cm/y until about 4,000 year ago when rates slowed to 0.04 cm/y (Williams et al., 1999). In the past century, ESLR rates have accelerated and are estimated at 0.17 ± 0.05 cm/y (IPCC, 2007). Many areas of the northwestern Gulf of Mexico are presently experiencing a higher rate of relative sea level rise as a consequence of regional subsidence effects (White and Tremblay, 1995). Current regional rates of sea level rise

along the Gulf Coast are 0.3 to 0.6 cm/y in TX (with highest rates occurring in Galveston at about 0.7 cm/y), 0.9 to 1.2 cm/y in deltaic wetlands of LA, and 0.0 to 0.3 cm/y in AL and FL (NOAA, 2006). These rates represent averages over a period of 30 years or more and include data through 2006.

Subsidence and faulting in the northwest Gulf of Mexico/Galveston area are converting wetlands to open water at above average rates in response to these higher than ESLR rates. For example, approximately 10,700 ha of wetland regions were inundated and lost throughout Galveston Bay during the 1950's to 1989 (White and Tremblay, 2002). The Trinity-Galveston area has experienced the majority of wetland loss in Texas, while areas in the Nueces fluvial-deltaic system have only experienced an estimated loss of 130 ha since the 1950's (White et al., 2002). The major causes of this wetland loss in the Galveston Bay area have been identified as human-induced subsidence through groundwater and hydrocarbon withdrawal, regional faulting, and river dams and reservoirs which reduce delivery of fluvial sediment to the estuary for mineral trapping by coastal saline wetlands in the bays. Many regional faults also underlie the bays and may locally induce more rapid subsidence on the downthrown side of the fault (White and Tremblay, 2002). Subsidence combined with ESLR rates are thought to exceed local rates of vertical accretion in Galveston Bay *Spartina* wetlands, which have been estimated at ~0.20 cm/y (White and Tremblay, 2002; Ravens et al., 2009). Long-term averages of marsh vertical accretion rates are higher in the bayhead deltaic regions near the major riverine mineral sediment sources to the bays: 0.51 cm/y for the Trinity delta (Galveston Bay) and 0.26 cm/y for the Nueces (Corpus Christi and

Port Aransas) (White et al., 2002). Marsh accretion rates in Louisiana deltaic wetlands are much higher (0.8 to 1.3 cm/y; White and Tremblay, 2002) but are also experiencing significantly higher regional sea level rise rates due to compaction of the thick Holocene sediment section and a host of other anthropogenic factors (Penland et al., 1990). Recent work by Perry and Mendelssohn (2009) in Louisiana deltaic wetlands is the only study to date that examines differences in accretion rates in marshes and mangrove wetlands in the Gulf. In fact, they report similar accretion rates of 0.2 to 0.3 $g/m^2/d$, 0.6 to 0.7 cm/y, and 0.5 to 0.6 cm/y in short-term, medium-term, and decadal-scale, respectively.

In addition to sea level rise, the Gulf of Mexico may be experiencing increased storm frequency with climate change. Several climate models have predicted increased storm frequencies, intensities, and duration (Knutson and Tuleya, 2004; Emanuel, 2005; Webster et al., 2005; Knutson et al., 2010). The frequency of hurricane episodes is connected to sea surface temperature (SST) variability in the northern Atlantic related to the Atlantic Multi-decadal Oscillation (AMO) (Kerr, 2005). Less hurricane activity is observed when SST is cooler and increased hurricane frequencies are connected to warmer conditions (cool and warm phases of the AMO). Eight hurricanes were recorded in 26 years from 1968 to 1994 during a cool phase compared to 14 hurricanes over 13 years (1995 to 2008) during a recent warm phase in the Gulf of Mexico (Poore et al., 2009). North Atlantic SST recorded from a Mg/Ca record in the Pigmy Basin in the northern Gulf indicate temperatures were as warm or slightly warmer than today 1000 to 1400 years before present (Richey et al., 2007). Examined over a longer timeframe, a comparative study by Wallace and Anderson (2010) shows little variation in storm

activity in south Texas over the past 5,000 years, despite high fluctuations in temperature and climate during this time. Results conclude there is no apparent link between climate change and hurricane probability in the northwestern Gulf of Mexico (Wallace and Anderson, 2010). If SST continues to warm throughout the Gulf of Mexico, increases in warm phases of AMO and frequencies of hurricanes may occur into the 21st century.

Avicennia colonies are widespread throughout the Gulf of Mexico and prevalent across the Caribbean from southern Florida and the Bahamas to Mexico (Tomlinson, 1986). It is one of the most geographically widespread mangrove genera at present (Dodd, 2002), and is hypothesized to have migrated westward after evolving in the Tethys Sea (Saenger, 1998). *Avicennia* were more tropically restricted throughout the Pleistocene but existed in the northern Gulf of Mexico for millions of years prior to this epoch (Sherrod and McMillan, 1981). Genetic variation occurs in western and eastern mangrove colonies along the Gulf Coast, suggesting that population divergence occurred after Pleistocene recolonization, thus *Avicennia* has been present in TX for 100s to 1000s of years (Sherrod and McMillan, 1985; McMillan and Sherrod, 1986). Conversely, native marsh environments started forming 3,000 to 4,000 years ago along the TX coast and currently dominate wetlands throughout the Gulf of Mexico (Sherrod and McMillan, 1985).

A. germinans is the most cold-tolerant species of mangrove and is the most common species found along the TX Gulf Coast (McMillan and Sherrod, 1986). The first known record of *Avicennia* occurrence in TX was in 1853 at the mouth of the Rio Grande River (Sherrod and McMillan, 1981). Although black mangroves have existed in

13

restricted colonies along the TX coast throughout the past century, variations in population density and extent have followed environmental change (freeze frequencies), with populations expanding and contracting from three main Texas core areas: 1) Cavallo Pass, Calhoun County, 2) Harbor Island, Nueces County, and 3) Port Isabel-South Bay area, Cameron County. All three settings are situated in areas of low topographic relief behind barrier islands or on shorelines inside major passes. In addition to these three geographic concentrations, smaller communities of mangroves have persisted for some time in areas between the aforementioned populations. In the northern coast at Sabine Pass, mangroves date back to the 1930's to 1950's but may no longer exist in this region. In the central coast, concentrations of mangroves at Harbor Island are recorded in photographs from the 1900's and have been well documented since the 1930's. Throughout the southern coast, mangrove populations in South Bay and several km north of the Rio Grande date back to the 1980's, and Long Island and San Martin Lake populations were documented from 1969 to 1980 (Sherrod and McMillan, 1981). South of Corpus Christi, TX, mangroves are sparse, stunted, and stressed in the northern region of the Laguna Madre, and are absent from this location to south of Baffin Bay (Madrid et al., 2008). *Avicennia* is sparse along the northern Texas coast, with no known populations between Galveston and the LA border (Sherrod and McMillan, 1981).

CHAPTER 3

Materials and Methods

3.1 FIELD METHODS

Field sites of adjacent and inter-grown *Avicennia* mangrove and *Spartina* marsh populations in similar geomorphological settings were selected in back-barrier areas near Port Aransas and Galveston, TX (two sites each). Port Aransas consisted of the Harbor Island (27° 51' 50.25"N, 97° 3' 35.36"W) and Mud Island (27° 56' 32.24"N, 97° 1' 38.14"W) sites, both situated along the Lydia Ann Channel, north of Mustang Island (Fig. 3). Harbor Island is a flood tidal delta (Sherrod and McMillan, 1981) which is entirely mangrove-dominated at present, but was of interest because of past reversals in mangrove versus marsh vegetation associated with freezes in the 1980's – the last to significantly impact mangrove populations along the Texas coast. Sub-freezing conditions that occurred in December, 1983 induced a mortality rate of approximately 80-85 percent of Texas mangrove populations (McMillan and Sherrod, 1986), with Harbor Island experiencing a mortality of 85 percent mangrove loss and Galveston 95 percent or greater (Sherrod and McMillan, 1985). Additional impacts on mangrove colony expansion occurred during a freeze event composed of multiple fronts in December, 1989; although the amount of damage is unknown, multiple fronts may induce more severe effects (Everitt et al., 1996; Buskey et al., 1997; personal communication with Edward Buskey). A remote sensing study in late 1980's suggests that mangroves in

Figure 3: Harbor Island and Mud Island field localities at Port Aransas, plotted on U.S Geological Survey digital orthophoto quadrangle (DOQ) aerial photos taken in 2004.

Figure 4:   Galveston East field locality, plotted on U.S Geological Survey digital orthophoto quadrangle (DOQ) aerial photos taken in 2004.

Figure 5: Galveston West field locality, plotted on U.S Geological Survey digital orthophoto quadrangle (DOQ) aerial photos taken in 2004.
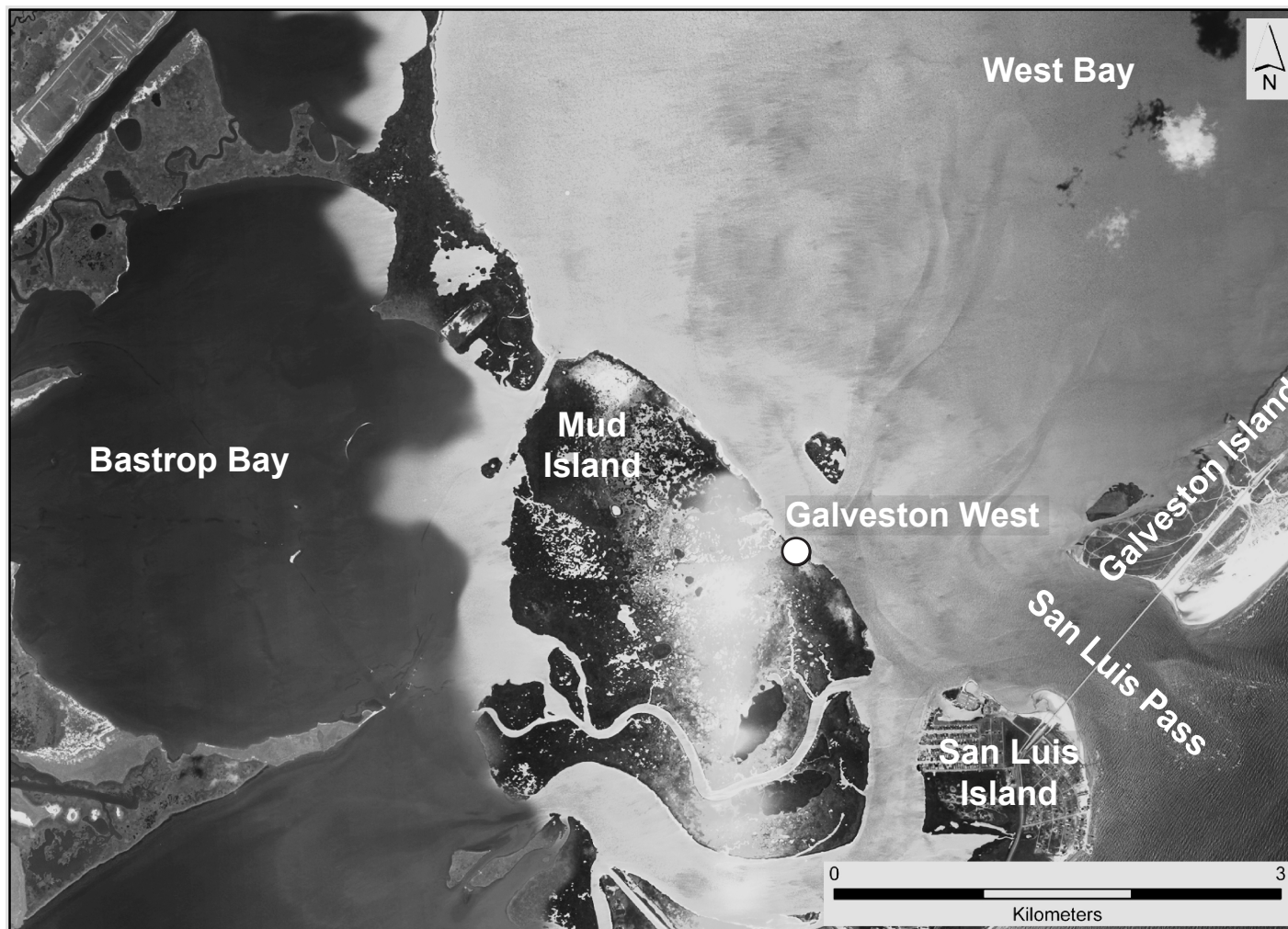
South Texas and at Harbor Island had fully recovered before the 1989 freeze episode (Everitt and Judd, 1989), and once again after the 1989 freeze (Everitt et al., 1996). The 1983 and 1989 freezing events are believed to have impacted *Avicennia* populations within the Galveston area to a greater extent; after the 1983 freeze mangrove populations reduced to less than 5 percent of the original (Everitt and Judd, 1989; Everitt et al., 1996). Port Aransas mangrove colonies were thick and flourishing during the present study in July, 2009, with individual tree sizes reaching one to two meters in height (Fig. 6A-B).

Galveston study areas and representative mangrove populations are located on another Mud Island (hereafter referred to as Galveston West; 29° 5' 20.82"N, 95° 8' 35.17"W) on the flood tide delta at the West end of Galveston Island and at East Beach (29° 19' 53.44"N, 94° 45' 1.15"W), hereafter referred to as Galveston East. The Galveston East site (Fig. 4) is located directly adjacent to the entrance to the Bolivar Roads tidal inlet, to which it is attached by a tidal channel, and the Galveston West site (Fig. 5) is situated immediately adjacent of the San Luis Pass tidal inlet. Individual tree sizes at the Galveston sites during the field study in October, 2009 were approximately 30 to 50 cm in height, and mangrove colonies were scattered and mixed with marsh grasses (Fig. 6C). These smaller sizes of mangrove colonies relative to the Port Aransas sites are likely a function of colony age, but could be either a product of slower colony recovery after the diebacks of the 1980's, or dispersal pathways controlling the time of establishment of the colony.

Figure 6: Field photographs of Port Aransas Mud Island in July 2009 showing mangrove-dominated (A) and the transition (B) between marsh and mangrove areas. Trees are one-two meters in height. Notice the brown, unhealthy appearance of salt marsh in (B). (C) Galveston West mixed mangrove and salt marsh in October 2009. Height of GPS antenna is approximately 46 cm.

A.

C.

B.

3.1.1 Elevation

Elevation surveys were completed for each of the four field areas with the purpose of observing any elevation differences with respect to wetland vegetation type. A base station was established at each field area using a tripod-mounted Trimble NetRS GPS receiver, positioned to record spatial data over at least a 24 hour period in order to achieve cm-scale accuracy of antenna location and elevation. Collected data was recorded and later post-processed through OPUS (Online Positioning User Service) after the surveys for spatial correction; the resultant latitude and longitude (reference frame North American Datum of 1983 (NAD83) and associated UTM coordinates) and orthometric height (North American Vertical Datum of 1988 [NAVD88], GEOID09 except for the Port Aransas Mud Island site, processed with GEOID03) were used as the final base station location. A PVC tube benchmark was hammered into the soil prior to setting up the NetRS receiver in order to allow the receiver to be moved to multiple sites during the field deployment and to allow for future work in the area. A transit topographic system (involving an electronic theodolite and stadia measuring rod) was subsequently used to record points of elevation over the field area at +/- 1 cm accuracy. Horizontal azimuth (degrees, minutes, seconds converted to decimal degrees-direction from base station), 90° height (m-elevation), and vertical azimuth (degrees, minutes, seconds converted to decimal degrees-distance from base station-angle subtracted from 90°) were recorded and later spatially referenced back to the base station locality and converted into latitude and longitude coordinates. Elevation contour maps were created

with ArcMap© software (ESRI, Inc., Redlands, California) using the Inverse Distance Weighting interpolation in the Spatial Analyst tool.

3.1.2 Core Sampling

Peat auger cores from marsh and mangrove areas were collected for sampling of organic matter content, pore water chemistry, Pb/Cs radiotracer geochronology, sediment strength and grain size, porosity, and pigment and lignin-phenol biomarkers of organic matter sources(s). Augering was selected as the coring method to avoid core compaction (foreshortening) associated with many coring techniques. Cores were cut on site and sub-sampled the same day in a field lab prior to freezing for analysis and storage at university labs. Cores were sub-sampled at every two to 22 cm depth, and then every other two cm to a depth of 50 cm. After 50 cm, two cm sub-sampling was done every 10 cm for the remaining length of the core.

3.2 LABORATORY METHODS

3.2.1 Bulk Properties and Organics

Strength measurements were taken on the core half prior to sub-sampling using a hand-held shear vane tester (Geonor/03535; range 0 to 200 kPa) inserted vertically at intervals in the core. Grain size and porosity data were subsequently evaluated in the lab utilizing sub-sampled core intervals. Grain size (percent gravel/sand/silt/clay) was analyzed utilizing a combined wet sieve and pipette technique (Folk, 1968). Soil porosities were calculated from freeze dried and wet weights. Sediment organic content

was measured using two distinct parameters: as weight percentages of live root organics (sieved and picked by hand to obtain the "green" stem and root material), followed by weight loss on ignition at 550°C to determine the overall organic matter content (minus the live rooting). As live rooting was found to be highly variable across depth intervals, integrated values were calculated for the upper 14 to 18 cm rooted zone (see section 4.4). Weight organic loss on ignition (hereafter referred to as percent organic matter; section 4.3) was also averaged over the upper 18 to 20 cm surface zone (representing a period of post-wetland colonization) as well as over entire core intervals to facilitate inter-comparison of mangrove and marsh areas.

3.2.2 Sediment Accumulation

Total sediment accumulation rates (mineral + organic) were measured using the particle-reactive radiotracers ^{210}Pb and ^{137}Cs measured by gamma spectrometry (planar and well geometry LEGE detectors) of freeze-dried sediment intervals. Samples were freeze-dried and finely ground and subsequently packed and sealed for a period of ≥ 21 days prior to counting to allow Pb to in-grow to secular equilibrium. Samples were counted for at least 24 h and activities were calculated following the methods outlined in Allison et al. (2007). A best-fit linear regression of the natural log of excess ^{210}Pb (^{210}Pb$_{xs}$) with depth below any surface mixed layer of homogenous activity was used to determine the sediment accumulation for the past ~100 years (Nittrouer and Sternberg, 1981). ^{137}Cs (T½ = 30 years) is the product of fallout from atmospheric testing of thermonuclear weapons that began in 1954. Two time markers for ^{137}Cs with depth were

23

utilized: the depth of maximum ^{137}Cs penetration (1954), and the depth of maximum ^{137}Cs fallout in the northern hemisphere (1963 according to Chmura and Kosters, 1994). ^{137}Cs rates were calculated by dividing the depth of the 1954 or 1963 peak occurrence in the core by the number of years passed; errors were derived by extrapolating across the core interval represented by that particular year. Final accumulation rates were depth-corrected to a standard core porosity (60%) to expand or contract interval depths (to allow for inter-comparison of sites in linear terms; see Allison et al., 2007), and were converted from linear accumulation rates (consolidation-corrected cm/y) to mass accumulation rates (g/cm^2/y).

3.2.3 Soil Pore Water Geochemistry

Salinity, pH, and redox potential (Eh) were measured on pore water data from each sub-sampled core interval. pH and Eh data were measured on cores thawed in a nitrogen atmosphere glove bag by inserting electrodes directly into the sediment and taking an average of five readings. pH was measured using a Micro pH electrode (PHR-146B, Ag/AgCl internal reference, Lazar Research Laboratories). Eh was measured using a VWR sympHony Glass Combination Redox electrode (Ag/AgCl internal reference). Both measurements were collected with a pH/mv/TEMP meter (JENCO Electronics, LTD. Model No. 6230). Electrodes were thoroughly rinsed with distilled water between sample insertions. The pH electrode was measured against known pH 4, 7, and 10 standard buffers every three samples to evaluate electrode reliability. Micro pH electrode instrumentation error was calculated by taking differences of measured versus

known pH buffer readings at the beginning and end of a measuring period and dividing by the known buffer value. The following are errors reported for known pH 4, 7, and 10 buffers: 0.00 to 0.15 (beginning of sampling period) and 0.30 to 0.99 (end of sampling period) (pH 4), 0.05 to 0.07 and 0.08 to 0.25 (pH 7), and 0.00 to 0.01 and 0.00 to 0.03 (pH 10). Redox calibration solutions (Zobel's solution (Nordstrom and Wilde, 1998); Redox Calibration Solution (S-146 OPR, Lazar Research Laboratories)) were used to evaluate Eh electrode confidence at the beginning and end of an analysis series. Electrodes were dipped into dilute hydrochloric acid prior to the next analytical series in order to dissolve any remaining sediments or sulfides. The redox electrode was rubbed with fine emery paper and stored in non-distilled water overnight; a dilute pH 7 buffer solution was used for pH electrode storage.

Salinity readings were taken from extracted pore waters in the open atmosphere immediately following the completion of pH and Eh glove bag measurements. A fraction of each sample interval was wrapped into glass microfiber filter paper (Whatman 70 mm), placed into a hand-held press with 63 μm stainless steel sieve filters (Advantech NO. 230) and squeezed. Extracted water droplets were collected with a glass stir rod into a refractometer for salinity measurements (Sper Scientific, Digital Refractometer 300035).

3.2.4 Statistical Testing

A *t*-test calculation was applied to multiple mangrove and marsh datasets for every component of data in order to evaluate statistical significance of differences

observed between cores and between wetland types. A preliminary test that evaluates equality of variances between datasets (F-test) was applied in order to determine which type of *t*-test to utilize (equal or unequal variance). If the probability (one-tail *p*-value) was less than 0.05, variances were assumed to be unequal. After variance was determined, the appropriate *t*-test was applied. If the two-tailed *p*-value was less than 0.05, evidence existed to reject the null hypothesis of equal means between two datasets (therefore there is a significant difference between mangrove and marsh data) (TexaSoft, 2008). *T*-test data is reported as a mean score for individual groups (*p* = two-tailed *p*-value).

CHAPTER 4

Results

4.1 ELEVATION

Results of the GPS/theodolite surveys at Port Aransas Mud Island suggest mangrove vegetated areas are on average four cm higher in elevation than surrounding marsh areas using statistical comparisons (*t*-test; Table 1) of the >90 percent and <10 percent mangrove areas. Several theodolite transects at Port Aransas Mud Island crossed single mangroves surrounded by marsh, and these also display one to two cm higher elevations (locations in Fig. 7A, vegetation patterns in Fig. 7B). Because Port Aransas Harbor Island is entirely mangrove colonized, elevation data cannot be compared by wetland type, however Harbor Island mangroves are within the same elevation range as Mud Island mangroves (18 to 20 cm above mean sea level, referenced to NAVD88 using a GEOID model). While the >90 percent mangrove areas are one to two cm higher on average than the <10 percent mangrove sites at Galveston East and West, these differences are not statistically significant (Table 1). The concentration of mangroves growing at Galveston East occurs along a topographic low (Fig. 8), while the small patch of mangroves at Galveston West (Fig. 9) grows along a topographically high bankside levee on the island. This suggests that pre-existing geomorphology is also a control on the elevation patterns observed at the Galveston field sites, given that these topographic features cut across mangrove-marsh transitions.

Table 1: Average elevations for mangrove and marsh vegetated regions for each field site. A *t*-test was performed to evaluate statistical differences (*p*-values in chart) between mangrove and marsh datasets; *p*-values of <0.05 represent statistical significance and are notated with an asterisk (*). All statistical *t*-test results were calculated over arrays of point elevations within >90% and <10% mangrove vegetated areas.

Location	Average Elevation (m)	Error	*p*-value
Port Aransas Mud			
>90% Mangrove	0.182	± 0.014	*9.012E-06
<10% Mangrove	0.139	± 0.033	
Galveston East			
>90% Mangrove	0.307	± 0.045	0.147
<10% Mangrove	0.281	± 0.056	
Galveston West			
>90% Mangrove	0.483	± 0.006	0.194
<10% Mangrove	0.474	± 0.027	

Figure 7:   Elevation (A) and vegetation (B) patterns at Port Aransas Mud Island. In the elevation map, warmer colors represent higher elevations and arrows indicate the location of single mangroves within a marsh area discussed in the text. In the vegetation map, categories are based on field observations of areas containing more than 90% mangroves, mixed mangrove and marsh, and less than 10% mangroves.
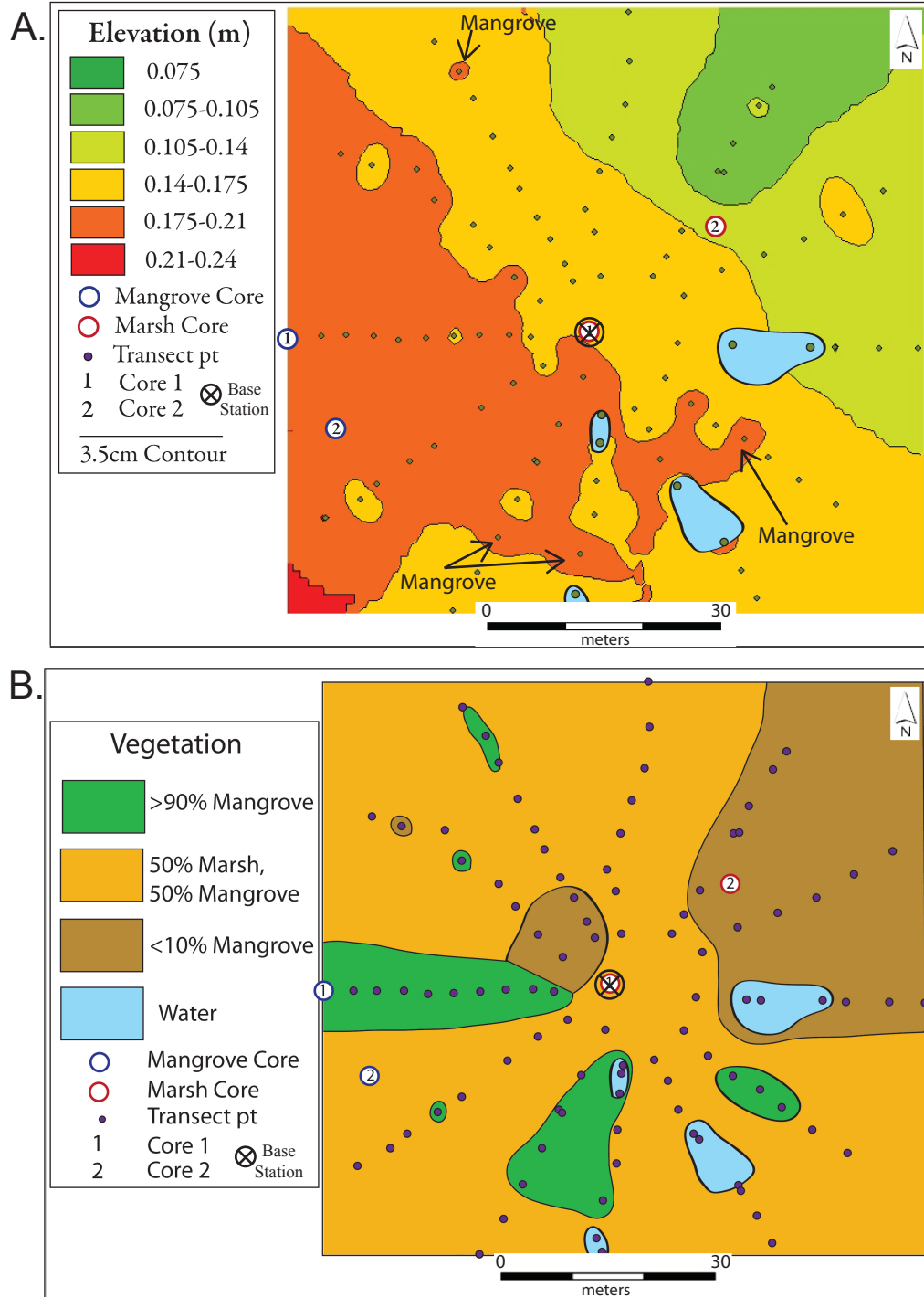
Figure 8:   Elevation (A) and vegetation (B) patterns at Galveston East. Elevation and
              vegetation patterns are the same as in Figure 7.
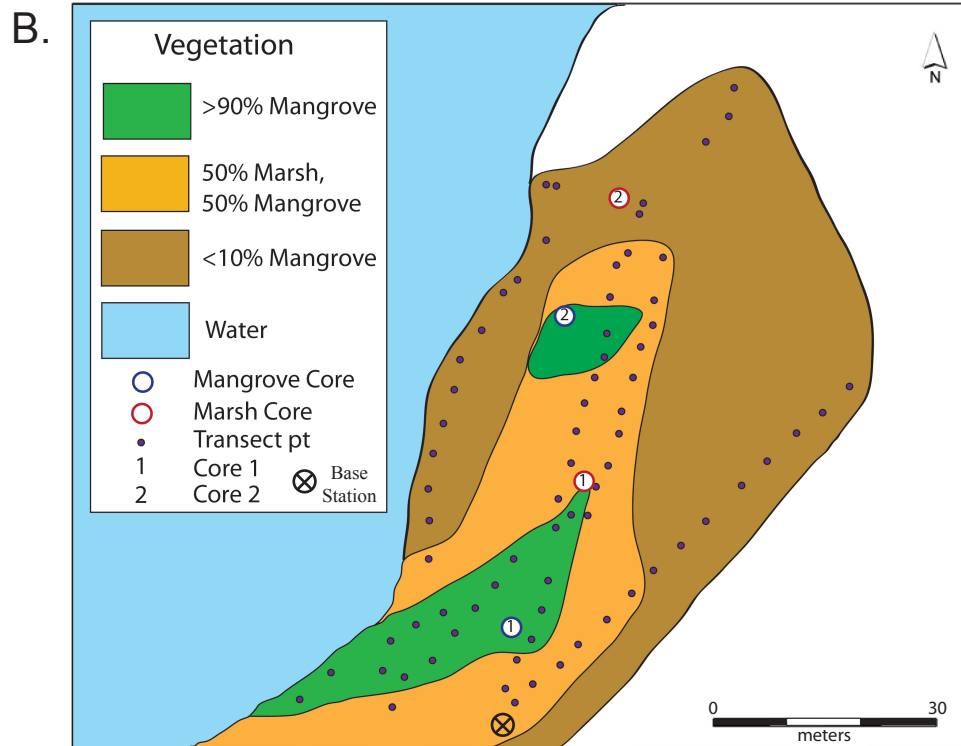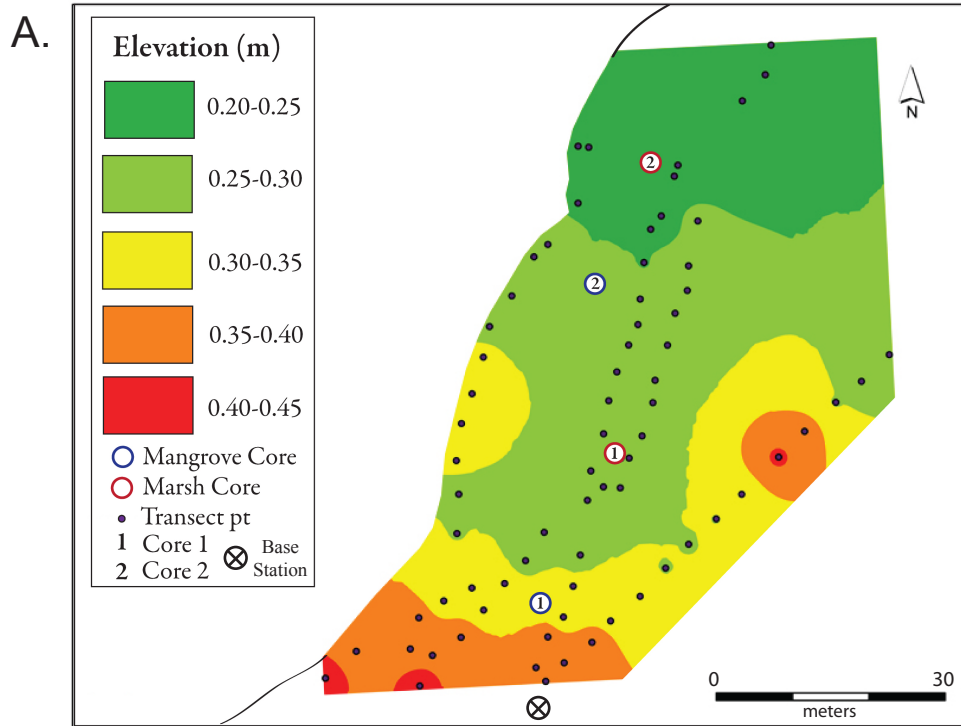
Figure 9:   Elevation (A) and vegetation (B) patterns at Galveston West. Elevation and
              vegetation patterns are the same as in Figure 7.
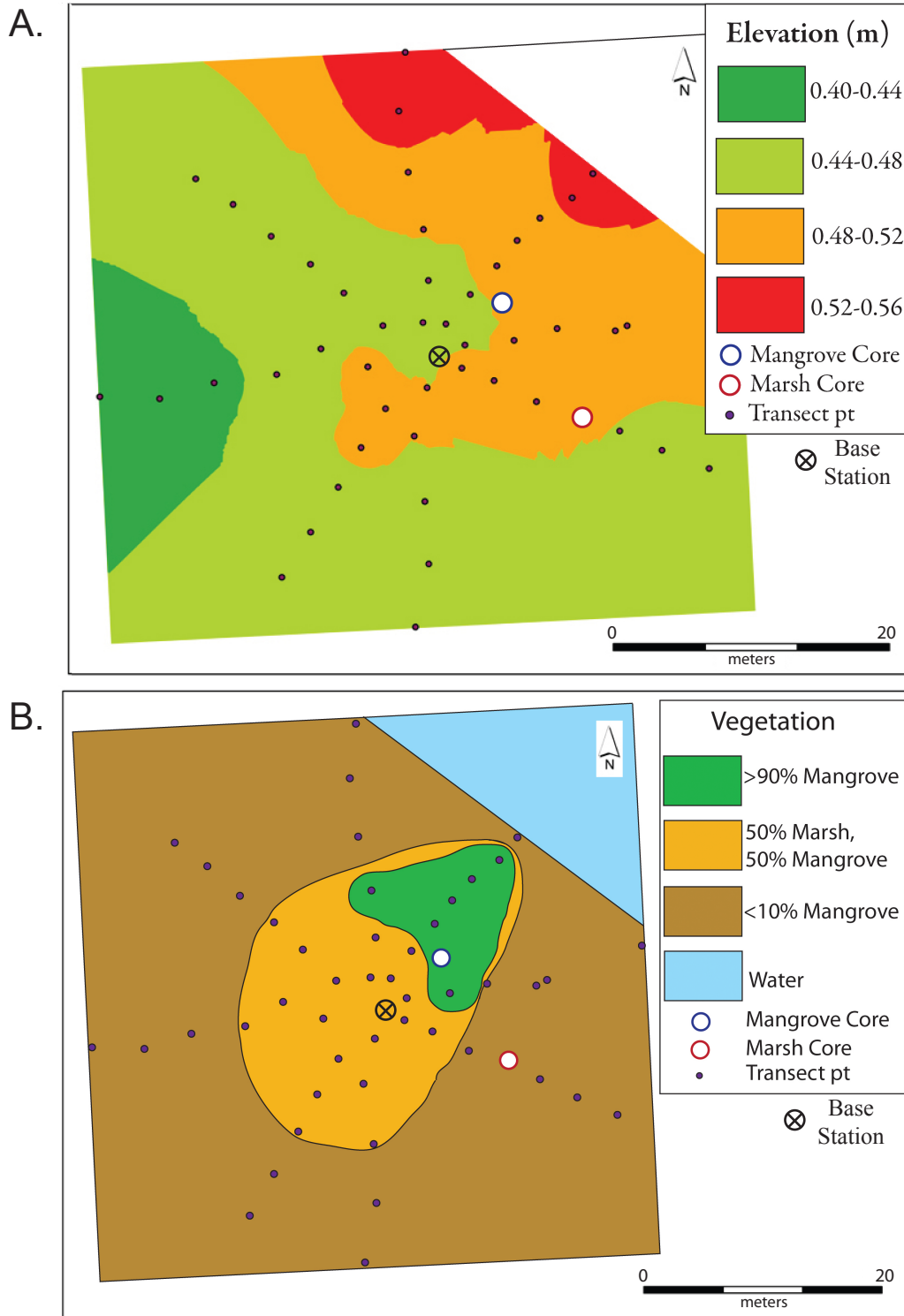
Percent error was calculated using the standard deviation of all elevation points and included in >90 percent and <10 percent mangrove classifications for every field location.

4.2 RADIOCHEMICAL SEDIMENT ACCUMULATION RATES

Excess ^{210}Pb activities in surficial sediments range from 6.8 to 8.6 dpm/g within Port Aransas sediments, and 5.6 to 7.3 and 7.1 to 7.6 dpm/g within Galveston East and West cores. Plots of consolidated depth versus decay-induced declining excess ^{210}Pb activities used to calculate sediment accumulation rates have relatively high R^2 values for most sites (Fig. 10A). Table 2 displays multi-core averaged linear accumulation rates (LAR) with total mass accumulation rates (MAR) listed in parentheses. Single core LARs range from 0.31 ± 0.04 to 0.77 ± 0.15 cm/y in mangroves and 0.17 ± 0.03 to 0.36 ± 0.03 cm/y in marsh at Port Aransas. Galveston East LAR ranges are 0.62 ± 0.12 to 0.82 ± 0.10 cm/y (mangroves) and 0.31 ± 0.14 cm/y (marsh). MARs in single mangrove and marsh cores, respectively, ranged from 0.19 to 0.46 and 0.10 to 0.22 g/cm^2/y at Port Aransas and 0.37 to 0.49 and 0.18 g/cm^2/y at Galveston East. ^{210}Pb rates were excluded from one marsh core from Galveston East and from both Galveston West core sites calculations because of a low R^2 value (<0.6) in the linear regression curves; rates are also not calculated for Harbor Island sediments because of variable downcore ^{210}Pb activities (Fig. 10B-C).

^{137}Cs (1963) mineral accumulation rates are based on the peak in fallout activity associated with thermonuclear atmospheric testing in the northern hemisphere (Chmura

Figure 10: Examples of downcore ^{210}Pb linear regression curves utilized to calculate sediment accumulation rates. (A) shows and example of a high R^2 linear regression, while (B-Galveston West) and (C- Port Aransas Harbor Island) show examples of low R^2 values rejected for sediment accumulation calculations. Reasons for this variability downcore are discussed in the text.
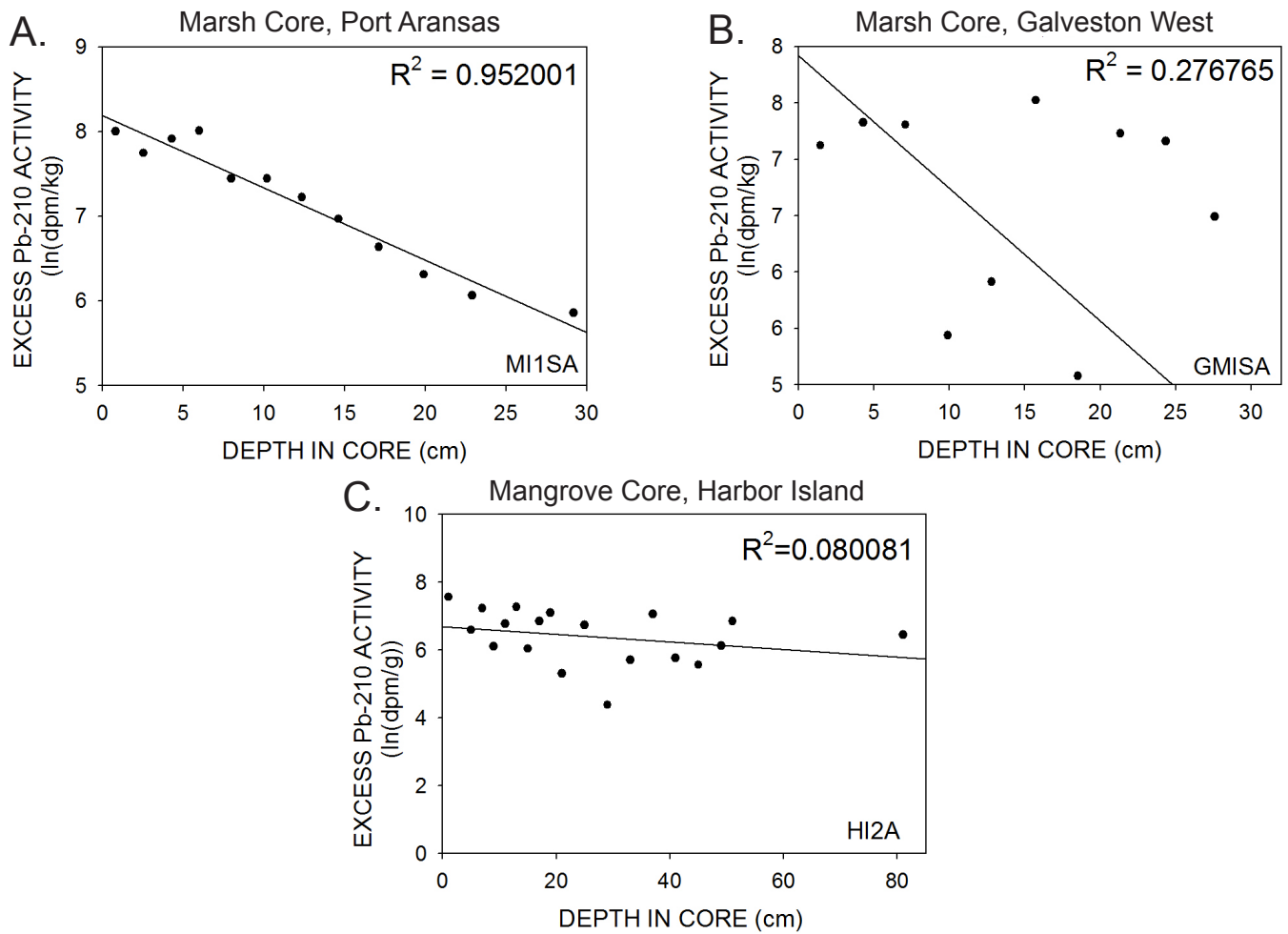
Table 2: Radiochemical sediment accumulation rate averages for mangrove and marsh field sites, represented as linear accumulation rates in cm/y and mass accumulation rates in (g/cm^2/y). ^{210}Pb and ^{137}Cs counting was completed prior to organic loss on ignition measurements. Statistical significance (*p*-value) notated with an asterisk (*).

Location	^{137}Cs (1954) cm/y (g/cm2/y)	^{137}Cs (1963) cm/y (g/cm2/y)	^{210}Pb cm/y (g/cm2/y)	*p*-value		
				Cs 1954	Cs 1963	Pb
Port Aransas Mud						
Mangrove	1.31 ± 0.07 (0.79)	0.74 ± 0.21 (0.45)	0.54 ± 0.15 (0.32)	0.429	*0.026	0.385
Marsh	1.59 ± 0.17 (0.95)	0.18 ± 0.06 (0.11)	0.26 ± 0.04 (0.16)			
Galveston East						
Mangrove	1.04 ± 0.08 (0.62)	0.50 ± 0.10 (0.30)	0.72 ± 0.16 (0.43)	0.652	0.751	0.313
Marsh (^{210}Pb single core)	0.95 ± 0.09 (0.57)	0.45 ± 0.10 (0.27)	0.31 ± 0.14 (0.18)			
Galveston West						
Mangrove	0.74 ± 0.06 (0.45)	0.41 ± 0.06 (0.24)	R^2 < 0.4	N/A (single cores)		
Marsh	1.16 ± 0.07 (0.70)	0.22 ± 0.06 (0.13)	R^2 < 0.3			

and Kosters, 1994). This input radiotracer age marker generated lower rates than those calculated from the basal horizon, corresponding with the onset of thermonuclear testing in 1954, by an average range of 0.5 to 1.0 cm/y. ^{137}Cs (1963) LARs range from 0.41 to 0.74 cm/y (mangrove) and 0.18 to 0.45 cm/y (marsh) compared to ^{137}Cs (1954) rates of 0.74 to 1.31 cm/y (mangroves) and 0.95 to 1.59 cm/y (marsh). MAR follow similar trends (see Table 2). Fig. 11A shows a typical curve used for these calculations; activity reflects non-steady state fallout of bomb-products with one major peak representing the 1963 peak of maximum activity and is followed by a progressive decrease in activity with depth as the data approach the 1954 atmospheric onset. ^{137}Cs accumulation rates were not calculated for Harbor Island sediments because downcore variable ^{137}Cs activities make it difficult to select an exact point of maximum atmospheric peak or onset (Fig. 11B-C). Multiple core averaged errors for all site marsh versus mangrove comparisons were calculated utilizing the square root of the sum of squares of individual core errors (with the exception of Galveston West cores which represent single core error).

Statistical comparison of ^{210}Pb LARs from marsh and mangrove sites (each averaged from two cores; Table 2) show mangrove sites exhibit more than twice the accumulation rate of marshes at the Port Aransas and Galveston East study sites, however, these differences are not statistically significant given the inter-core variability. ^{137}Cs (1963) LARs are also higher in mangrove sediments at all three sites, however there is only statistical significance at Port Aransas (Table 2). No consistent or statistical trends are apparent from ^{137}Cs (1954) calculated LARs, with marsh rates higher at Port

35

Figure 11: Examples of downcore ^{137}Cs activity plots showing the location of time-markers utilized for calculating sediment accumulation rates. Example (A) shows a core with a well-defined 1963 peak and 1954 onset. The other examples (B, C) show cores where sediment accumulation time markers were not definitive either because of multiple 1963 peak possibilities and/or a poorly defined depth for onset of activity.
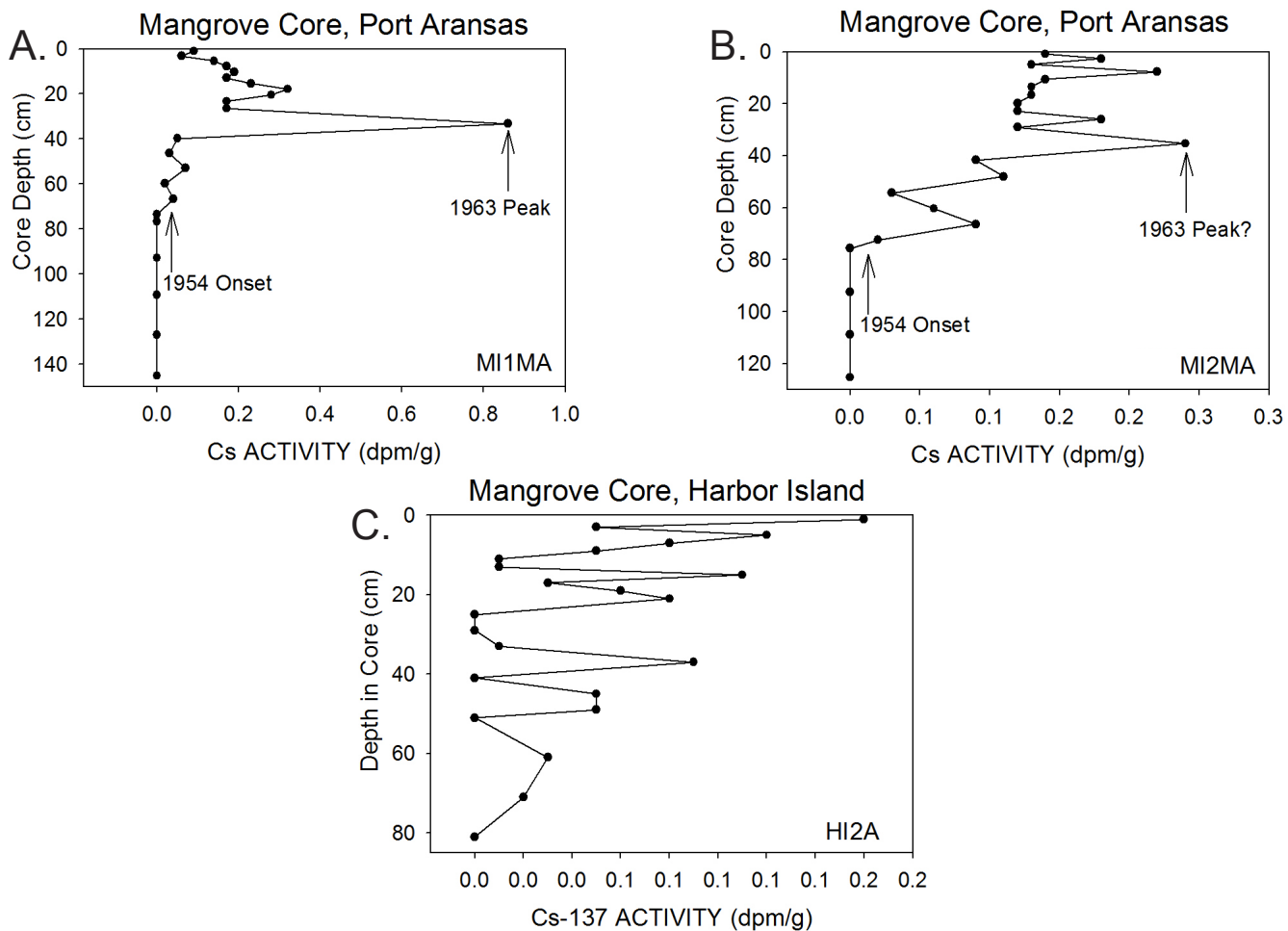
Aransas. Galveston West accumulation rates were not statistically tested for Pb or Cs because these rates represent single cores and are not comparable with a *t*-test.

4.3 ORGANIC ACCUMULATION RATES

Percent soil organic matter was measured as the weight of organic loss on ignition at 550°C following removal of live roots. These analyses indicate that organic matter content is low at every site when averaged over the entire core, ranging from only 0.49 to 1.36 percent (Table 3). However, much of the organic matter is concentrated in a near surface interval and represents the accumulation (mineral and organic) of post-wetland colonization. When only the wetland interval depths are considered, average percent organic matter increases to 0.58 to 2.45 percent (Table 3). This depth averaging was carried out in order to compensate for the observed large sample-to-sample variability in percent organic matter and was selected where percent organics first dropped to a site specific background level characteristic of deeper in the core (20 cm at Port Aransas Mud Island, 18 cm at Galveston East, and 20 cm at Galveston West, see Fig. 12). Errors in Table 3 were calculated based on the standard deviation of all sample points used for an integrated calculation for each core: mangrove and marsh core averages of errors for two cores were then obtained by square root of the sum of the squares of individual core errors. The low volumes of percent organic matter suggest that the majority of sediment accumulation observed with the radiotracers (see calculated ^{210}Pb and ^{137}Cs rates in Table 2) is the product of mineral trapping.

37

Table 3:   Organic loss on ignition represented as averaged percentages over entire core depths and wetland intervals (20 cm at Port Aransas, 18 cm at Galveston East, and 20 cm at Galveston West; actual wetland depths vary between mangrove and marsh cores). Statistical significance (*p*-value) notated with an asterisk (*).

Location	Ignition Loss (%/cm) Entire Core	Error	Ignition Loss (%/cm) Wetland Interval	Error	*p*-value Entire Core	Wetland
Port Aransas Mud						
Mangrove	0.85	± 0.83	1.44	± 1.09	0.113	*0.003
Marsh	1.36	± 2.11	2.45	± 2.52		
Port Aransas Harbor						
Mangrove	0.49	± 0.66	0.58	± 0.67		
Galveston East						
Mangrove	0.62	± 0.53	0.70	± 0.51	0.837	0.714
Marsh	0.59	± 0.63	0.88	± 0.81		
Galveston West						
Mangrove	0.59	± 0.79	0.90	± 0.20	0.419	0.215
Marsh	0.74	± 0.33	1.00	± 0.28		

Figure 12:   Downcore plots of percent organic matter loss on ignition at Port Aransas Mud Island (A), Galveston East (B), and Galveston West (C). Mangrove and marsh cores are represented with closed blue squares and red triangles, respectively. Dashed lines indicate depth to the base of the organic-rich interval emplaced after the establishment of a wetland.
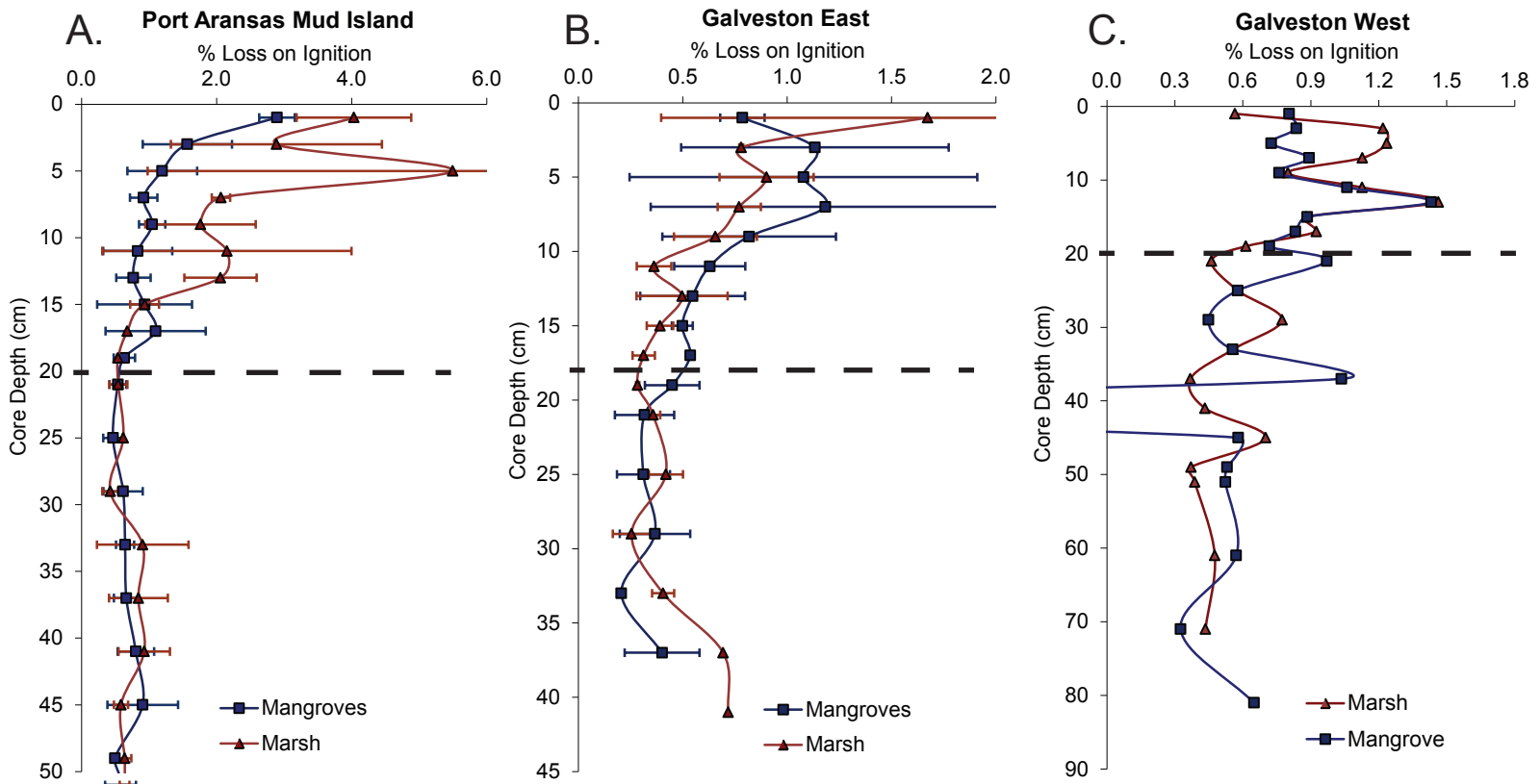
With the exception of the entire core intervals in Galveston East, the integrated values for organic loss on ignition are higher in marsh soils than in mangrove core data for both the entire core and wetland intervals of every site, however marsh sediments only exhibit a statistically higher percent in the wetland interval at Port Aransas Mud Island (as observed from averaged values and statistical t-tests completed over entire interval and wetland depths of averaged mangrove and marsh cores, Table 3).

4.4 LIVE ROOTING

Live rooting organics were measured as weight percent of total sediment weight for each depth interval. Because of sample variability with depth (see Fig. 13), these values were averaged over the entire actively rooted soil interval to allow inter-comparison of marsh and mangrove cores. The depth to the base of the actively rooted interval was selected where sample live root weights in any core at the site (marsh or mangrove) first dropped below 0.5 percent of total dry sediment weight (14 cm at Port Aransas, 14 cm at Galveston East, and 18 cm at Galveston West, Fig. 13). Error is calculated in the same method as section 4.3. Average live root organics over rooted intervals range from 1.13 to 2.41 percent in mangrove and 1.03 to 1.69 percent in marsh sediments (Table 4).

T-test results of this averaging are shown in Table 4: percent live rooting in the rooted interval is statistically higher in mangroves than marshes at Port Aransas Mud Island and Galveston West. While also higher in mangroves at Galveston East, this difference is not statistically significant.

Figure 13: Downcore plots of live root organic percentages at Port Aransas Mud Island (A), Galveston East (B), and Galveston West (C) core locations. Mangrove and marsh cores are represented with closed blue squares and red triangles, respectively. Dashed lines represent the base of the rooted interval used in calculations, as discussed in the text.
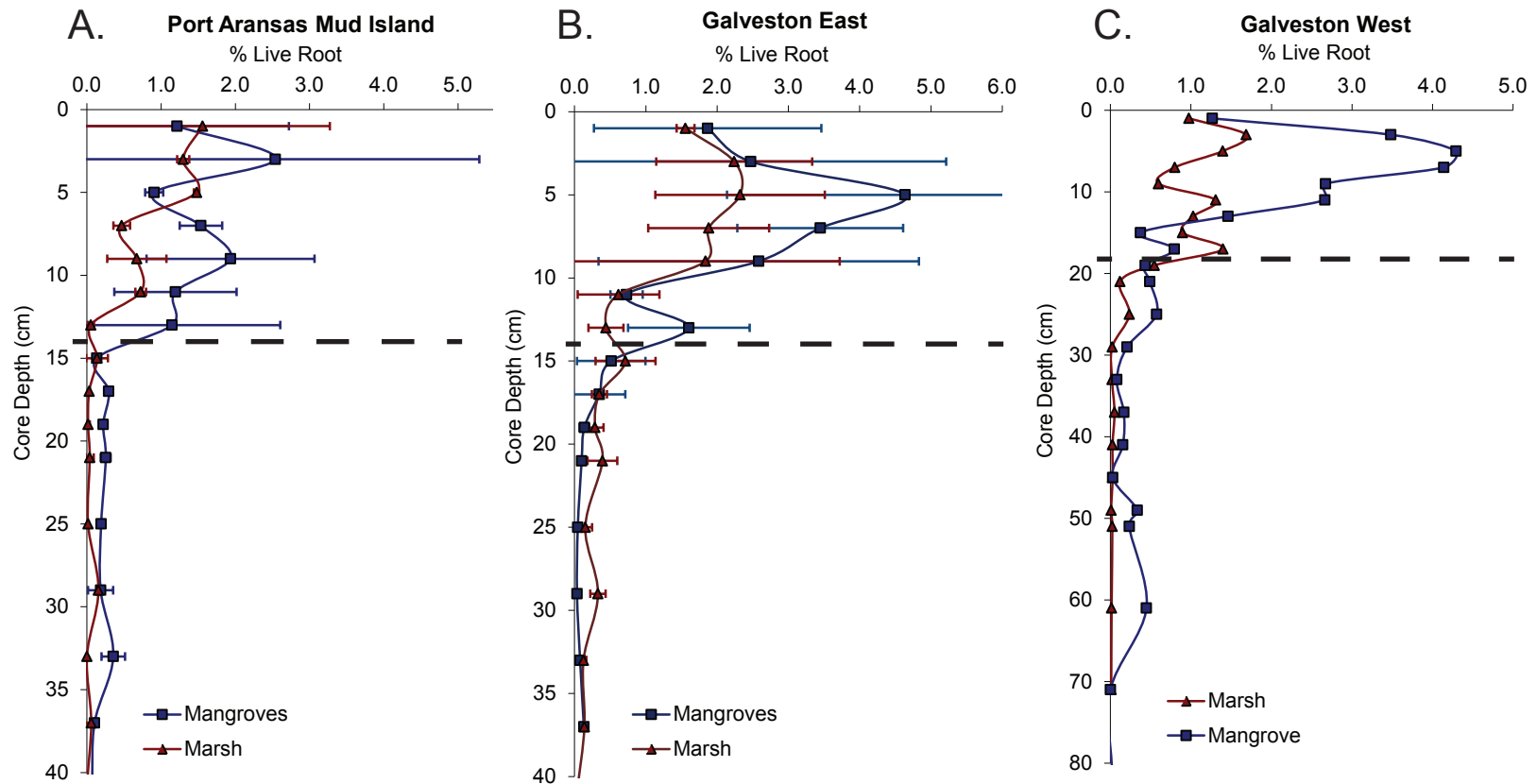
Table 4: Live root organics represented as averaged percentages over rooted depth intervals (where organic values reached <0.5%, approximately 14 cm at Port Aransas, 14 cm at Galveston East, and 18 cm at Galveston West; actual rooted depths vary between mangrove and marsh cores). Statistical significance (*p*-value) notated with an asterisk (*).

Location	Live Root (%/cm)	Error	*p*-value
Port Aransas Mud			
Mangrove	1.64	± 1.51	*0.028
Marsh	1.03	± 0.91	
Port Aransas Harbor			
Mangrove	1.13	± 2.17	
Galveston East			
Mangrove	2.41	± 1.92	0.139
Marsh	1.69	± 1.29	
Galveston West			
Mangrove	2.35	± 1.40	*0.001
Marsh	1.06	± 0.37	

4.5 BULK PROPERTIES

Grain size analyses were only conducted for the Port Aransas Mud Island and Galveston West sites. Galveston and Port Aransas sites are similar, with Galveston sediments averaging 3 percent higher sand and 4 percent lower clay content. Grain size over the wetland depth (loss on ignition organic-rich interval from section 4.3) showed an average (mangrove and marsh data combined) of 60 percent (54 to 70 percent range) sand+gravel (gravel is shell material), 10 percent (7 to 13 percent range) silt and 30 percent (23 to 36 percent range) clay at Port Aransas. Below the wetland interval, samples were less variable and slightly more sand rich and silt/clay poor (67 percent (59 to 73 percent) sand+gravel, 8 percent (5 to 14 percent) silt, and 25 percent (20 to 30 percent) clay) (Table 5, Fig. 14A). At Galveston West, averaged grain sizes displayed 63 percent (50 to 78 percent) sand+gravel, 11 percent (1 to 18 percent) silt, and 26 percent (15 to 33 percent) clay over combined mangrove and marsh wetland depths (Table 5). Pre-wetland intervals averaged 64 percent (53 to 77 percent) sand+gravel, 6 percent (0 to 14 percent) silt, and 29 percent (23 to 38 percent) clay (Fig. 14B). In Port Aransas, once core depths of 40 cm are reached, there is very little grain size fluctuation. A small increase in sand+gravel content (corresponding decrease in silt and clay) occurs at a depth of eight cm, followed by a larger sand+gravel increase at a depth of 22 cm (Fig. 14A). Within Galveston West data, a sharp drop in the sand+gravel fraction occurs at a depth of 10 cm within mangrove soils followed by a gradual increase up to a depth of 26 cm. An inversion point between mangrove and marsh sand+gravel and clay fractions occurs at approximately eight and 20 cm core depths (Fig. 14B). Graphical errors (error

Table 5: Grain size, porosity, strength, and statistical *t*-test results calculated over averaged mangrove and marsh data for wetland intervals: Port Aransas=20 cm, Galveston East=18 cm, Galveston West=20 cm. Statistical significance (*p*-value) notated with an asterisk (*). Errors represent standard deviation over averaged core intervals.

Location	Grain Size (Frequency %)						Porosity		Strength (kPa)	
	Sand+Gravel		Silt		Clay					
	Average	*p*-value	Average	*p*-value	Average	*p*-value	Average	*p*-value	Average	*p*-value
Port A Mud										
Mangrove	61.36 ± 5.12	0.283	9.46 ± 1.65	0.468	29.18 ± 4.33	0.311	0.64 ± 0.06	*0.014	20.80 ± 2.84	*0.000
Marsh	58.90 ± 4.45		10.07 ± 1.90		31.03 ± 3.23		0.72 ± 0.06		11.60 ± 2.07	
Port A Harbor										
Mangrove	N/A						0.48 ± 0.05	N/A	25.10 ± 1.71	N/A
Galveston East										
Mangrove	N/A						0.61 ± 0.05	0.861	8.95 ± 1.44	0.245
Marsh							0.60 ±0.07		7.94 ± 2.11	
Galveston West										
Mangrove	63.50 ± 7.43	0.864	8.65 ± 5.99	0.084	27.86 ± 5.50	0.054	0.59 ± 0.03	0.835	6.27 ± 1.74	0.244
Marsh	63.06 ± 3.38		12.81 ± 4.23		24.12 ± 1.76		0.59 ± 0.03		7.10 ± 1.37	

Figure 14:   Grain size distributions for averages of two cores/wetland type for Port Aransas Mud Island core data (A) and single cores from Galveston West (B). Years before present are plotted according to [210]Pb (A) and [137]Cs (1963) geochronologies (B). Mangroves and marsh are represented by open squares and closed triangles, respectively. Grain size is subdivided into silt (4-63 µm-green), clay (<4 µm- red), and sand+gravel (>63 µm-blue) fractions. Dashed line indicates depth to the base of the wetland interval as shown in Figure 12.

A.   Port Aransas Mud Island Grain Size Distribution

B.   Galveston West Grain Size Distribution
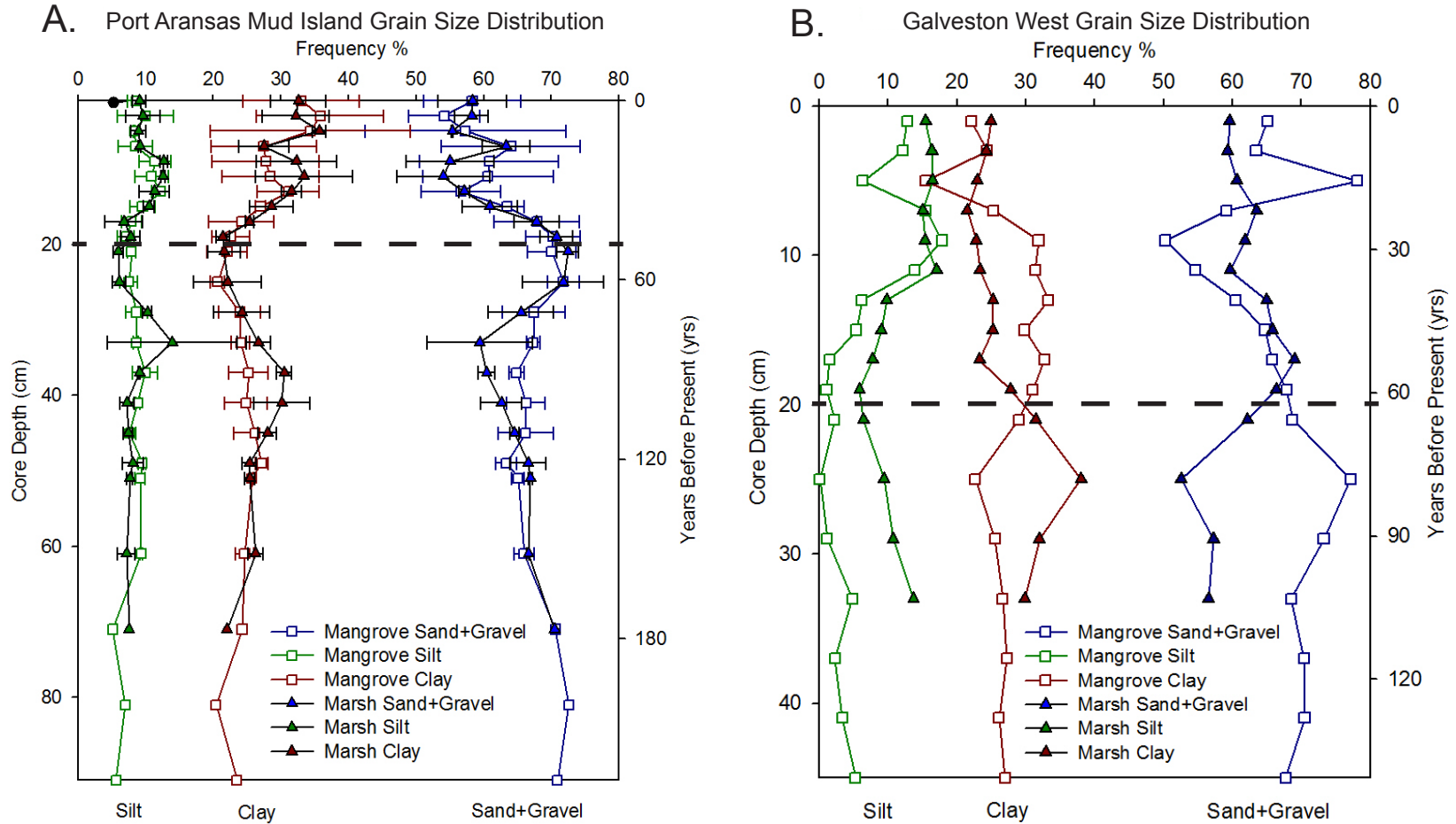
bars on averaged plotted data) for all grain size, porosity, and strength curves are based on the standard deviation of averaged mangrove and marsh core data. Errors in Table 5 of wetland intervals are the standard deviations of averaged values over those depths.

Average porosities at Port Aransas are 0.48 (0.44 to 0.59 range), 0.64 (0.57 to 0.75 range), and 0.72 (0.61 to 0.82 range) within wetland soil intervals of Harbor Island mangroves and Mud Island mangroves and marsh, respectively (Table 5). Following the same order, pre-wetland soil porosity averages are 0.44 (0.43 to 0.46), 0.52 (0.48 to 0.55), and 0.50 (0.45 to 0.54); increased porosities correlate to the onset of wetland development. All porosity trends within Port Aransas gradually decline in the upper 15 to 20 cm and reach steady levels past this wetland depth (Fig. 15A). Galveston East and West porosities range from 0.61 (0.53 to 0.67) to 0.59 (0.54 to 0.62) (mangroves) and 0.60 (0.51 to 0.70) to 0.59 (0.51 to 0.62) (marsh), respectively over wetland depths (Table 5). Pre-wetland soil intervals exhibit lower porosities as in Port Aransas, but still decrease with depth; averages are 0.46 (0.43 to 0.49) and 0.47 (0.43 to 0.52) at Galveston East and 0.46 (0.42 to 0.52) and 0.45 (0.42 to 0.47) at Galveston West in mangrove and marsh cores, respectively. Porosity linearly decreases with depth in Galveston East and in step-like intervals with a sharp decrease from 12 to 20 cm in Galveston West (Fig. 15B-C).

Soil strength averaged 20.8 (17 to 25 range) kPa and 11.6 (9.0 to 14.5 range) kPa in mangrove and marsh cores from Port Aransas Mud Island and 25.1 (23.5 to 27.5) kPa in Harbor Island mangroves over wetland intervals (Table 5). Below these depths values ranged from 11.7 (8.5 to 14) to 30.8 (14 to 39) kPa in Mud Island mangroves and marsh

Figure 15: Porosity plots with depth for Port Aransas (A) and Galveston East (B) and West (C) core locations. (A) Mud Island mangroves (closed blue squares) and marsh (red triangles) are compared to Harbor Island mangroves (green squares). (B-C) Mangrove and marsh cores are represented with closed blue squares and red triangles, respectively. Dashed line indicates depth to the base of the wetland interval as shown in Figure 12.

47
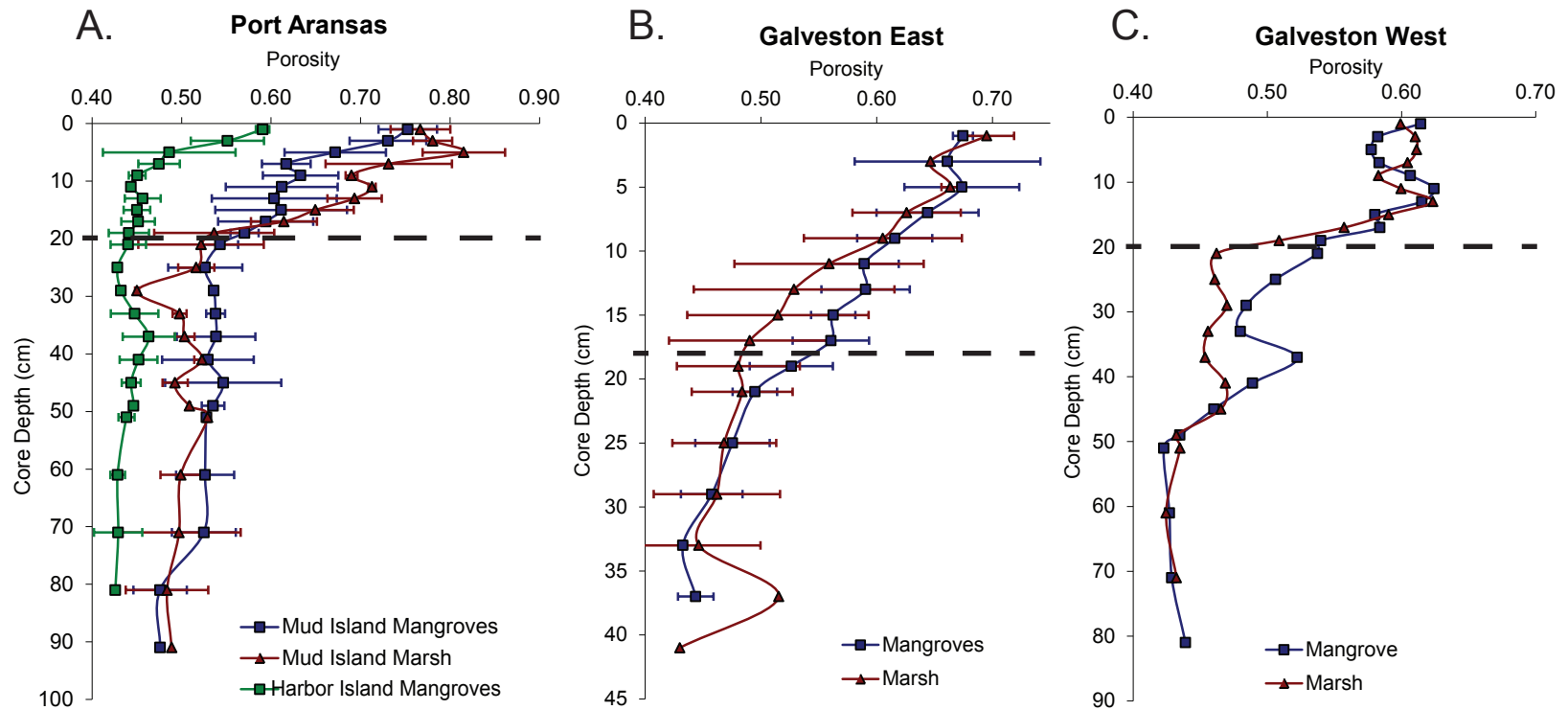
and 24.1 (20 to 29) kPa in Harbor Island mangroves. Pre-wetland soil strengths were stable in mangrove cores but increased with depth up to 44 cm in marsh cores at Port Aransas (Fig. 16A). Galveston East strengths ranged in averages of 9.0 (7.5 to 11) kPa and 7.9 (6.0 to 12) kPa over wetland depths and 7.7 (6.0 to 9.0) kPa and 7.6 (5.0 to 13) over pre-wetland intervals in mangrove and marsh cores, respectively (Table 5, Fig. 16B). Multi-core averaged soil strengths from Galveston West exhibited values of 6.3 (4.0 to 10) kPa and 7.1 (6.0 to 10) kPa in mangrove and marsh core data over the wetland interval (Table 5). Pre-wetland mangrove soil strengths averaged 6.3 (4.0 to 8.0) kPa and marsh 7.4 (5.0 to 13) kPa; strength appears to increase with depth after 30 cm beneath the wetland layer (Fig. 16C). Both Galveston East and West soil strength patterns oscillate up and down over entire wetland depths.

There are no statistical differences between mangrove and marsh grain size data at Port Aransas Mud Island or Galveston West sites, however the clay fraction is 4 percent higher on average within the mangrove soil interval at Galveston West site (Table 5, Fig. 14B). Statistically significant differences exist in porosity and strength trends at Port Aransas; porosities are lower in mangrove soils by approximately 0.08% and strengths are higher in mangrove sediments by approximately 9.0 kPa over wetland intervals from Mud Island (Table 5, Fig. 15A and 11A). Harbor Island mangrove soils exhibit lower porosities by approximately 0.16 to 0.24% and higher strengths of 4.0 to 13 kPa within the wetland interval compared to Mud Island mangroves and marsh, respectively (Fig. 15A and 11A). In Galveston East and West soils, no statistical difference exists in averaged mangrove and marsh porosity or soil strength over wetland depths. Average

Figure 16: Sediment strength with depth in kilopascals (kPa) for Port Aransas (A) and Galveston East (B) and West (C) core locations. (A) Mud Island mangroves (blue squares) and marsh (red triangles) are compared to Harbor Island mangroves (green squares). (B-C) Mangrove and marsh cores are represented with closed blue squares and red triangles, respectively. Dashed line indicates depth to the base of the wetland interval as shown in Figure 12.
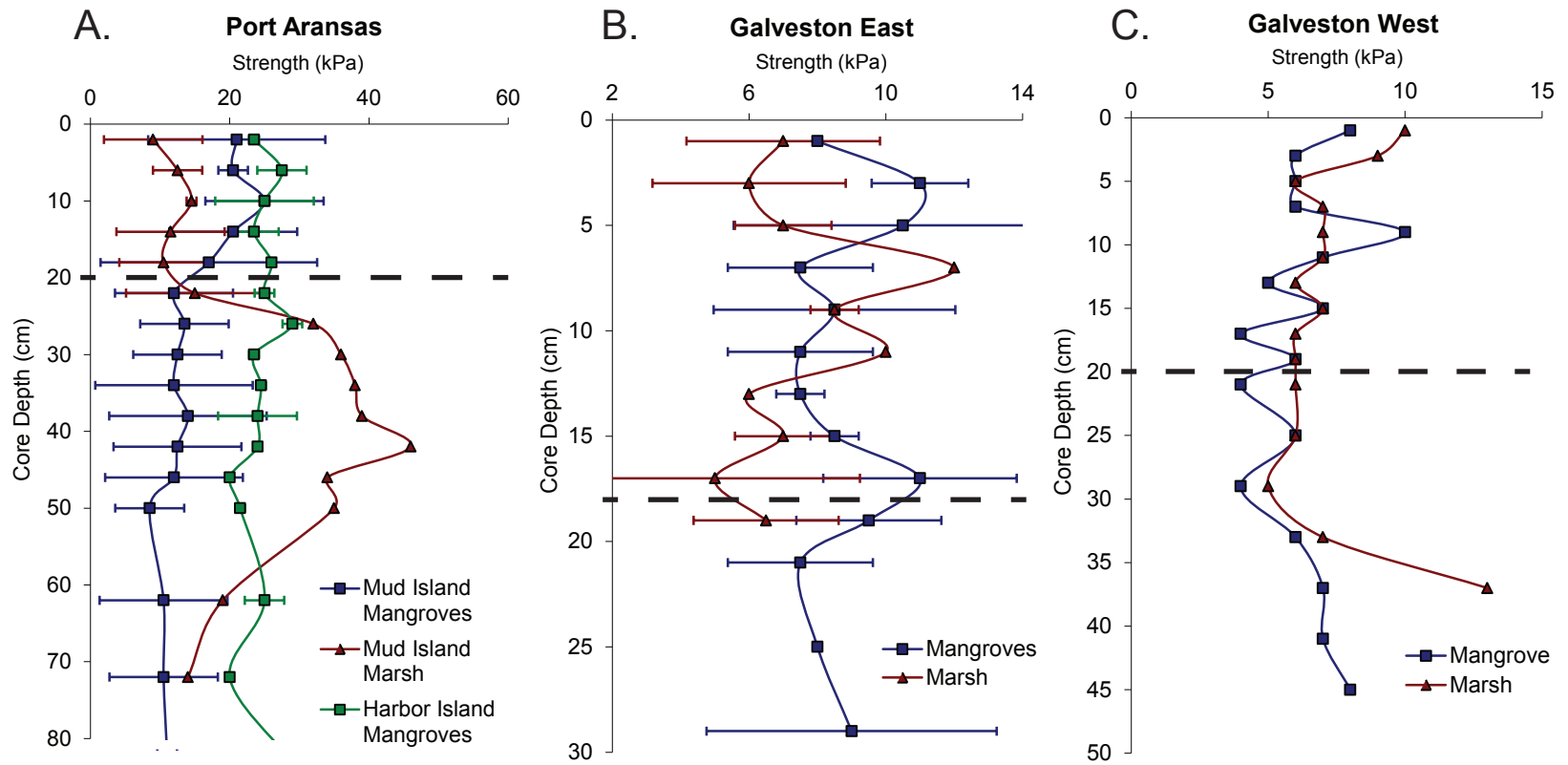
porosities are nearly the same between both wetland types. Mangrove strength values average slightly higher at Galveston East and lower at Galveston West by about 1.0 and 0.8 kPa, respectively (Table 5, Fig. 15B-C and 11B-C).

4.6 PORE WATER GEOCHEMISTRY

4.6.1 Salinity

Soil pore water salinity levels in Port Aransas ranged from values of approximately 60 (Mud Island marsh sediments) to 80 and 140 in Mud Island and Harbor Island mangrove sediments, respectively. Mangrove soil salinity levels remain consistently 10 to 30 higher than marsh salinities throughout the entire core depth (Fig. 17A, Table 6). Harbor Island mangrove pore water salinities, after an initial decrease over the upper 0 to 5 cm, track closely with mangrove salinities from Mud Island (Fig. 17A). Galveston pore water salinities ranged in values of approximately 20 to 40 at the East site and 35 to 85 (mangrove) and 64 to 89 (marsh) at the West site (Fig. 17B). Graphical error was calculated by taking the standard deviation of the averaged core data. Error in Table 6 of rooted and below rooted intervals are the standard deviations of averaged values over those depths.

For statistical comparison, the cores were subdivided into the live rooted interval (outlined in section 4.4) and the deeper core. The live rooted interval was used rather than the organic-rich wetland interval (derived in section 4.3) because active root processes are likely to show the strongest effect on soil pore water properties. At Port Aransas Mud Island, mangrove salinities were higher and statistically significant in both

Figure 17:   Downcore salinity data for Port Aransas (A) and Galveston (B) core locations. (A) Mud Island mangroves (blue squares) and marsh (red triangles) are compared to Harbor Island mangroves (green squares). (B) Galveston mangroves (East closed blue square, West open blue square) are compared to marsh (East closed red triangle, West open red triangle). Dashed lines represent the base of the rooted interval as shown in Fig. 13.
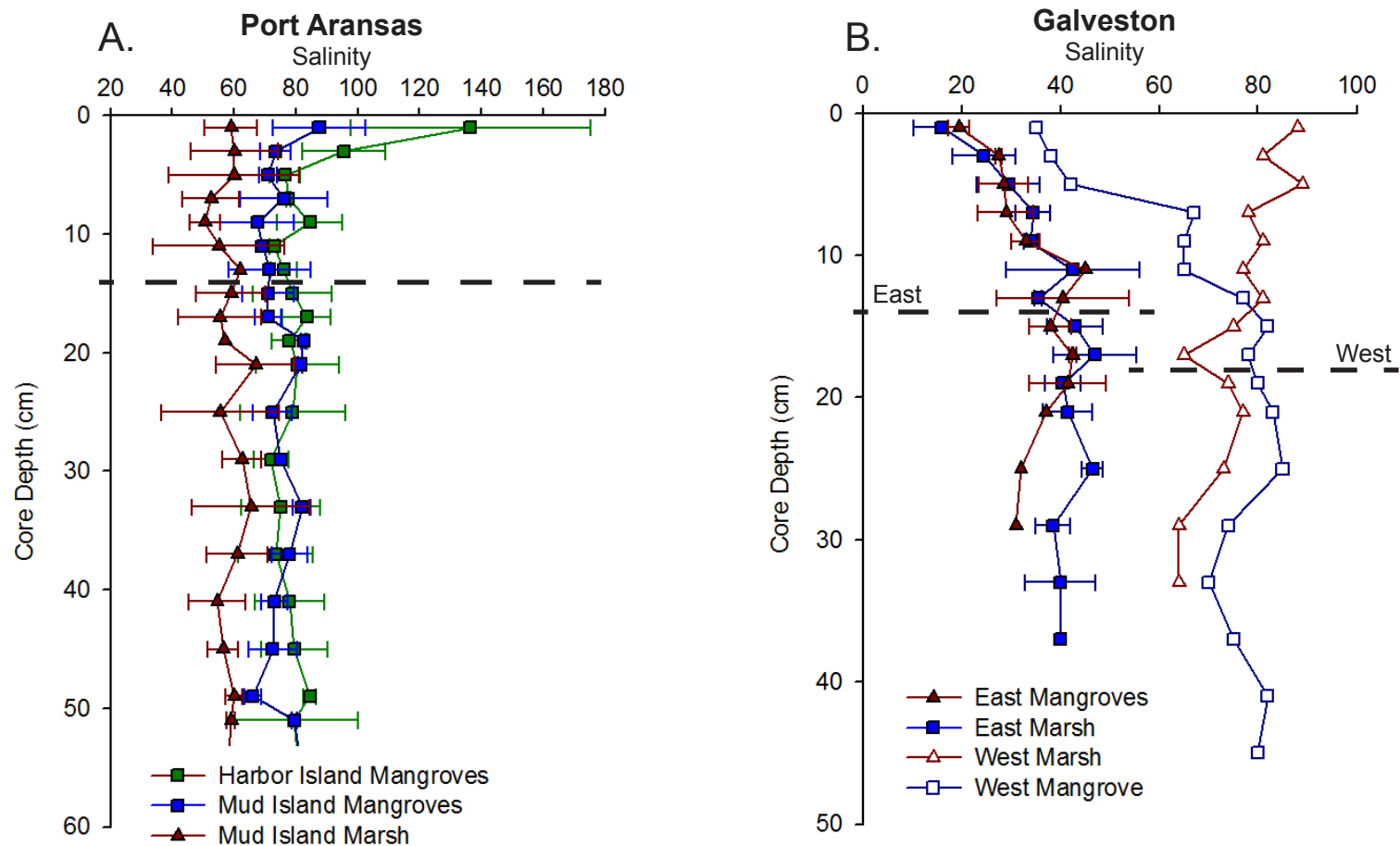
Table 6: Geochemistry averages and statistical *t*-test results calculated over averaged mangrove and marsh core data for rooted and below rooted intervals: Port Aransas=14 cm, Galveston East=14 cm, Galveston West=18 cm. Statistical significance (*p*-value) notated with an asterisk (*). Errors represent standard deviation over averaged core intervals.

Location	Salinity				pH				Redox Potential (Eh)			
	Rooted Interval		Below Rooted		Rooted Interval		Below Rooted		Rooted Interval		Below Rooted	
Port A Mud	Average	*p*-value	Average	*p*-value	Average	*p*-value	Average	*p*-value	Average	*p*-value	Average	*p*-value
Mangrove	73.71 ± 6.69	*0.000	76.19 ± 5.29	*1.436 E-10	8.11 ± 0.82	*0.026	9.01 ± 0.19	0.514	101.70 ± 44.70	*0.038	80.62 ± 30.07	*0.040
Marsh	56.17 ± 4.11		59.39 ± 3.84		9.04 ± 0.27		8.94 ± 0.34		22.11 ± 75.58		12.13 ± 109.58	
Port A Harbor	88.50 ± 22.47	N/A	78.85 ± 3.72	N/A	8.23 ± 0.57	N/A	8.81 ± 0.19	N/A	145.90 ± 45.54	N/A	233.51 ± 15.17	N/A
Mangrove												
Galveston East												
Mangrove	34.06 ± 9.74	0.645	41.17 ± 2.79	0.093	8.67 ± 0.26	0.119	8.98 ± 0.03	*0.022	48.06 ± 32.28	0.343	76.72 ± 50.51	0.551
Marsh	31.86 ± 8.56		37.00 ± 4.74		8.49 ± 0.17		8.87 ± 0.07		33.80 ± 23.45		55.57 ± 34.61	
Galveston West												
Mangrove	62.90 ± 18.09	*0.020	78.43 ± 5.50	*0.037	8.29 ± 0.39	0.805	8.85 ± 0.06	*0.007	131.70 ± 86.13	0.153	254.17 ± 75.40	*0.000
Marsh	79.44 ± 7.14		70.40 ± 6.02		8.25 ± 0.26		8.96 ± 0.05		180.11 ± 47.04		33.04 ± 46.00	

the rooted interval and the deeper interval. No statistical difference between mangrove and marsh salinities exists at Galveston East in either the rooted or deeper intervals. There is a statistically significant increase in Galveston West marsh pore water salinities by an average difference of 16.5 within the rooted interval, relative to the mangroves (Table 6, Fig. 17B). Past this rooted depth mangroves are statistically higher by an average difference of eight.

4.6.2 pH

Port Aransas soil pore water pH values range from approximately 7.0 to 9.0 in mangrove cores and approximately 8.0 to 9.5 in marsh cores. Below the rooted interval, all pH values in mangrove and marsh systems converge and reach relatively stable values within a pH range of 8.0 to 9.0 (Fig. 18A). pH ranges between 8.2 to 9.0 in Galveston East soils and 7.8 to 9.0 in West core data. Galveston East pH gradually increases downcore with a sharp decrease in marsh pH at 13 cm depth (Fig. 18B). Galveston West mangrove and marsh pH exhibit similar patterns and oscillate throughout the rooted horizon; deeper pH levels become steady downcore (Fig. 18C). Graphical error was calculated by taking the standard deviation of the combined 10 measurements for each set of averaged core data. Error in Table 6 of rooted and below rooted intervals are the standard deviations of averaged values over those depths.

Port Aransas Mud Island mangrove and marsh pH in soil pore waters are statistically different, with a lower pH in mangrove cores in the rooted interval; Harbor Island mangroves lie within a similar pH range as Mud Island mangroves (Fig. 18A,

53

Figure 18: Downcore pH data for Port Aransas (A) and Galveston East (B) and West (C) core locations. (A) Mud Island mangroves (blue squares) and marsh (red triangles) are compared to Harbor Island mangroves (green squares). (B-C) Mangrove and marsh cores are represented with closed blue squares and red triangles, respectively. Dashed lines represent the base of the rooted interval as shown in Fig. 13.
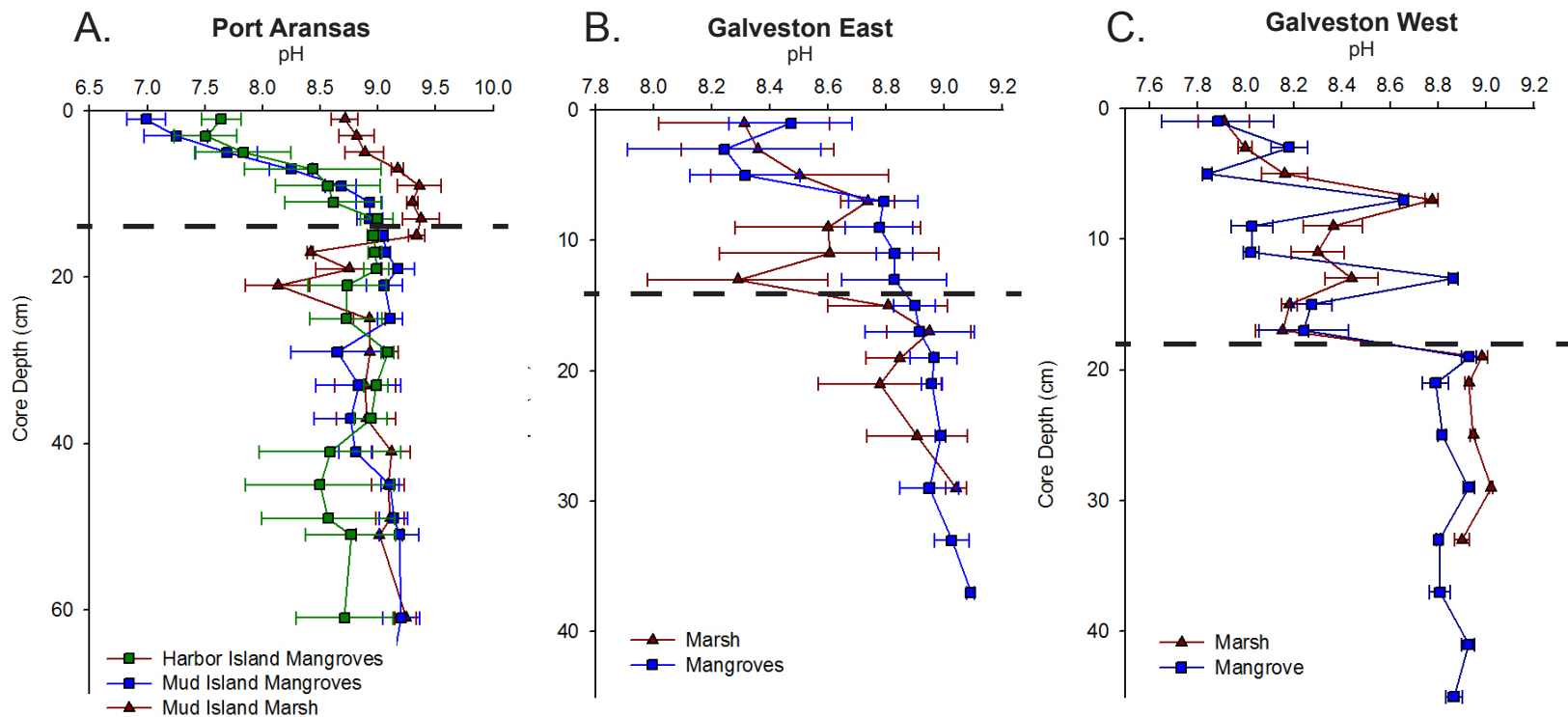
Table 6). No statistically significant difference exists between marsh and mangrove pH throughout rooted intervals at either Galveston location, however there appears to be statistically higher mangrove pH at Galveston East and lower mangrove pH at Galveston West in deeper post-rooted depths (each is only a difference of 0.1 pH, see Table 6).

4.6.3 Redox Potential (Eh)

Redox potential (Eh) values in soil pore waters at Port Aransas range from -248 to 270 mv: Mud Island marsh values range from -248 to 107 mv, while Mud Island mangrove values range from 27 to 158 mv compared to 75 to 270 mv in Harbor Island mangroves. Mud Island soils exhibit a gradual decrease in redox potential over the rooted interval, with the exception of a sharp Eh decline in Mud Island marsh soils at 14 cm depth. In Harbor Island mangrove soils, a sharp decrease in Eh over the upper eight cm is followed by rapid Eh increase from eight to 16 cm. Below 20 cm depth, redox values merge and stabilize around zero to 150 mv (Mud Island sediments) and 200 to 270 mv (Harbor Island sediments) (Fig. 19A). Galveston East pore water redox potentials oscillate within a range of approximately -15 to 150 mv throughout the entire core. Eh values exhibit a wide range of approximately -60 to 400 mv (mangrove core data) and -40 to 260 mv (marsh core data) at Galveston West. Values appear to trend in opposite directions between the two systems (Fig. 19B). Redox potential error is calculated in the same method as pH error in 4.6.2.

There is statistical difference between Mud Island mangrove and marsh pore water redox potentials in both the rooted and below-rooted intervals; mangroves exhibit

Figure 19:   Redox potential (Eh) with depth in cores in Port Aransas (A) and Galveston (B) sediments.   A) Mud Island mangroves (blue squares) and marsh (red triangles) are compared to Harbor Island mangroves (green squares). (B) Galveston mangroves (East closed blue square, West open blue square) are compared to marsh (East closed red triangle, West open red triangle).   Dashed lines represent the base of the rooted interval as shown in Fig. 13.

A.   **Port Aransas Redox Potential**

B.   **Galveston Redox Potential**
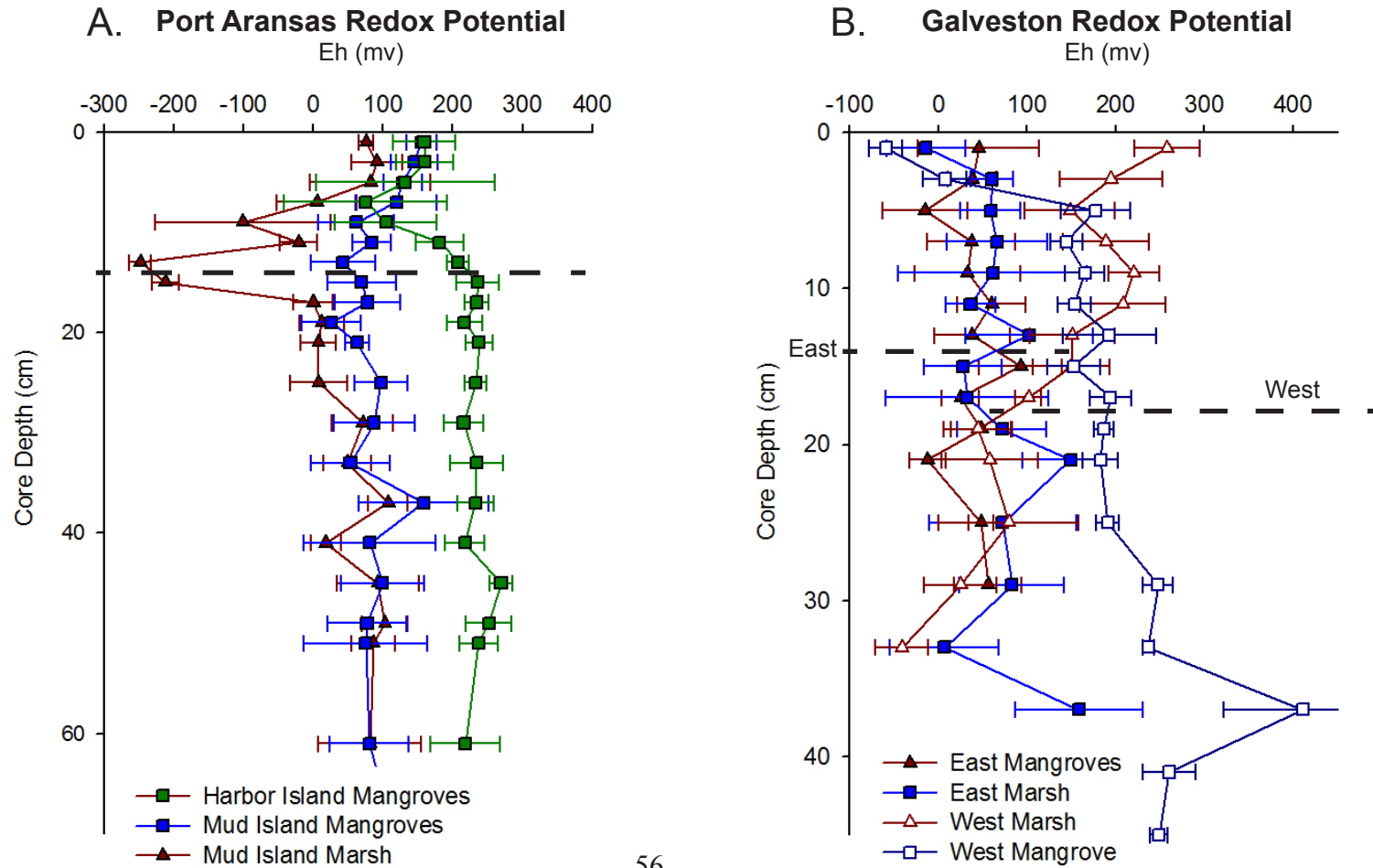
higher (more positive) redox values within the rooted horizon compared to deeper intervals and are substantially greater than marsh values over the same depth (by an average of approximately 80 mv over rooted interval and 68 mv below rooted). Harbor Island mangroves exhibit even higher Eh values than mangroves at Mud Island (by an average of approximately 44 mv within rooted zone) however redox potentials appear to actually increase with depth (Fig. 19A, Table 6). No statistical distinction is present between mangrove and marsh soils at Galveston East, but mangrove soils are on average higher in redox potential. At Galveston West mangroves are statistically higher in Eh than marsh values by an average of 221 mv below rooted depths. As in Harbor Island soils, redox potentials within Galveston mangrove pore waters appear to increase with depth (Fig. 19B, Table 6).

CHAPTER 5

Discussion

5.1 RESISTANCE TO SEA LEVEL RISE

Eustatic sea levels are projected to rise from 20th century rates of 0.17 ± 0.05 cm/y to approximately 0.4 cm/y over the 21st century (IPCC, 2007). Present estimates of the rates along the TX Coast are 0.3 to 0.6 cm/y with the highest rates of 0.68 cm/y occurring in Galveston (NOAA Tides and Currents, 2006). The increase in rates at Galveston relative to other areas of the TX coast is linked to subsidence from groundwater withdrawal: rates reach a maximum of 1.6 cm/y or more at Virginia Point, an area situated northwest of Galveston West and East site locations (White and Tremblay, 2002). Accelerating sea level rise likely will result in submergence (or retreat) of coastal saline wetlands in the Gulf and elsewhere where the combined effects of mineral and organic accumulation and root volume soil displacement cannot keep pace.

Wetland loss patterns are indicators of where wetlands are already not keeping pace with relative sea level rise rates in the Gulf of Mexico and elsewhere, although these patterns are complicated by other natural (e.g., wave attack, etc.) and anthropogenic (e.g., fluid withdrawal, canalization, urbanization, etc.) factors. The highest rates of wetland loss in the U.S. are present in the Mississippi deltaic plain in Louisiana, where rates average 26 to 30 km^2/y (Barras et al., 2003). Outside of clearly anthropogenic causes like canalization, the bulk of this loss during the decade 1990 to 2000 has been attributed to

58

shoreline retreat from wave attack (Wilson and Allison, 2008), and interior ponding. The latter has directly been attributed to failure to keep pace with relative sea level rise, due in part to starvation of riverine mineral input and rapid compactional subsidence (Penland et al., 2000). Future wetland loss in Louisiana is projected as a net total of 1,329 km^2 over the period of 2000 to 2050 (Barras et al., 2003). In south Texas, a coastal vulnerability index (CVI) developed by Pendleton et al. (2004) predicts an average CVI of 11.27 (high ranking) for Padre Island, with this zone of higher erosion vulnerability extending north to the Corpus Christi-Port Aransas region. An estimated 10,700 ha of wetlands were permanently lost in the Galveston Bay area from the 1950's to 1989, a rate that doubled over the period from the 1930's to 1950's, and has primarily been attributed to anthropogenic subsurface fluid withdrawal. Since the 1970's wetland loss rates have declined in the Galveston Bay region due to a cessation of fluid withdrawal (White and Tremblay, 2002). More than 2,000 ha of wetland loss in the Galveston and Corpus Christi Bay areas (study area locations) occurred in the fluvial-deltaic (bay head) systems of the Trinity, Lavaca-Navidad, and Nueces Rivers in the 1950's to 1980's, with an estimated loss of 130 ha (8 ha/y) within the Nueces system (near Port Aransas, Texas). Continued wetland loss is predicted in these bay systems because aggradation rates are hypothesized to be unable to keep pace with future rates of relative sea level rise in the area (White et al., 2002).

Locally higher elevations are observed in mangrove vegetated areas at Port Aransas Mud Island. Mangroves are on average four cm higher in elevation than surrounding marsh and one to two cm higher at several points where single mangroves

are found in a marsh patch (Fig. 7, Table 1). Although no statistically significant elevation differences are observed at the Galveston sites, averaged mangroves values are slightly higher than adjacent marshes (Table 1). Pre-existing geomorphology appears to be a strong control on the elevation patterns observed at the Galveston field sites. At Galveston East, >90 percent mangrove concentrations grow along a topographic swale (Fig. 8), while the small patch of mangroves at Galveston West (Fig. 9) occurs along a topographically high island rim levee. In general, significant elevation gain is concentrated within the more mature (1 to 2 m high and high tree density) mangrove systems at Port Aransas (Fig. 7), relative to shorter stature (30 to 50 cm) and lower tree densities observed at the Galveston sites. This suggests a greater age for the Port Aransas mangrove colonies. This age difference is likely a combination of two factors: proximity to established seed colonies, and the faster recovery of Port Aransas mangroves to freezing episodes in the 1980's (Everitt et al., 1996). Evidence for the former factor is apparent in that most back-barrier colonies are found adjacent to tidal inlets in the coastal barrier, suggesting that coastal currents are an important seed dispersal pathway (Rabinowitz, 1978; Krauss et al., 2008). Sherrod and McMillan (1981) found that even larger trees (less than 1 m in height) in Galveston were only seven years old (although determining age from mangrove wood can be difficult due to non-seasonal habitats; Tomlinson, 1986).

A final factor in establishment of new colonies may be that settlement of the waterborne seeds preferentially takes place along local elevation highs during tidal or storm inundation. The floating seeds require quiescent settings to enable sufficient time

for them to take root (Rabinowitz, 1978; Sherrod and McMillan, 1985). A recent study by Perry and Mendelssohn (2009) examined mangrove expansion into a salt marsh in the Mississippi delta in Louisiana and attained comparable elevation results to the present study. Averaged mangrove elevations were found to be slightly higher than in adjacent salt marshes, however accretion rates were found to be similar between the two systems, which led them to suggest initial establishment took place at a previously elevated site. No differences were found in organic matter content (Perry and Mendelssohn, 2009).

Possible reasons for different results of accumulation rates and organic variability between Louisiana and Texas studies include the use of different methodologies in accumulation rate and organic calculations, sediment substrate, and the age of the mangrove systems. Dating techniques used by Perry and Mendelssohn (2009) involved a single core utilizing the ^{137}Cs 1963 peak, whereas this study calculated rates for both 1954 and 1963 ^{137}Cs horizons as well as ^{210}Pb rates from two cores for every field site. Calculation of organic content also varied between studies; this study calculated sieved and dried weights of live root organics as well as organic loss on ignition, while the Louisiana study calculated subsurface biomass using in-growth core methods. Sediments in the Louisiana study were silt/clay rich (~70 percent) compared to Texas sediments (30 to 40 percent). Calculations in the Texas study were further differentiated into wetland and pre-wetland and rooted and non-rooted intervals. Finally, mangroves in Port Aransas, Texas may be more mature than those in the Louisiana study. Mangroves in the Louisiana study are likely more comparable to the Galveston sites than the more mature

61

Port Aransas setting as they are young (13 to 15 years old) and cover an aerial extent of only 28 to 50 m^2 (Perry and Mendelssohn, 2009).

Total (mineral + organic) sediment accumulation is consistently higher in averaged mangrove ^{210}Pb and ^{137}Cs (1963) rates at each Port Aransas and Galveston locality. Mangrove increases in sediment accumulation are statistically significant only at Port Aransas Mud Island in rates utilizing ^{137}Cs (1963) peak data. Although this statistical difference is only apparent in ^{137}Cs (1963) calculations (Table 2), these rates are more reliable than 1954 rates because the data differences in activity in the peak method are several tenths of a dpm/g, while the depth limit (1954) method relies on very low changes in activity near the detection limit (<0.02 dpm/g). ^{137}Cs (1963) rates are also more consistently comparable at each field location with ^{210}Pb rates. This is an important support for the ^{137}Cs (1963), given that Cs is capable of desorption and migration in the presence of varying pore water salinities, unlike Pb (Santschi et al., 1983). A reliance only on ^{210}Pb sediment accumulation rates is also not possible due to the presence of several cores with poor R^2 fits to the decay profile (Fig. 10). Variable grain size may explain the low R^2 values within ^{210}Pb data from Galveston West cores (Fig. 14B). If ^{137}Cs (1963) dates are more reliable indicators of sediment accumulation over ^{137}Cs (1954), then increased mangroves rates are present at Galveston West as well (no statistical comparison because of single cores at this site). In general, the greatest differences in accumulation between mangrove and marsh systems is present at Port Aransas, where the mangroves are more mature and developed compared to Galveston systems (Table 2).

62

Percent organic matter is lower in the organic-rich mangrove soil interval at all three sites but only statistically significant at Port Aransas Mud Island (Tables 2 and 3). This increase in the marshes may be ascribed either to higher deposition rates of grass litter or lower soil decomposition rates relative to the mangrove areas: higher redox potentials found within oxygenated mangrove soils at this location may increase decay rates in mangrove organics (further discussed in section 5.3 and 6). While this organic increase in marsh sites is a component of the total accumulation measured by the radiotracers (Pb and Cs), observed percent organic matter content is so low (<2 percent) that most of the observed elevation gain and increased accumulation rates at the mangrove sites can be confidently ascribed to increased mineral trapping. Given the increased barrier to flow during submergence episodes provided by the larger and denser mangrove stands at Port Aransas, it is to be expected that this differential would be most noticeable at this site. Interestingly, this increased trapping does not extend to any significant difference in the grain size character of the trapped particulates – which may reflect the limited grain size range of suspended material in these back-barrier settings.

Increased percent live rooting, which can be assumed to relate to increased root volumes, is also present in the mangrove colonies relative to adjacent marshes. Higher live rooted volumes within mangroves may increase elevations through soil displacement outward and upward with growth (Wells and Coleman, 1981), and the ability of the aboveground root complex to bind and trap sediment (Scoffin, 1970, referencing *Rhizophora mangle*). Averaged live rooting percentages are consistently higher in mangrove sediments at every location, with statistically significant higher volumes at

63

Port Aransas and Galveston West sites (Table 4). However, since percent live root organics are low (Fig. 13), this is likely a relatively small factor in elevation increase relative to mineral trapping. This may represent only a fraction of true live root volumes as cores were extracted from single-spot locations and mangrove roots are laterally extensive and complex by nature (Tomlinson, 1986) compared to salt marsh grasses.

Even if periodic freezes along the Texas coast occur in the future with climate amelioration, albeit with a reduced frequency, it is important to note from the present results how rapidly mangrove colonies can impact sediment accumulation rates and elevation. Mangrove colonies have been expanding along the Texas coast over the past 20 to 26 years (at least in Port Aransas) since the last major freezes of 1983 and 1989 (Sherrod and McMillan, 1985). An average accumulation increase of 0.19 to 0.56 cm/y within mangrove sediments (Table 2) would locally increase elevations by 1.0 cm in 1.8 to 5.3 years and by approximately 4.0 to 15 cm in 20 to 26 years (assuming immediate colonization). In Port Aransas, averaged increased mangrove elevations of 4.0 cm and increased average sediment accumulation rates of 0.28 to 0.56 cm/y relative to adjacent marshes will have a significant advantage over lower-lying marsh vegetated areas at present rates of relative sea level rise for this section of the TX coast (0.3 to 0.6 cm/y, NOAA Tides and Currents, 2006). These rates can also be utilized to estimate the relative importance of mineral trapping versus root displacement: an average (maximum) elevation increase of 4.0 cm in the approximate 20 to 26 year age of Port Aransas mangroves (calculated from freeze incidents of 1983 and 1989) yields a total increase in accumulation rate of 0.2 cm/y, closely approximating the 0.28 to 0.56 cm/y differential in

mangrove: marsh sediment accumulation rates in the area, and suggests that live rooting is a less important factor in increased elevation of mangrove areas. It should be noted that these rates are based on 60% soil porosity: the higher porosities characteristic of the wetland soil interval at Port Aransas (Fig. 15A) suggest that this elevation differential will be even higher. Rates of relative sea level rise are higher in Galveston (0.68 to 1.6 cm/y; White and Tremblay, 2002; NOAA Tides and Currents, 2006), making this factor less important here in ultimate wetland survival. Maximum accumulation rates of Texas mangrove systems remain unknown given their present relatively juvenile stage, but can be expected to continue to increase trapping efficiency and leaf litter fall as tree size and colony density increase with age. It is clear however, that mangrove wetlands rapidly develop higher soil elevations that will be competitively advantageous with the predicted ESLR acceleration in the 21st century.

5.2 RESISTANCE TO WAVE ATTACK

Changing future climate is also predicted to enhance weather extremes and to increase cyclonic storm frequency and intensity (IPCC, 2007). Increased wave attack associated with more frequent and stronger tropical landfalls may be expected to cause an increase in wetland loss rates along coastal saline wetland shorelines. Hurricane landfalls in the Gulf of Mexico have increased over the past 40 years, from eight major hurricanes that occurred during 1968 to 1994 to 14 hurricanes occurring over the period of 1995 to 2008 (Poore et al., 2009). The index of cyclonic destructive potential, based on the total dissipation of power over the lifetime of a cyclone, has increased significantly since the

1970's as a result of longer storm lifetimes and greater intensities; potential hurricane destructiveness may increase with climate warming (Emanuel, 2005). Wave energy is related to the square of the wave height, which determines the amount of sediment mobilization and transport (Pendleton et al., 2004). In general, wave erosion of wetland shorelines is minimal with wave heights less than 0.17 m and significant at heights greater than 0.3 m (Ravens et al., 2009). There is also a positive feedback in that increased open water fetch associated with retreating wetland shorelines can be expected to lead to greater wave height at the shoreline (Scavia et al., 2002).

Direct evidence of the mechanisms and magnitude of wetland loss from cyclonic storms has been recorded for recent Gulf hurricanes. Hurricane Ike in 2008 made landfall with hurricane force winds along a 180 km segment of the upper Texas coast with maximum hurricane wind speeds of 175 km/hr, storm surges up to 5 m, and a maximum (offshore) wave height of 6 m. Hurricane Ike generated 50 to 150 m of barrier beach shoreline erosion, with an extreme 3.0 m elevation change at Bolivar (area of maximum devastation) and 30 cm of elevation change near Galveston, Texas. Overall damage consisted of beach erosion, shoreline retreat, scarping of dune faces, sand deposited inland from shoreline, and distressed vegetation (Doran et al., 2009). The surge from Hurricane Ike developed new and expanded on previously formed interior marsh ponds. Preliminary estimates indicate this storm was responsible for >405 ha (~4 km^2) of marsh loss in Louisiana. In addition to wetland interior ponding, anastomosing channels were generated through intermediate marsh areas. This event distressed wetlands which were still recovering from previous hurricanes (Barras, 2009). In 2005

hurricanes Rita and Katrina were responsible for approximately 562 km^2 of wetland loss in the Mississippi delta of Louisiana. Lost wetlands included 324 km^2 of fresh, 259 km^2 of intermediate, 104 km^2 of brackish and 78 km^2 of saline marshes (Barras, 2006). Much of this loss was in two forms: marsh shoreline edge retreat from wave attack in regions subjected to the largest waves, and loss of inland, fresher marshes adjacent to the Mississippi River. The latter were high organic, low mineral marshes and experienced rip-up of the entire organic mat. These observations suggest strong variability in loss is induced by factors such as sediment strength and organic content as well as degree of exposure to waves.

Resistance to wave attack at wetland shorelines may be expected to be directly related to soil strength, which is itself controlled by degree of consolidation, grain packing and size, organic content, and the binding properties of roots. As discussed in section 5.1, live rooting in the upper organic-rich sediment interval (Fig. 13) is consistently higher in mangrove soils at all sites, with statistically significant higher volumes at Port Aransas Mud Island and Galveston West sites (Table 4). Direct measurements of soil strength made in the present study correlate in part with the most densely rooted intervals. Strengths are on average higher in mangrove sediments in the more mature Port Aransas site, and indistinguishable at the Galveston sites (Table 5). Porosities are statistically lower in mangroves over wetland soil intervals at Port Aransas ((Fig. 16A, Table 5) and are clearly a contributing factor to observed increases in soil strength in addition to increased rooting density. No variation in porosity is observed over wetland soil intervals at the Galveston sites, however intervals enriched in silt/clay

in Galveston West marsh sediments below 24 cm depth correspond to increased marsh strength (Fig. 14B, 11C), demonstrating the importance of grain size as well as porosity and rooting on sediment strength.

A study by Feagin et al. (2009) emphasizes that wetland soil strength and erosional patterns are dependent on the size and type of organic material present in addition to the soil type. Finer organics (such as the finer root matrix in mangrove root systems) are believed to moderate erosional impact, whereas larger plant fractions may heighten erosion (McKee and McGinnis, 2002; Feagin et al., 2009). The type of soil does not appear to effect patterns in strength or porosity differences between the two wetland types because there is no statistical variation in grain size over upper wetland intervals. Perry and Mendelssohn (2009) found no statistical variance in grain size and slightly lower porosities within mangrove sediments in their Mississippi delta wetland comparison, consistent with results from this study. The absence of distinct sediment strength and porosity trends in Galveston mangroves may once again be attributable to the relative youth of these systems. Inconsistencies may also be influenced by local changes in geomorphic conditions.

Feagin et al. (2009) concluded that coastal vegetation may better serve as a defense against continual sea level rise and tidal action as opposed to breaking waves. An inadequate sediment supply combined with a high relative sea level rate is suggested as the primary cause for salt marsh shoreline erosion rather than wave height in West Bay area (Fig. 5) near the Galveston West study site (Ravens et al., 2009). These studies examined salt marsh vegetation specifically and do not take mangrove presence into

68

consideration. One important difference between mangrove and salt marsh vegetation to consider during storms and wave inundation is that mangroves are physically taller and stronger structures compared to salt marsh grass stems. Numerous studies have demonstrated the ability of mangroves to dissipate wave energy during storm events (Mazda et al., 1997; 2006; Massel et al., 1999; Quartel et al., 2007; Tanka et al., 2007). The density and diameter of roots and trunks in a mangrove forest were shown to strongly affect the rate of wave energy attenuation and drag (Massel et al., 1999). Mazda et al. (2006) demonstrated the ability of mangroves to substantially damp wave energy during storms dependent on wave height, water level, and mangrove species and vegetative condition. Mangroves are believed to provide coastal protection by inducing drag forces and friction through their complex rooting network of trunks, branches, and aerial roots (Quartel et al., 2007; Tanka et al., 2007).

A final factor to consider regarding storm resistance is the geomorphic setting of a wetland area. The sand-dominated back-barrier island settings of this study exhibit a limited range of grain size and organic content. Stronger heterogeneity in grain size may be expected in deltaic settings where mud-rich suspensions are supplied from the river. Resulting differences in soil fertility (due to grain size and dissolved nutrients delivered by river water) may also impact growth rates of the mangroves. Further, wetland substrates in the Mississippi delta region tend to be relatively starved of mineral sediment, leading to organic contents of approximately 30 percent (Wilson and Allison, 2008), which may further impact soil strength. As mentioned previously, although it was

69

not associated with floral type, increased soil strength at Galveston West appears to correlate with an increase in the fine clay and silt fraction (Fig. 14B, 11C).

5.3 **ALTERATIONS TO SOIL GEOCHEMISTRY AND IMPACT ON ORGANIC CARBON**

SEQUESTRATION

If mangroves continue to expand in the Gulf of Mexico and elsewhere at the expense of salt marsh habitat in the 21st century, observed subsurface changes in geochemistry may affect diagenetic processes and carbon storage. The more mature mangrove systems at Port Aransas that have persisted and recolonized through periods of dieback over the past century (Sherrod and McMillan, 1981) exhibit increased pore water salinities, more acidic pH, and increased redox potentials relative to adjacent marshes. Increased salt build up in Port Aransas mangroves may limit transpiration activity and subsequent carbon gain (Passioura et al., 1992). Differences in soil pH and Eh, in addition to affecting diagenetic remineralization rates of organic matter, may also selectively alter the character of organic matter sequestered, which, if eroded and supplied to the estuary, could have an impact on estuarine food webs as significant as the direct input of leaf litter (mangroves) vs. grass stems (salt marsh).

In Port Aransas mangroves, pore water pH is significantly more acidic in the rooted zone but similar to marsh values below this interval (Fig. 18A). Redox potentials in Mud Island mangroves are significantly greater over the entire core interval, with higher values contained within the zone of active root growth. Lower pH may result from rooting activity, negative correlation to redox potential, organic decay, or a

combination of the above. pH produces significant effects on the chemical solubility (ion exchange), nutrient availability, and organic matter decomposition in soils (McCauley et al., 2003). Cation availability and ion exchange are directly related to pH; basic cations (Ca, Mg, K, Na) are less likely to be exchanged or leached when pH is higher, whereas lower pH increases the amount of hydrogen ions available for exchange and releases cations into the soil water. Nutrients are most available in pH ranges of 6.5 to 8 (macronutrients: N, K, Ca, Mg, S) and 5 to 7 (micronutrients: B, Cu, Fe, Mn, Ni, An). Nutrients exist in smaller amounts and are more difficult to exchange outside these ranges. Highly acidic soils (pH of 5 or lower) exhibit low levels of microbial activity, which in turn may affect organic decomposition (McCauley et al., 2003). If mangrove expansion continues, pH may be lowered over a wider region, significantly affecting the surrounding biota and soil diagenesis.

Pore water pH variation in Galveston site soils exists in the below-rooted depths only, where it is statistically higher in East and lower in West mangroves. No significant Eh variation occurs at Galveston East, but mangroves exhibit statistically higher Eh at West over the deeper core and significantly lower Eh in the upper four cm (Table 6). Observed increases in Eh over the deeper core in Galveston West mangroves (Fig. 19B) may result from increased oxygen transport via water migration through the more permeable sand layers located below 20 cm in the mangrove core (Fig. 14B). Increased tidal flushing and drainage were surmised to increase oxygen availability in a salt marsh stand located on the Georgia coast in a study by Wiegert et al. (1983). Lack of observed

Port Aransas geochemical trends at Galveston sites are probably the result of the relative youth of these colonies.

Lower pH and increased Eh may affect the oxidation and degradation of organic matter during diagenetic reactions and whether sulfur oxidation or sulfur reduction is the dominant organic decay process. The observed increase in acidity in Port Aransas mangrove pH's may be explained by organic matter decomposition and associated sulfur oxidation, which acidifies sediment and lowers pH (Marchand et al., 2004) with the production of sulfuric acid (Twilley and Rivera-Monroy, 2009). This occurs as sulfides oxidize and produce substantial quantities of sulfuric acid during sediment transitions between reduced and oxidized zones, via the following reactions: $FeS_2 + 7/2O_2 + H_2O \rightarrow Fe^{2+} + 2SO_4^{2-} + 2H^+$, and $FeS_2 + 14Fe^{3+} + 8H_2O \rightarrow 15Fe^{2+} + 2SO_4^{2-} + 16H^+$ (Singer and Stumm, 1970; Clark et al., 1998; Twilley and Rivera-Monroy, 2009). Although sulfate reduction may dominate early diagenetic processes in mature mangrove systems and is higher in salt marshes than in mangrove sediments (Alongi, 1998), the introduction of oxygen into the sediment via rooting may increase aerobic respiration and associated sulfur oxidation to the point that it dominates organic decay processes in young forests (Alongi et al., 1998; 2000). Rates of salt marsh and mangrove organic decay are similar (Alongi, 1998), but higher live rooted volumes and woody material may lengthen the duration of mangrove decomposition and promote reduced pH compared to marsh systems at Port Aransas. pH may also be lowered if there is an uptake of NH_4^+ or via root respiration of CO_2 (Alongi et al., 1998).

A negative correlation between pH and Eh exists as suboxic decay of organic matter lowers sulphur content, increases Eh, and depresses pH (Marchand et al., 2004). Increased Eh over the rooted interval in Port Aransas Mud Island mangroves agrees with increased acidity and is attributed to the ability of mangroves to oxidize sediments as roots translocate oxygen from the atmosphere to the sediment through aerial root (pneumatophore) gas exchange (Andersen and Kristensen, 1988). Higher elevation and better drainage may also contribute to increased Eh observed in mangroves (Perry and Mendelssohn, 2009). A slight Eh depression over depths of approximately 2 to 14 cm and 4 to 10 cm in Mud Island and Harbor Island mangrove sediments, respectively, corresponds to an upper reduction zone geochemical model of mangrove oxidation (Clark et al., 1998) linked to maximum root abundance (15 to 38 cm deep in the model). As discussed previously, measured live root depths at Port Aransas may not fully represent maximum depths of rooting. Increased oxidation promotes aerobic respiration and sulfur oxidation during organic decay, which may lower sulfide levels in surrounding pore waters (Bianchi et al., 1999). A correlation between higher redox potentials and lower sulfide concentrations was found near the aerial roots in *Rhizophora mangle* and *Avicennia germinans* mangroves (McKee et al., 1988).

Higher redox potentials observed within mangrove sediments at Port Aransas may partly explain why mangroves appeared healthier compared to the brown, senescent appearance of salt marsh (Fig. 6B). This marsh character may also be a function of exposure to hypersalinity as discussed below. Low Eh, observed over depths of 10 to 18 cm in Port Aransas salt marsh (Fig. 19A), inhibits root growth and photosynthesis in

Spartina (Pezeshki, 1997). Although strong evidence exists within the more mature Port Aransas mangroves to suggest oxidation of the sediment associated with live rooting activities, and is supported by other studies (Scholander, 1955; Thibodeau and Nickerson, 1986; Andersen and Kristensen, 1988, McKee et al., 1988), this trend was also observed in a salt marsh study by Howes et al. (1981). Eh was oxidized over depth ranges of 10 cm containing the largest volume of live rooted biomass compared to sediments lacking salt marsh. There was a larger increase in Eh in sediment from tall versus short grass. A positive feedback loop is suggested of higher oxidation increasing plant production which further oxidizes sediment (Howes et al., 1981). No evidence of salt marsh oxidation within the rooting zone is observed in Port Aransas however Galveston West marsh exhibits high Eh values over the suggested rooted depth of 10 to 15 cm (Fig. 19B). If salt marsh does indeed locally increase Eh over shallow rooted depths, more mature mangrove systems appear to do this to a greater extent and possibly over deeper subsurface intervals (marsh live root depths range from 10 to 20 cm (Howes et al., 1981; Blum, 1993; Ravit, 2006) compared to mangrove depths of 3 to 45 cm (root exchange, gas activity) and 10 to 15 cm (feeding/drinking roots) (Passioura, 1992; Clark et al., 1998; McKee, 2000; Marchand et al., 2004).

Pore water salinities are higher over entire core depths in Port Aransas mangroves relative to adjacent marshes, with similar average values above and below the rooted zone (Fig. 17A, Table 6). No statistically significant difference in pore water salinity exists at Galveston East, and at Galveston West salinities are lower in mangrove rooted intervals (possibly complicated by grain size) and statistically divergent over entire core

depths. Again, differences in Port Aransas and Galveston systems are likely attributed to the maturity of mangrove colonies and their ability to impact soil salinities. A study by Passioura et al. (1992) suggests that mangroves may salinize the soil via transpiration activity, which excludes salt content as water is conducted through the root system. Because salinity trends in Port Aransas mangroves extend past the rooted interval, increased salinities cannot be attributed to this factor alone. Another component to consider when observing higher salinities within mangrove core data is the presence of mangrove trees in a wetland setting. Plants with low transpiration rates (associated with high salt concentrations) may develop in poorly flushed intertidal environments (Passioura et al., 1992) where salt buildup may increase over time. Mangroves may be subjected to more evaporation in a higher topographic setting as rain water is transported to lower areas in the region. A study by Marchand et al. (2004) in French Guiana observed basal salinities that were either greater or equal to surface salinities over mangrove core depths during a dry season with minimal freshwater input; lower surface salinities were attributed to rainfall and inundation by low salinity coastal waters. Unable to explain increased salinities over deeper core intervals with transpiration processes (which occur in the upper 30 cm of cable root activity), they suggested a density driven convection process which diffuses surface salt accumulation downward. High salinity levels in Port Aransas mangroves are most likely attributable to a combination of rooted salt build up (Passioura et al., 1992) and density driven convection processes (Marchand et al., 2004). Although averages in Table 5 indicate no differences between salinities in rooted versus lower depths at Port Aransas Mud Island, the highest salinities occur in the

75

upper 6 cm. High surficial salt concentration combined with permeable sand layers should make density driven convection possible.

Avicennia are known to have a wide tolerance to salinity variation and can persist in hypersaline environments (Sherrod and McMillan, 1985). Pore water salinities in well-developed mangrove forested areas were found to be significantly higher than in sediments where mangroves were lacking (Smith, 1987). Typical trauma to plant biochemical processes induced from hypersalinity is not commonly observed in *Avicennia*, however it may cause physically shorter stature of trees by inhibiting water uptake and reducing growth (Krauss et al., 2008). Concentration of salt along the root margins can also occur quickly relative to the lifespan of an individual tree and may limit transpiration rates (Passioura et al., 1992). In contrast, *Spartina* is highly sensitive to hypersalinities, which may limit marsh growth and height (Howes et al., 1981). Louisiana has had recent episodes of "brown marsh" where massive salt marsh dieback events take place in a season (McKee et al., 2004). Possible triggers are thought to include extended periods of drought, high pore water salinities, heat, evaporation and low river discharge, but mangroves were observed to remain unharmed by these conditions (Coastal Wetlands Planning, Protection and Restoration Act Task Force, 2000; McKee et al., 2004). Although higher salinities may reduce overall mangrove growth, existing data suggests mangroves appear to have a competitive advantage in high pore water salinity settings. By actively increasing pore water salinities, they may in effect "poison" *Spartina*, allowing for more rapid expansion in favorable climatic conditions.

Carbon storage in Gulf coastal estuaries may change with continued mangrove expansion. Averaged soil organic content is consistently higher in marsh sediment, particularly in Port Aransas where mangroves are further developed, suggesting reduced carbon sequestration with mangrove dominance. Conversely, higher redox potentials in mangrove sediments, which reflect the presence of oxygen, may have a positive increase on plant production. Oxygen is essential for nutrient uptake and root growth, which promote plant productivity and carbon assimilation (Howes et al., 1981; Pezeshki, 1997). Organic accumulation is impacted by levels in pH and Eh, which control the rates of organic decay. Lower pH and higher Eh found within Port Aransas mangrove sediments may correlate to increased suboxic decay of organic material. The Mississippi delta mangrove: marsh comparison study by Perry and Mendelssohn (2009) found an increase in cellulytic degradation in mangroves compared to salt marshes, with both leaves and roots of *Avicennia* found to degrade at a faster rate than *Spartina*, however this trend was observed in only one month over a one year study. Total below-ground production and carbon fixation were similar between both wetland types over the one year study. While stems, leaves, and roots may decay more quickly, mangrove wood is more sustainable long term than salt marsh grasses which dieback annually and become incorporated into the soil. The lack of production differences between the two wetland types may be related to the size and age of the recently introduced mangroves: mangroves in this study are young, representing a growth period of 15 to 20 years since the last major freeze of 1989 (same event as in the present Texas study), and it is possible with warming climate that future mangroves will attain larger biomass and production differences (Perry and

Mendelssohn, 2009). At present size and distribution, net carbon storage appears to be relatively equal between the two wetland types of the Mississippi delta wetland study. In this study, trends found within more mature mangrove systems at Port Aransas suggest a stronger divergence in carbon storage between mangrove and marsh wetlands. Higher live root volumes and lower percent sediment organics in mangrove soils indicate the importance of tree age and density as a control on carbon sequestration and type of organic matter present.

CHAPTER 6

Conclusions

With the onset of global warming, climate projections include rising sea levels, increased storm frequencies, and climate moderation in temperate latitudes. Presently, coastal saline wetlands along the Gulf of Mexico are primarily *Spartina* salt marshes, however the black mangrove, *Avicennia*, has been suggested in several studies to be expanding into marsh territory as a result of reduced freeze frequency and intensity. Although mangrove and salt marsh wetlands fulfill similar ecological roles, the differences between these two systems are substantial, and the replacement of salt marsh with mangrove vegetation will likely have ecological and societal significance if mangrove habitat expansion continues in the 21st century.

Mangroves may have increased resistance to sea level rise by increasing elevation through mineral and organic accumulation and root displacement. The present study demonstrates that even the relatively young and small mangroves at Port Aransas have increased local elevations on the order of 4 cm. This increase in elevation is attributed mainly to an increase in mineral trapping efficiency, demonstrated by an increase in total (mineral+organic) sediment accumulation rate of 0.28 to 0.56 cm/y measured by radiotracers relative to adjacent marshes. The trapping by the canopy does not appear to preferentially trap different grain size fractions (such as fine silts or clays) relative to adjacent marshes. Given that root volumes are also higher in mangrove soils studied, sediment displacement via rooting is likely a contributing factor to differential elevation

increase, but their relatively low density suggests it is a minor factor relative to mineral trapping. Organic accumulation is actually lower in the mangrove soils relative to adjacent marshes, but again, low organic contents suggests this is a minor factor on observed elevation differences. Increased mineral accumulation and elevation differential in mangrove areas at Port Aransas suggest these systems are currently accreting enough sediment to keep pace with current rates of relative sea level rise in this region.

Port Aransas mangrove systems also exhibit higher soil strengths, which may favor a reduction in wetland edge wave erosion during cyclonic or winter storms or from erosion by tidal currents. Higher soil strength has multiple causality: increased live rooting volumes, which bind sediments, and lower porosities (perhaps due to the reduced organic content) are observed in the more mature Port Aransas mangroves. The physical stature (e.g., canopy structure) of mangrove colonies may also contribute to dampening storm and wave attack by increased friction caused by the canopy structure (e.g., pneumatophores and a dense network of tree trunks, branches, and leaves).

Along with physical changes below the subsurface, the more mature mangroves at the Port Aransas sites induce chemical changes by lowering pore water pH and increasing redox potential and salinity, all of which occur mainly within the rooted zone. Subsurface oxidation may increase plant production, but may increase diagenetic decomposition of organic matter as well, agreeing with the observed reduction in organic content of mangrove soils horizons relative to adjacent marshes. Increased redox potential and sediment acidification will affect diagenetic and organic decay processes by

promoting sulfur oxidation and cation exchange and possibly decreasing soil sulfides, which may increase rates of organic decay. These observations suggest that continued mangrove expansion will likely lead to a reduction in wetland carbon sequestration, and will alter the character of organic carbon sequestered, producing more leaf litter and woody material over salt marsh grass blades. The wide salinity tolerance of mangroves may lend a competitive advantage over salt marsh vegetation with continued expansion as salinities are increased.

Finally, most of the above trends are confined within the Port Aransas study sites, where mangroves are physically taller, more mature, and composed of a denser vegetative and root network. Port Aransas mangrove colonies have had more time to generate elevation and substrate strength differences, and to create a unique soil geochemical signature. Mangrove colonies at the Galveston study sites are younger, less dense, and physically shorter, and many of these differential characteristics with adjacent marshes (except perhaps mineral sediment accumulation and live root density) are not observed. This demonstrates the relative rapidity that these substrate differences can develop, given that both areas were likely colonized since the 1980's.

The location of all study sites in back-barrier lagoonal settings, which are relatively low energy, low mineral input, and low organic productivity, limits the extrapolation of present results to other coastal saline wetland settings of the Gulf (e.g., deltaic, bay head, etc.). However, it can be inferred that distinctly different trends in grain size, sediment accumulation, sediment strength, and geochemistry are likely present in these settings, resulting from increased mineral and nutrient input from rivers. In the

lowest latitude areas of the Gulf (e.g., South Texas and the Florida Everglades) where mangrove systems are older and better-developed, observed trends may be accentuated. There is strong evidence that, as mangroves mature with decreasing freeze impact, these wetlands, wherever they colonize in the Gulf, are likely to better keep pace with relative sea level rise and offset erosional impacts of sea level rise, tidal fluctuations, and storm waves, relative to *Spartina* areas. Geochemical evidence suggests these systems will also significantly influence diagenetic processes by promoting sulfur oxidation and introducing increased oxygen and cation exchange into chemical reactions. Mangroves may also alter the character of sequestered organic matter and regionally increase salinities, allowing for a competitive advantage over hypersaline-sensitive salt marsh grasses.

Appendix A – Trimble NetRS Unit Setup, Field Procedure, and Data Processing

1. **Equipment necessary for Trimble NetRS Data Collection:**

A. GPS Antenna (Zephyr Antenna Part No. 41249-00 DC4906 recommended)

B. Tripod

C. Trimble NetRS Receiver and associated equipment

    1. NetRS receiver

    2. Antenna cable

    3. Internet crossover cable for computer connection

    4. Power and Network plug

    5. Trimble power supply, cables

    6. 24hr battery, cables, alligator clips

    7. Battery charger

    8. Measuring tape/stick (cm)

    9. Tri-Brack

    10. Field laptop

2. **Installing Trimble NetRS Software onto laptop**

    Insert software disk into laptop and follow installation setup.

3. **Connecting laptop to Trimble NetRS receiver unit**

    To create a connection between the NetRS unit and a computer:

A. Connect one end of orange cross-over cable to NetRS unit and the other end to laptop internet port

B. Establish laptop connection that uses correct IP address:

    1. Control Panel→Network Connections

2. Right-click on Local Area Connection (LAN)

3. Properties→General Tab→Internet Protocol→Properties

4. Select "Use the following IP address"

5. Enter IP address: **192.168.0.41** and

Subnet mask: **255.255.255.0**

6. Ok

C. Launch internet at IP address **http://192.168.0.40**

D. Turn on Trimble NetRS receiver-network icon should be green

4.   Creating a new Trimble NetRS recording session

Creating a new session prior to field set-up is recommended:

A. Open Trimble network connection

B. Data Logging→Create New Session

C. Select a name you will remember, i.e. "Mud Island_1"

D. Set recording time (for a 24hr session enter 1440 min-all times are Universal Coordinated Time-UTC)

E. Select Manual Logging

F. Select T00 format→Options: 15 sec/1 minute

G. Select Smooth Code/Carrier Phase

5.   Setting Up a Benchmark for Universal Coordinates

To setup a universal GPS benchmark using a Trimble NetRS unit:

A.   Insert benchmark piping into ground to mark position for future work.

B.   Mount antenna tripod directly over benchmark

1. Tripod feet should be firmly planted into ground

2. Connect tri-brack to top surface of tripod

3. Use side viewer on tri-brack to site to benchmark position and center tripod

4. Use tri-brack thumbscrews to level tripod

C. Place antenna onto tripod mount by screwing antenna base into tri-brack

D. Record/measure:

1. "Orthogonal height" (antenna height-height of ground/benchmark base to Antenna Reference Point, usually base of antenna)

2. Antenna type

E. Set-up Trimble Net-RS Unit

1. Battery pack-black, round end of cord connects to Trimble Net RS unit, +/- ends connect to battery

2. Connect orange cross-over cable to laptop Ethernet and Trimble Net RS

3. Open Trimble website **http://192.168.0.40**, turn on receiver unit and make sure laptop is connected

4. Locate previously created project, make sure settings are correct, <u>Enable Project</u>-receiver will begin recording once satellites are located

5. Once recording has started, disconnect laptop and leave Trimble unit running-collect when recording session is complete

6. Files will be saved as "NetRSUT1**2009**0618**1530**b.T00"

   Trimble Unit, **Year**, month/date, **time**, file type

6.   Downloading data from Trimble NetRS receiver

Requires conversion of **.T00** files into **.dat** and **RINEX**:

A. Save **.T00 file** and rename in shorter format (ensure **.T00** format remains, ex. **MI01.T00**)

B. Open command prompt window

C. Change window properties to allow cut and paste options: click on small icon on left→Properties→Edit options→Quick Edit mode

D. To copy/paste, highlight txt and right-click copy, right-click paste

E. Change directory path to location of the .T00 file:

    1. Execute command "**chdir**" to full path of folder name containing file:

      Chdir C:\Documents and Settings\Name\Desktop\GPS_Data

F. Install executable code on C drive (1st time only)

    1. Create folder for GPS software on **C:\drive**

    2. Copy all .exe files

      →**runpkr00.exe** (Trimble CD)

      →**dat2rin.exe** (Trimble.com)

    3. Control panel→System→Advanced→Environment Variables, edit path variable by attaching the the following to the existing values:**;C:\Trimble**

G. Now files are ready to be translated into **.dat** and **RINEX** format

7.   **Translating the data from Trimble NetRS receiver**

    Fist translate **.T00** file into **.dat** file

A. Command line entry:

    runpkr00 –dv MI01.T00 (will create new file **MI01.dat** into the same folder)

    Translate **.dat** file into **RINEX** format

B. Command line entry for observation program UTIG (UT Institute for Geophysics), observer R.S. Comeaux (RSC), agency UTIG, antenna code G0 (Zephyr Geodetic Antenna L1/L2 compact antenna with ground plane)and signal to noise levels s1 and s2 on frequencies L1 and L2 are to be retained:

    dat2rin –rUTIG –oRSC –AUTIG –aG0 –s1 –s2 MI01.dat

C. This creates two files in the same directory:

1. **MI01.09o** $\rightarrow$ **RINEX observation** file (used in data processing .09 designates year 2009)

2. **MI01.09n** $\rightarrow$ **RINEX navigation** file

8.   Processing data from Trimble NetRS receiver

Now it is time to send the **RINEX observation** file **MI01.09o** off for processing and correction using OPUS (Online Positioning User Service) of the National Geodetic Survey (US territories):

A. Connect to OPUS home page:

http://www.ngs.noaa.gov/OPUS/

B. Enter required information:

1. Email address

2. **RINEX observation** file location (DATA file)

3. Antenna type

4. Orthogonal height

C. Then keep the default options and select "Upload to STATIC" processor for data session >2hrs

D. You will receive an email with your corrected data in a few minutes to an hour that will look like the following:

FILE: UT_MI01.obs 000083247

NGS OPUS SOLUTION REPORT

========================

All computed coordinate accuracies are listed as peak-to-peak values.   For additional information: www.ngs.noaa.gov/OPUS/Using_OPUS.html#accuracy

USER: r.comeaux@mail.utexas.edu   DATE: July 27, 2009

RINEX FILE: ut_m182r.09o   TIME: 16:31:04 UTC

SOFTWARE: page5 0903.24 master11.pl 081023

START: 2009/07/01 17:46:00

EPHEMERIS: igs15383.eph [precise]   STOP: 2009/07/02 17:46:00

NAV FILE: brdc1820.09n   OBS USED: 60603 / 62392 : 97%

ANT NAME: TRM41249.00 NONE   # FIXED AMB: 125 / 205 : 61%

ARP HEIGHT: 0.9285   OVERALL RMS: 0.015(m)

REF FRAME: NAD_83(CORS96)(EPOCH:2002.0000)

ITRF00 (EPOCH:2009.4993)

X: -689846.988(m)   0.012(m)   -689847.685(m)   0.012(m)

Y: -5596339.142(m)   0.039(m)   -5596337.660(m)   0.039(m)

Z: 2970844.812(m)   0.012(m)   2970844.603(m)   0.012(m)

LAT: 27 56 32.24113   0.013(m)   27 56 32.25623   0.013(m)

E LON: 262 58 21.86269 0.010(m)   262 58 21.83076   0.010(m)

W LON: 97 1 38.13731   0.010(m)   97 1 38.16924   0.010(m)

EL HGT: -25.834(m)   0.038(m)   -27.156(m)   0.038(m)

ORTHO HGT: 0.775(m)   0.075(m) [NAVD88 (Computed using GEOID03)]

UTM COORDINATES   STATE PLANE COORDINATES

UTM (Zone 14)   SPC (4204 TXSC)

88

Northing (Y) [meters]	3092375.565	4013714.045
Easting (X) [meters]	694089.640	794166.671
Convergence [degrees]	0.92467993	0.96647005
Point Scale	1.00006498	1.00015577
Combined Factor	1.00006904	1.00015983

US NATIONAL GRID DESIGNATOR: 14RPR9409092376(NAD 83)

BASE STATIONS USED

PID   DESIGNATION   LATITUDE   LONGITUDE DISTANCE(m)

DK7573   KVTX   KINGSVILLETX2006   CORS   ARP   N273245.407 W0975334.345   95980.6

DF4377   TXCC   CORPUS   CHRISTI   R2   CORS   ARP   N274426.854 W0972630.011   46529.2

DK7565 ARP7 ARANSAS PASS 7 CORS ARP N275018.051 W0970332.220 11933.7

NEAREST NGS PUBLISHED CONTROL POINT

AH1130   SKIFF 1934   N275559.875 W0970236.489   1882.2

This position and the above vector components were computed without any knowledge by the National Geodetic Survey regarding the equipment or field operating procedures used.

Appendix B – List of Field Site and Core Locations

Location	Wetland	Core	Length	Easting	Northing
(UTM Zone 14)					
	Base Station Location			**694089.640**	**3092375.564**
Port Aransas	Mangrove	MI1M A, B, C	92 cm	694051.049	3092374.793
Mud Island	Mangrove	MI2M A, B, C	82 cm	694057.158	3092363.153
	Marsh	MI1S A, B, C	92 cm	694089.640	3092375.564
	Marsh	MI2S A, B, C	82 cm	694105.737	3092388.876
Port Aransas	**Base Station Location**			**691022.909**	**3083644.298**
Harbor Island	Mangrove	HI1 A, B, C	72 cm	691022.909	3083644.298
	Mangrove	HI2 A, B, C	82 cm	690988.751	3083621.946
(UTM Zone 15)					
Galveston East	**Base Station Location**			**330052.051**	**3245987.119**
	Mangrove	GIEM1 A, B, C	38 cm	330053.184	3246000.070
	Mangrove	GIEM2 A, B, C	38 cm	330062.546	3246041.108
	Marsh	GIES1 A, B, C	34 cm	330064.236	3246018.861
	Marsh	GIES2 A, B, C	42 cm	330070.686	3246056.666
Galveston West	**Base Station Location**			**291415.302**	**3219756.165**
	Mangrove	GMIM A, B, C	82 cm	291419.438	3219760.301
	Marsh	GMIS A, B, C	72 cm	291425.062	3219751.455

Appendix C – Radioisotope Activity Raw Data

Core ID: **GIEM1A**   Location: Galveston East

Sample ID (in cm)	xs Pb-210	xs err	Ra-226	Cs-137	Cs err
0-2	1.41	0.19	0.51	0.07	0.03
2-4	1.12	0.13	0.37	0.09	0.01
4-6	0.89	0.15	0.38	0.15	0.03
6-8	0.48	0.12	0.42	0.10	0.02
8-10	0.58	0.18	0.43	0.15	0.04
10-12	0.28	0.14	0.44	0.13	0.04
12-14	0.31	0.16	0.39	0.19	0.04
14-16	0.47	0.17	0.41	0.22	0.04
16-18	0.82	0.17	0.47	0.20	0.04
18-20	0.61	0.13	0.50	0.24	0.03
20-22	0.44	0.17	0.43	0.17	0.04
24-26	0.15	0.13	0.39	0.20	0.03
28-30	0.09	0.12	0.39	0.09	0.03
32-34	0.07	0.13	0.36	0.02	0.03
36-38	-0.05	0.11	0.37	0.04	0.03

Core ID: **GIEM2A**   Location: Galveston East

Sample ID in cm	xs Pb-210	xs err	Ra-226	Cs-137	Cs err
0-2	1.02	0.15	0.43	0.09	0.03
2-4	0.78	0.28	0.41	0.09	0.04
4-6	0.77	0.22	0.49	0.11	0.04
6-8	0.83	0.19	0.33	0.08	0.04
8-10	0.62	0.16	0.38	0.12	0.04
10-12	0.82	0.21	0.44	0.13	0.04
12-14	0.83	0.19	0.39	0.14	0.04
14-16	0.67	0.16	0.38	0.21	0.03
16-18	0.39	0.10	0.33	0.11	0.02
18-20	0.67	0.19	0.39	0.17	0.04
20-22	0.50	0.16	0.38	0.15	0.03
24-26	0.26	0.16	0.39	0.06	0.04
28-30	0.31	0.15	0.43	0.09	0.03
32-34	0.11	0.11	0.37	0.02	0.03
36-38	0.12	0.11	0.32	0.00	0.00

Core ID: **GIES1A**   Location: Galveston East

Sample ID (in cm)	xs Pb-210	xs err	Ra-226	Cs-137	Cs err
0-2	0.93	0.34	0.76	0.06	0.07
2-4	0.26	0.22	0.54	0.05	0.04
4-6	0.53	0.23	0.52	0.01	0.05
6-8	0.27	0.15	0.47	0.06	0.03
8-10	0.12	0.22	0.47	0.07	0.04
10-12	0.24	0.22	0.43	0.13	0.04
12-14	0.10	0.18	0.41	0.09	0.04
14-16	-0.19	0.18	0.55	0.09	0.04
16-18	-0.13	0.18	0.52	0.10	0.04
18-20	-0.01	0.12	0.44	0.05	0.03
20-22	-0.34	0.19	0.54	0.05	0.04
24-26	0.01	0.17	0.49	0.06	0.03
28-30	-0.07	0.19	0.36	0.00	0.00
32-34	0.05	0.18	0.44	0.00	0.00

Core ID: **GIES2A** Location: Galveston East

Sample ID (in cm)	xs Pb-210	xs err	Ra-226	Cs-137	Cs err
0-2	1.03	0.24	0.60	0.10	0.04
2-4	0.93	0.23	0.48	0.04	0.04
4-6	1.00	0.23	0.49	0.01	0.04
6-8	1.17	0.28	0.55	0.06	0.04
8-10	1.06	0.25	0.59	0.03	0.05
10-12	0.50	0.25	0.45	0.07	0.04
12-14	0.47	0.21	0.57	0.06	0.03
14-16	-0.07	0.20	0.60	0.10	0.04
16-18	0.02	0.22	0.53	0.12	0.04
18-20	-0.04	0.24	0.52	0.16	0.05
20-22	-0.14	0.20	0.57	0.08	0.04
24-26	0.40	0.20	0.44	0.03	0.04
28-30	0.35	0.14	0.47	0.06	0.03
32-34	0.07	0.16	0.48	0.06	0.03
36-38	-0.07	0.20	0.48	0.03	0.04
40-42	-0.37	0.19	0.40	0.00	0.00

Core ID: **GMIMA**   Location: Galveston West

Sample ID (in cm)	xs Pb-210	xs err	Ra-226	Cs-137	Cs err
0-2	1.94	0.73	0.79	0.02	0.08
2-4	1.44	0.47	0.66	0.04	0.05
4-6	1.28	0.65	0.94	0.06	0.07
6-8	0.55	0.68	0.84	0.14	0.08
8-10	0.99	0.67	0.81	0.06	0.08
10-12	0.36	0.62	0.87	0.02	0.07
12-14	1.10	0.61	0.94	0.15	0.07
14-16	1.03	0.53	0.92	0.08	0.06
16-18	0.94	0.65	0.92	0.06	0.08
18-20	1.73	0.67	0.82	0.14	0.08
20-22	0.94	0.61	0.98	0.06	0.08
24-26	-0.35	0.67	0.78	0.14	0.07
28-30	0.49	0.49	1.02	0.00	0.00
32-34	0.45	0.65	1.13	0.00	0.00
36-38	-0.12	0.61	0.99	0.00	0.00
40-42	0.98	0.62	0.93	0.00	0.00
44-46	1.09	0.61	0.93	0.00	0.00
48-50	-1.13	0.30	1.13	0.00	0.00
50-52	-0.24	0.43	1.02	0.06	0.05
60-62	-0.52	0.40	0.82	0.04	0.05
70-72	-0.81	0.25	0.81	0.04	0.07
80-82	-0.33	0.61	1.05	0.00	0.00

Core ID: **GMISA**   Location: Galveston West

Sample ID (in cm)	xs Pb-210	xs err	Ra-226	Cs-137	Cs err
0-2	1.24	0.62	1.02	0.05	0.06
2-4	1.52	0.55	1.00	0.11	0.06
4-6	1.49	0.75	1.09	0.16	0.08
6-8	0.23	0.66	1.25	0.23	0.08
8-10	0.37	0.59	0.98	0.07	0.07
10-12	1.85	0.69	1.00	0.18	0.08
12-14	0.16	0.07	0.11	0.02	0.01
14-16	1.38	0.44	1.00	0.13	0.04
16-18	1.29	0.52	0.92	0.21	0.05
18-20	0.66	0.36	0.85	0.15	0.04
20-22	-0.09	0.44	1.11	0.13	0.06
24-26	0.18	0.38	0.93	0.04	0.03
28-30	-0.13	0.60	1.02	0.08	0.07
32-34	0.66	0.63	0.98	0.00	0.00
36-38	1.06	0.61	1.02	0.09	0.07
40-42	0.76	0.61	1.20	0.00	0.00
44-46	0.04	0.42	1.15	0.00	0.00
48-50	-0.09	0.54	1.06	0.03	0.07
50-52	0.14	0.55	0.97	0.00	0.00
60-62	1.40	0.62	0.75	0.05	0.07
70-72	0.27	0.55	0.95	0.00	0.00

Core ID:	**MI1MA**	Location: Port Aransas Mud Island			

Sample ID (in cm)	xs Pb-210	xs err	Ra-226	Cs-137	Cs err
0-2	2.28	0.33	0.77	0.09	0.05
2-4	1.40	0.30	0.93	0.06	0.06
4-6	1.57	0.33	0.98	0.14	0.06
6-8	0.98	0.28	0.97	0.17	0.05
8-10	0.89	0.20	1.31	0.19	0.03
10-12	0.41	0.43	1.38	0.17	0.04
12-14	0.37	0.21	1.32	0.23	0.03
14-16	0.51	0.22	1.35	0.32	0.04
16-18	0.40	0.17	1.20	0.28	0.03
18-20	0.18	0.27	1.01	0.17	0.05
20-22	-0.19	0.24	0.95	0.17	0.05
24-26	-0.72	2.59	8.05	0.86	0.40
28-30	0.21	0.22	1.01	0.05	0.05
32-34	-0.02	0.16	0.91	0.03	0.03
36-38	-0.02	0.21	0.82	0.07	0.04
40-42	0.10	0.24	0.87	0.02	0.05
44-46	-0.16	0.21	0.83	0.04	0.04
48-50	-0.47	0.28	0.99	0.00	0.00
50-52	-0.23	0.24	1.09	0.00	0.00
60-62	-0.15	0.23	0.99	0.00	0.00
70-72	-0.38	0.18	0.89	0.00	0.00
80-82	-0.35	0.23	0.81	0.00	0.00
90-92	-0.13	0.25	0.78	0.00	0.00

		Location: Port			
Core ID:	**MI2MA**	Aransas Mud Island			

Sample ID (in cm)	xs Pb-210	xs err	Ra-226	Cs-137	Cs err
0-2	3.30	0.41	0.71	0.14	0.06
2-4	1.93	0.24	0.71	0.18	0.03
4-6	0.86	0.21	0.70	0.13	0.04
6-8	0.81	0.25	0.85	0.22	0.04
8-10	0.58	0.22	0.78	0.14	0.04
10-12	0.69	0.20	0.75	0.13	0.04
12-14	0.49	0.19	0.66	0.13	0.04
14-16	0.40	0.20	0.72	0.12	0.04
16-18	0.48	0.17	0.73	0.12	0.03
18-20	0.80	0.20	0.65	0.18	0.04
20-22	0.27	0.17	0.68	0.12	0.04
24-26	0.52	0.17	0.65	0.24	0.04
28-30	0.18	0.18	0.69	0.09	0.04
32-34	0.43	0.16	0.77	0.11	0.03
36-38	0.35	0.20	0.83	0.03	0.04
40-42	0.34	0.16	0.76	0.06	0.03
44-46	0.04	0.17	0.82	0.09	0.04
48-50	0.04	0.20	0.71	0.02	0.03
50-52	-0.06	0.17	0.70	0.00	0.00
60-62	0.22	0.17	0.57	0.00	0.00
70-72	0.08	0.17	0.64	0.00	0.00
80-82	-0.06	0.12	0.69	0.00	0.02

Core ID:	**MI1SA**	Location: Port Aransas Mud Island			

Sample ID (in cm)	xs Pb-210	xs err	Ra-226	Cs-137	Cs err
0-2	2.98	0.38	0.63	0.10	0.06
2-4	2.31	0.28	0.60	0.05	0.03
4-6	2.73	0.35	0.76	0.17	0.05
6-8	3.01	0.35	0.67	0.17	0.05
8-10	1.71	0.31	0.76	0.15	0.03
10-12	1.71	0.28	0.83	0.15	0.05
12-14	1.37	0.22	0.95	0.18	0.03
14-16	1.06	0.23	0.85	0.14	0.04
16-18	0.76	0.27	0.77	0.14	0.04
18-20	0.55	0.19	0.66	0.12	0.04
20-22	0.43	0.14	0.70	0.13	0.02
24-26	0.35	0.17	0.69	0.15	0.04
28-30	-0.17	0.18	0.69	0.01	0.03
32-34	0.06	0.18	0.74	0.07	0.04
36-38	-0.03	0.16	0.80	0.00	0.00
40-42	-0.09	0.18	0.79	0.04	0.04
44-46	0.06	0.14	0.73	0.05	0.03
48-50	-0.21	0.16	0.84	0.01	0.04
50-52	-0.10	0.17	0.77	0.00	0.04
60-62	-0.18	0.15	0.73	0.03	0.03
70-72	0.05	0.21	0.71	0.01	0.03
80-82	-0.02	0.14	0.75	0.01	0.03
90-92	-0.01	0.16	0.83	0.00	0.20

Core ID: **MI2SA**   Location: Port Aransas Mud Island

Sample ID (in cm)	xs Pb-210	xs err	Ra-226	Cs-137	Cs err
0-2	2.88	0.28	0.48	0.12	0.03
2-4	3.67	0.41	0.63	0.27	0.05
4-6	5.24	0.54	0.84	0.34	0.07
6-8	1.22	0.25	0.65	0.10	0.04
8-10	1.09	0.23	0.85	0.25	0.05
10-12	0.90	0.25	1.00	0.28	0.05
12-14	0.90	0.19	0.91	0.20	0.03
14-16	0.53	0.20	0.85	0.24	0.04
16-18	0.31	0.18	0.82	0.18	0.04
18-20	0.04	0.19	0.58	0.12	0.03
20-22	0.26	0.21	0.62	0.13	0.03
24-26	-0.21	0.17	0.80	0.13	0.04
28-30	0.17	0.16	0.71	0.00	0.00
32-34	0.28	0.15	0.76	0.06	0.03
36-38	-0.03	0.16	0.67	0.04	0.04
40-42	-0.35	0.23	0.83	0.08	0.04
44-46	-0.01	0.18	0.91	0.02	0.04
48-50	-0.03	0.22	0.84	0.02	0.04
50-52	0.15	0.20	0.80	0.01	0.04
60-62	0.00	0.14	0.73	0.01	0.02
70-72	0.04	0.12	0.68	0.00	0.00
80-82	-0.11	0.14	0.74	0.01	0.03

Core ID: **HI1A**

Location: Port Aransas
Harbor Island

Sample ID (in cm)	xs Pb-210	xs err	Ra-226	Cs-137	Cs err
0-2	1.00	0.68	0.88	0.23	0.08
2-4	0.97	0.72	0.87	0.05	0.08
4-6	0.00	0.64	0.81	0.04	0.07
6-8	0.58	0.41	0.93	0.00	0.05
8-10	1.19	0.61	0.83	0.05	0.07
10-12	-0.25	0.57	0.77	0.09	0.06
12-14	-0.08	0.53	0.73	0.01	0.07
14-16	1.42	0.59	0.71	0.00	0.07
16-18	0.53	0.44	0.82	0.00	0.00
18-20	0.19	0.52	0.75	0.05	0.06
20-22	0.24	0.57	0.97	0.13	0.07
24-26	0.58	0.58	0.88	0.00	0.00
28-30	0.42	0.59	0.94	0.03	0.07
32-34	0.53	0.64	0.91	0.01	0.07
36-38	-0.66	0.44	0.78	0.01	0.05
40-42	0.47	0.57	0.74	0.16	0.07
44-46	-0.04	0.55	0.70	0.09	0.07
48-50	0.04	0.58	0.91	0.05	0.07
50-52	-0.36	0.52	0.67	0.04	0.06
60-62	0.62	0.62	0.91	0.04	0.07
70-72	0.23	0.29	0.60	0.00	0.00

Core ID:	**HI2A**	Location: Port Aransas Harbor Island			

Sample ID (in cm)	xs Pb-210	xs err	Ra-226	Cs-137	Cs err
0-2	1.93	0.66	0.77	0.16	0.07
2-4	-0.03	0.56	0.63	0.05	0.07
4-6	0.73	0.60	0.64	0.12	0.07
6-8	1.38	0.44	0.50	0.08	0.04
8-10	0.45	0.54	0.60	0.05	0.06
10-12	0.88	0.60	0.54	0.01	0.07
12-14	1.43	0.57	0.68	0.01	0.06
14-16	0.42	0.52	0.73	0.11	0.06
16-18	0.95	0.39	0.65	0.03	0.05
18-20	1.21	0.62	0.57	0.06	0.07
20-22	0.20	0.52	0.74	0.08	0.06
24-26	0.84	0.53	0.59	0.00	0.00
28-30	0.08	0.50	0.78	0.00	0.06
32-34	0.30	0.55	0.74	0.01	0.07
36-38	1.16	0.59	0.83	0.09	0.07
40-42	0.32	0.37	0.62	0.00	0.00
44-46	0.26	0.49	0.64	0.05	0.06
48-50	0.46	0.55	0.71	0.05	0.06
50-52	0.94	0.52	0.52	0.00	0.00
60-62	-0.30	0.53	0.60	0.03	0.06
70-72	-0.21	0.32	0.51	0.02	0.04
80-82	0.63	0.51	0.53	0.00	0.00

Appendix D – Organic Raw Data

Galveston East

GIEM1A Sample Interval (in cm)	% Live Root	% Organic Matter	GIEM2A Sample Interval (in cm)	% Live Root	% Organic Matter
0-2	0.738	0.710	0-2	2.994	0.861
2-4	0.531	0.680	2-4	4.410	1.586
4-6	2.870	0.489	4-6	6.403	1.667
6-8	2.625	0.591	6-8	4.269	1.774
8-10	0.993	0.523	8-10	4.173	1.112
10-12	0.568	0.509	10-12	0.889	0.749
12-14	1.000	0.369	12-14	2.207	0.725
14-16	0.853	0.462	14-16	0.175	0.533
16-18	0.604	0.544	16-18	0.089	0.527
18-20	0.185	0.542	18-20	0.090	0.356
20-22	0.124	0.216	20-22	0.075	0.417
24-26	0.062	0.221	24-26	0.029	0.401
28-30	0.013	0.247	28-30	0.055	0.486
32-34	0.017	0.201	32-34	0.139	0.209
36-38	0.102	0.274	36-38	0.159	0.528

GIES1A

Sample Interval (in cm)	% Live Root	% Organic Matter
0-2	1.468	2.575
2-4	3.014	0.773
4-6	1.482	1.060
6-8	1.281	0.697
8-10	0.507	0.515
10-12	0.212	0.304
12-14	0.267	0.342
14-16	0.417	0.346
16-18	0.274	0.274
18-20	0.203	0.278
20-22	0.244	0.382
24-26	0.084	0.361
28-30	0.253	0.191
32-34	0.155	0.368

GIES2A

Sample Interval (in cm)	% Live Root	% Organic Matter
0-2	1.644	0.770
2-4	1.466	0.786
4-6	3.163	0.742
6-8	2.482	0.843
8-10	3.167	0.797
10-12	1.023	0.421
12-14	0.614	0.651
14-16	1.012	0.436
16-18	0.424	0.350
18-20	0.373	0.289
20-22	0.540	0.334
24-26	0.217	0.476
28-30	0.404	0.318
32-34	0.096	0.443
36-38	0.139	0.694
40-42	0.033	0.718

Galveston West

GMIMA Sample Interval (in cm)	% Live Root	% Organic Matter
0-2	1.265	0.804
2-4	3.484	0.836
4-6	4.292	0.726
6-8	4.140	0.893
8-10	2.671	0.761
10-12	2.664	1.060
12-14	1.460	1.431
14-16	0.373	0.885
16-18	0.795	0.832
18-20	0.431	0.717
20-22	0.489	0.970
24-26	0.572	0.577
28-30	0.208	0.448
32-34	0.079	0.555
36-38	0.166	1.036
40-42	0.154	-2.801
44-46	0.027	0.580
48-50	0.335	0.530
50-52	0.233	0.523
60-62	0.447	0.571
70-72	0.000	0.325
80-82	0.019	0.649

GMISA Sample Interval (in cm)	% Live Root	% Organic Matter
0-2	0.976	0.565
2-4	1.688	1.219
4-6	1.396	1.236
6-8	0.798	1.127
8-10	0.597	0.799
10-12	1.308	1.127
12-14	1.028	1.463
14-16	0.896	0.879
16-18	1.399	0.924
18-20	0.545	0.614
20-22	0.120	0.461
24-26	0.234	0.577
28-30	0.022	0.774
32-34	0.019	0.557
36-38	0.051	0.368
40-42	0.026	0.433
44-46	0.027	0.701
48-50	0.009	0.371
50-52	0.023	0.388
60-62	0.014	0.476
70-72	0.010	0.435

Port Aransas Mud Island

MI1MA Sample Interval (in cm)	% Live Root	% Organic Matter	MI2MA Sample Interval (in cm)	% Live Root	% Organic Matter
0-2	0.149	2.706	0-2	2.280	3.080
2-4	0.596	1.098	2-4	4.482	2.033
4-6	0.993	1.559	4-6	0.820	0.830
6-8	1.334	1.063	6-8	1.738	0.776
8-10	1.136	1.184	8-10	2.736	0.908
10-12	1.776	1.192	10-12	0.610	0.472
12-14	2.178	0.949	12-14	0.113	0.587
14-16	0.164	1.430	14-16	0.102	0.438
16-18	0.290	1.621	16-18	0.300	0.572
18-20	0.250	0.744	18-20	0.190	0.520
20-22	0.208	0.451	20-22	0.302	0.625
24-26	0.163	0.363	24-26	0.221	0.569
28-30	0.305	0.821	28-30	0.065	0.410
32-34	0.243	0.550	32-34	0.467	0.739
36-38	0.104	0.534	36-38	0.103	0.793
40-42	0.133	0.614	40-42	0.000	0.994
44-46	0.000	0.536	44-46	0.000	1.276
48-50	0.015	0.461	48-50	0.010	0.530
50-52	0.018	0.414	50-52	0.000	0.740
60-62	0.000	0.433	60-62	0.000	0.461
70-72	0.000	0.461	70-72	0.020	0.667
80-82	0.153	0.396	80-82	0.000	0.471
90-92	0.055	0.365			

MI1SA Sample Interval (in cm)	% Live Root	% Organic Matter	MI2SA Sample Interval (in cm)	% Live Root	% Organic Matter
0-2	2.771	3.432	0-2	0.348	4.632
2-4	1.355	1.781	2-4	1.239	3.989
4-6	1.452	2.301	4-6	1.504	8.685
6-8	0.389	2.159	6-8	0.550	1.969
8-10	0.955	1.184	8-10	0.390	2.339
10-12	0.776	0.849	10-12	0.674	3.457
12-14	0.082	1.679	12-14	0.025	2.436
14-16	0.241	1.085	14-16	0.034	0.782
16-18	0.034	0.676	16-18	0.027	0.680
18-20	0.032	0.531	18-20	0.000	0.550
20-22	0.077	0.448	20-22	0.000	0.638
24-26	0.021	0.612	24-26	0.010	0.624
28-30	0.160	0.341	28-30	0.153	0.507
32-34	0.000	0.425	32-34	0.000	1.385
36-38	0.000	0.533	36-38	0.117	1.148
40-42	0.000	0.659	40-42	0.000	1.198
44-46	0.000	0.509	44-46	0.000	0.659
48-50	0.000	0.709	48-50	0.054	0.569
50-52	0.000	0.688	50-52	0.029	0.587
60-62	0.000	0.527	60-62	0.000	0.643
70-72	0.000	0.552	70-72	0.000	0.326
80-82	0.000	0.418	80-82	0.000	0.494
90-92	0.000	0.263			

Port Aransas Harbor Island

HI1A

Sample Interval (in cm)	% Live Root	% Organic Matter
0-2	6.662	3.387
2-4	1.162	0.749
4-6	0.285	0.370
6-8	1.609	0.543
8-10	0.597	0.585
10-12	0.980	0.497
12-14	0.760	0.373
14-16	0.204	0.462
16-18	0.000	0.443
18-20	0.000	0.953
20-22	0.000	0.412
24-26	0.052	0.456
28-30	0.177	0.422
32-34	0.092	0.482
36-38	0.038	0.599
40-42	0.053	0.467
44-46	0.000	0.456
48-50	0.000	0.456
50-52	0.000	0.496
60-62	0.039	0.506
70-72	0.000	0.281

HI2A

Sample Interval (in cm)	% Live Root	% Organic Matter
0-2	0.371	0.873
2-4	0.717	0.621
4-6	0.174	0.400
6-8	0.510	0.542
8-10	0.336	0.443
10-12	0.302	0.248
12-14	1.364	0.482
14-16	0.154	0.369
16-18	0.000	0.317
18-20	0.000	0.236
20-22	0.000	0.199
24-26	0.000	0.146
28-30	0.000	0.174
32-34	0.000	0.241
36-38	0.000	0.310
40-42	0.000	0.385
44-46	0.000	0.283
48-50	0.000	0.318
50-52	0.000	0.260
60-62	0.000	0.268
70-72	0.000	0.340
80-82	0.198	0.156

Appendix E – Grain Size Raw Data: Gravel, Sand, Silt, and Clay Fractions

Galveston West

GMIS

Sample ID (in cm)	% Gravel	% Sand	% Silt	% Clay
0-2	0.00	59.59	15.47	24.94
2-4	0.17	59.14	16.40	24.29
4-6	0.18	60.44	16.44	22.94
6-8	0.22	63.26	15.05	21.47
8-10	0.10	61.70	15.39	22.80
10-12	0.20	59.43	17.05	23.32
12-14	0.45	64.53	9.78	25.24
14-16	0.31	65.51	8.97	25.20
16-18	0.81	68.20	7.72	23.27
18-20	1.37	65.00	5.86	27.77
20-22	1.16	60.99	6.41	31.44
24-26	0.93	51.60	9.42	38.05
28-30	1.84	55.43	10.77	31.96
32-34	2.62	53.87	13.69	29.82

GMIM

Sample ID (in cm)	% Gravel	% Sand	% Silt	% Clay
0-2	1.67	63.45	12.79	22.09
2-4	1.30	62.16	12.13	24.40
4-6	0.96	77.19	6.38	15.47
6-8	1.38	57.79	15.49	25.33
8-10	1.38	48.91	17.85	31.86
10-12	2.03	52.63	13.94	31.40
12-14	3.80	56.68	6.23	33.29
14-16	2.15	62.58	5.41	29.86
16-18	1.37	64.36	1.55	32.72
18-20	1.48	66.42	1.08	31.02
20-22	0.80	67.95	2.24	29.01
24-26	0.78	76.40	0.13	22.69
28-30	0.22	73.06	1.17	25.54
32-34	0.29	68.24	4.82	26.65
36-38	0.19	70.21	2.34	27.26
40-42	0.10	70.40	3.39	26.10
44-46	0.05	67.66	5.26	27.02

Port Aransas Mud Island

MI1M

Sample ID (in cm)	% Gravel	% Sand	% Silt	% Clay
0-2	4.70	48.52	7.68	39.11
2-4	3.87	46.56	7.08	42.49
4-6	3.10	43.68	8.37	44.85
6-8	2.54	54.20	10.27	32.99
8-10	2.74	50.81	13.07	33.37
10-12	1.35	52.50	12.65	33.50
12-14	0.83	51.68	13.12	34.36
14-16	0.89	60.78	10.82	27.52
16-18	0.44	63.00	8.97	27.59
18-20	0.89	66.58	7.99	24.55
20-22	0.46	67.06	8.33	24.15
24-26	0.67	69.48	8.48	21.37
28-30	0.22	63.91	9.79	26.08
32-34	0.07	66.59	8.30	25.04
36-38	0.32	63.78	8.63	27.27
40-42	0.14	64.15	8.64	27.07
44-46	0.05	63.32	8.23	28.39
48-50	0.11	62.15	9.90	27.84
50-52	0.04	65.68	8.70	25.58
60-62	0.08	64.85	9.45	25.63
70-72	0.02	70.57	5.12	24.28
80-82	1.58	71.03	6.97	20.41
90-92	0.24	70.66	5.61	23.49

MI2M

Sample ID (in cm)	% Gravel	% Sand	% Silt	% Clay
0-2	3.77	59.66	9.62	26.95
2-4	4.14	53.72	12.96	29.19
4-6	2.32	65.47	8.26	23.95
6-8	0.68	70.64	6.72	21.96
8-10	1.72	66.36	9.74	22.17
10-12	0.62	66.86	9.17	23.36
12-14	0.49	60.33	11.33	27.85
14-16	0.41	64.83	8.27	26.49
16-18	0.38	72.00	6.88	20.75
18-20	0.96	72.12	6.25	20.67
20-22	0.29	72.29	7.48	19.94
24-26	0.36	73.10	6.64	19.91
28-30	0.42	70.30	7.52	21.76
32-34	0.73	67.32	8.87	23.08
36-38	0.07	65.57	11.19	23.17
40-42	0.06	68.25	9.08	22.62
44-46	0.33	68.77	6.95	23.95
48-50	0.11	64.31	9.09	26.49
50-52	0.13	64.30	9.75	25.82
60-62	0.05	67.03	9.25	23.67

MI1S

Sample ID (in cm)	% Gravel	% Sand	% Silt	% Clay
0-2	2.78	59.17	8.34	29.71
2-4	1.66	58.28	11.40	28.67
4-6	3.53	51.91	8.14	36.41
6-8	2.84	58.01	9.02	30.13
8-10	0.80	58.82	12.29	28.09
10-12	0.86	58.03	12.80	28.31
12-14	0.42	56.17	12.85	30.56
14-16	0.43	57.56	11.08	30.93
16-18	0.93	64.53	8.75	25.79
18-20	0.19	68.91	8.77	22.12
20-22	0.09	73.54	6.50	19.87
24-26	0.59	66.90	6.79	25.72
28-30	0.28	61.80	10.74	27.18
32-34	0.86	53.01	20.69	25.43
36-38	0.15	61.14	8.99	29.73
40-42	0.78	64.01	8.01	27.20
44-46	0.17	63.89	6.94	28.99
48-50	0.14	64.57	9.17	26.11
50-52	0.36	66.78	7.99	24.87
60-62	0.00	66.48	8.07	25.45
70-72	7.13	63.34	7.52	22.01

MI2S

Sample ID (in cm)	% Gravel	% Sand	% Silt	% Clay
0-2	4.75	49.97	9.79	35.49
2-4	3.42	53.05	7.81	35.72
4-6	3.60	51.65	9.73	35.03
6-8	2.43	63.39	9.30	24.89
8-10	0.88	49.57	13.06	36.49
10-12	0.73	48.46	12.35	38.46
12-14	0.50	57.16	9.75	32.59
14-16	0.62	63.16	9.90	26.31
16-18	0.45	69.76	4.84	24.96
18-20	0.40	72.10	6.76	20.73
20-22	0.28	71.02	5.40	23.30
24-26	0.53	75.50	5.40	18.57
28-30	0.37	68.58	9.78	21.27
32-34	0.08	64.85	7.13	27.94
36-38	0.13	59.46	9.17	31.24
40-42	0.04	60.43	6.47	33.07
44-46	0.11	64.98	7.87	27.04
48-50	0.09	68.34	6.98	24.59
50-52	0.07	66.65	7.35	25.93
60-62	0.11	66.64	6.25	27.00

Appendix F – Porosity and Strength Raw Data

Galveston East

GIEM1 Sample ID (in cm)	Porosity	Strength (kPa)	GIEM2 Sample ID (in cm)	Porosity	Strength (kPa)	GIES1 Sample ID (in cm)	Porosity	Strength (kPa)
0-2	0.668	8	0-2	0.681	8	0-2	0.712	5
2-4	0.604	12	2-4	0.718	10	2-4	0.646	8
4-6	0.638	14	4-6	0.709	7	4-6	0.669	6
6-8	0.613	9	6-8	0.675	6	6-8	0.593	12
8-10	0.593	11	8-10	0.639	6	8-10	0.557	9
10-12	0.568	9	10-12	0.610	6	10-12	0.501	10
12-14	0.563	7	12-14	0.617	8	12-14	0.467	6
14-16	0.576	9	14-16	0.549	8	14-16	0.459	6
16-18	0.584	9	16-18	0.537	13	16-18	0.441	8
18-20	0.552	8	18-20	0.501	11	18-20	0.443	5
20-22	0.481	9	20-22	0.508	6	20-22	0.453	6
24-26	0.453	8	24-26	0.498	8	24-26	0.437	13
28-30	0.439	6	28-30	0.476	12	28-30	0.423	
32-34	0.430	6	32-34	0.435		32-34	0.408	
36-38	0.433	8	36-38	0.454				

Galveston East

GIES2

Sample ID (in cm)	Porosity	Strength (kPa)
0-2	0.678	9
2-4	0.647	4
4-6	0.658	8
6-8	0.659	
8-10	0.654	8
10-12	0.617	10
12-14	0.590	6
14-16	0.570	8
16-18	0.540	2
18-20	0.518	8
20-22	0.515	
24-26	0.500	
28-30	0.501	
32-34	0.484	
36-38	0.515	
40-42	0.430	

Galveston West

GMIM

Sample ID (in cm)	Porosity	Strength (kPa)
0-2	0.61	8
2-4	0.58	6
4-6	0.58	6
6-8	0.58	6
8-10	0.61	10
10-12	0.62	7
12-14	0.62	5
14-16	0.58	7
16-18	0.58	4
18-20	0.54	6
20-22	0.54	4
24-26	0.51	6
28-30	0.48	4
32-34	0.48	6
36-38	0.52	7
40-42	0.49	7
44-46	0.46	8
48-50	0.43	
50-52	0.42	
60-62	0.43	
70-72	0.43	
80-82	0.44	

GMIS

Sample ID (in cm)	Porosity	Strength (kPa)
0-2	0.60	10
2-4	0.61	9
4-6	0.61	6
6-8	0.60	7
8-10	0.58	7
10-12	0.60	7
12-14	0.62	6
14-16	0.59	7
16-18	0.56	6
18-20	0.51	6
20-22	0.46	6
24-26	0.46	6
28-30	0.47	5
32-34	0.46	7
36-38	0.45	13
40-42	0.47	
44-46	0.47	
48-50	0.43	
50-52	0.43	
60-62	0.42	
70-72	0.43	

Port Aransas Mud Island

MI1M

Sample ID (in cm)	Porosity	Strength (kPa)
0-2	0.73	12
2-4	0.70	
4-6	0.71	19
6-8	0.64	
8-10	0.66	19
10-12	0.66	
12-14	0.65	14
14-16	0.66	
16-18	0.63	6
18-20	0.58	6
20-22	0.53	9
24-26	0.50	8
28-30	0.54	4
32-34	0.53	6
36-38	0.51	6
40-42	0.49	5
44-46	0.50	5
48-50	0.53	
50-52	0.53	4
60-62	0.55	5
70-72	0.50	10
80-82	0.45	
90-92	0.47	

MI2M

Sample ID (in cm)	Porosity	Strength (kPa)
0-2	0.78	30
2-4	0.76	
4-6	0.63	22
6-8	0.60	
8-10	0.60	31
10-12	0.57	
12-14	0.55	27
14-16	0.56	
16-18	0.56	28
18-20	0.56	18
20-22	0.56	18
24-26	0.56	17
28-30	0.54	20
32-34	0.55	22
36-38	0.57	19
40-42	0.57	19
44-46	0.59	12
48-50	0.54	
50-52	0.53	17
60-62	0.50	16
70-72	0.55	12
80-82	0.50	

MI1S

Sample ID (in cm)	Porosity	Strength (kPa)
0-2	0.79	4
2-4	0.77	
4-6	0.78	10
6-8	0.78	
8-10	0.69	14
10-12	0.72	
12-14	0.71	6
14-16	0.68	
16-18	0.64	6
18-20	0.58	8
20-22	0.57	
24-26	0.53	
28-30	0.45	
32-34	0.49	
36-38	0.51	
40-42	0.53	
44-46	0.50	
48-50	0.51	
50-52	0.53	
60-62	0.52	
70-72	0.55	
80-82	0.52	
90-92	0.48	

Port Aransas Mud Island

Port Aransas Harbor Island

MI2S

Sample ID (in cm)	Porosity	Strength (kPa)
0-2	0.74	14
2-4	0.80	
4-6	0.85	15
6-8	0.68	
8-10	0.69	15
10-12	0.71	
12-14	0.67	17
14-16	0.62	
16-18	0.59	15
18-20	0.49	22
20-22	0.47	32
24-26	0.50	36
28-30	0.45	38
32-34	0.50	39
36-38	0.50	46
40-42	0.52	34
44-46	0.48	35
48-50	0.51	
50-52	0.53	19
60-62	0.48	14
70-72	0.45	
80-82	0.45	

HI1

Sample ID (in cm)	Porosity	Strength (kPa)
0-2	0.585	24
2-4	0.522	
4-6	0.434	30
6-8	0.458	
8-10	0.444	30
10-12	0.443	
12-14	0.442	26
14-16	0.440	
16-18	0.438	26
18-20	0.425	26
20-22	0.426	28
24-26	0.430	24
28-30	0.435	25
32-34	0.429	28
36-38	0.443	24
40-42	0.437	20
44-46	0.436	22
48-50	0.448	
50-52	0.445	27
60-62	0.434	
70-72	0.410	

HI2

Sample ID (in cm)	Porosity	Strength (kPa)
0-2	0.596	23
2-4	0.580	
4-6	0.538	25
6-8	0.491	
8-10	0.457	20
10-12	0.444	
12-14	0.471	21
14-16	0.461	
16-18	0.465	26
18-20	0.457	24
20-22	0.454	30
24-26	0.427	23
28-30	0.430	24
32-34	0.466	20
36-38	0.484	24
40-42	0.467	20
44-46	0.451	21
48-50	0.445	
50-52	0.432	23
60-62	0.423	20
70-72	0.448	28
80-82	0.426	

Appendix G – Soil Geochemistry Raw Data

Galveston East

GIEM1 Sample ID (in cm)	Salinity	pH	Eh (mv)	GIEM2 Sample ID (in cm)	Salinity	pH	Eh (mv)	GIES1 Sample ID (in cm)	Salinity	pH	Eh (mv)
0-2	20	8.28	10.60	0-2	12	8.66	-38.40	0-2	18	8.57	-3.60
2-4	29	8.34	47.40	2-4	20	8.14	73.60	2-4	27	8.60	33.60
4-6	34	8.46	75.20	4-6	25	8.16	42.60	4-6	25	8.77	-47.80
6-8	37	8.86	115.60	6-8	32	8.72	16.60	6-8	25	8.81	65.80
8-10	33	8.80	157.40	8-10	35	8.75	-34.80	8-10	31	8.82	4.00
10-12	33	8.79	53.00	10-12	52	8.87	20.20	10-12	45	8.96	40.60
12-14	36	8.91	168.00	12-14	35	8.74	36.80	12-14	50	8.38	60.60
14-16	39	8.92	52.00	14-16	47	8.88	4.00	14-16	41	8.91	52.00
16-18	41	8.90	90.00	16-18	53	8.93	-24.80	16-18	42	9.00	16.80
18-20	38	8.92	40.00	18-20	43	9.00	104.00	18-20	47	8.86	45.20
20-22	38	8.97	195.60	20-22	45	8.94	102.60				
24-26	48	8.99	7.00	24-26	45	8.98	138.40				
28-30	41	8.99	117.00	28-30	36	8.90	49.00				
32-34	35	9.02	-47.20	32-34	45	9.03	60.80				
36-38	40	9.09	158.60								

Galveston East

GIES2

Sample ID (in cm)	Salinity	pH	Eh (mv)
0-2	21	8.06	94.40
2-4	28	8.11	43.20
4-6	32	8.23	17.00
6-8	33	8.66	8.80
8-10	35	8.38	61.40
10-12	45	8.25	79.60
12-14	31	8.20	15.60
14-16	35	8.70	134.20
16-18	43	8.89	33.00
18-20	36	8.83	52.20
20-22	37	8.78	-12.00
24-26	32	8.91	48.20
28-30	31	9.04	56.00

Galveston West

GMIM

Sample ID (in cm)	Salinity	pH	Eh (mv)
0-2	35	7.88	-59.00
2-4	38	8.18	7.80
4-6	42	7.84	177.20
6-8	67	8.66	144.60
8-10	65	8.03	165.60
10-12	65	8.02	153.80
12-14	77	8.86	193.00
14-16	82	8.27	152.80
16-18	78	8.24	194.40
18-20	80	8.93	186.80
20-22	83	8.79	183.00
24-26	85	8.82	191.00
28-30	74	8.93	247.80
32-34	70	8.80	237.00
36-38	75	8.81	411.20
40-42	82	8.93	260.20
44-46	80	8.87	249.00

GMIS

Sample ID (in cm)	Salinity	pH	Eh (mv)
0-2	88	7.91	257.80
2-4	81	8.00	194.80
4-6	89	8.16	148.20
6-8	78	8.77	189.20
8-10	81	8.36	220.60
10-12	77	8.30	208.00
12-14	81	8.44	150.80
14-16	75	8.18	150.00
16-18	65	8.15	101.60
18-20	74	8.98	44.20
20-22	77	8.93	57.80
24-26	73	8.95	79.40
28-30	64	9.02	25.00
32-34	64	8.90	-41.20

Port Aransas Mud Island

MI1M

Sample ID (in cm)	Salinity	pH	Eh (mv)
0-2	98	7.11	138.00
2-4	77	7.11	155.60
4-6	73	7.83	116.20
6-8	86	8.12	153.80
8-10	76	8.59	97.20
10-12	69	8.85	89.00
12-14	81	8.89	67.00
14-16	77	9.03	58.20
16-18	74	9.07	50.00
18-20	83	9.11	47.00
20-22	82	9.09	76.80
24-26	77	9.04	69.40
28-30	75	9.02	42.00
32-34	80	9.12	104.80
36-38	82	9.01	235.00
40-42	76	8.76	149.20
44-46	78	9.11	153.40
48-50	64	9.06	126.20
50-52	80	9.03	144.00
60-62	87	9.07	126.40
70-72	75	9.07	119.60
80-82	74	9.09	-45.40
90-92	80	9.15	-22.60

MI2M

Sample ID (in cm)	Salinity	pH	Eh (mv)
0-2	77	6.80	173.00
2-4	70	7.49	131.50
4-6	69	7.45	144.25
6-8	66	8.46	61.33
8-10	59	8.84	3.67
10-12	69	9.06	74.67
12-14	62	9.01	18.60
14-16	65	9.09	83.50
16-18	68	9.05	105.40
18-20	82	9.28	6.00
20-22	81	9.01	48.80
24-26	68	9.22	125.00
28-30		8.28	132.80
32-34	84	8.55	2.20
36-38	74	8.51	81.80
40-42	70	8.86	13.00
44-46	67	9.10	45.40
48-50	68	9.22	28.60
50-52	79	9.34	6.40
60-62	84	9.34	34.80

MI1S

Sample ID (in cm)	Salinity	pH	Eh (mv)
0-2	65	8.82	74.00
2-4	70	8.67	77.80
4-6	75	9.04	6.60
6-8	59	9.15	-27.40
8-10	47	9.53	-216.40
10-12	70	9.30	-20.67
12-14	62	9.37	-247.80
14-16	67	9.34	-212.20
16-18	65	8.42	0.00
18-20	57	8.51	-15.20
20-22	58	8.13	7.20
24-26	69	8.82	2.80
28-30	58	8.72	36.60
32-34	52	8.89	49.40
36-38	54	8.80	108.60
40-42	61	9.19	7.60
44-46	60	9.03	35.50
48-50	58	9.11	102.60
50-52	60	8.90	95.00
60-62	62	9.33	46.60

Port Aransas Mud Island

Port Aransas Harbor Island

MI2S

HI1

HI2

Sample ID (in cm)	Salinity	pH	Eh (mv)	Sample ID (in cm)	Salinity	pH	Eh (mv)	Sample ID (in cm)	Salinity	pH	Eh (mv)
0-2	53	8.60	77.60	0-2	164	7.53	119.60	0-2	109	7.76	198.80
2-4	50	8.96	105.20	2-4	105	7.31	157.20	2-4	86	7.71	164.00
4-6	45	8.73	157.40	4-6	73	8.22	15.20	4-6	80	7.45	249.20
6-8	46	9.20	37.40	6-8	78	8.99	-24.80	6-8	77	7.89	175.00
8-10	54	9.19	14.40	8-10	92	9.00	45.60	8-10	77	8.14	163.60
10-12	40			10-12	72	9.01	158.20	10-12	74	8.22	204.40
12-14				12-14	79	9.10	214.80	12-14	73	8.88	201.80
14-16	51			14-16	88	9.00	263.20	14-16	70	8.92	209.00
16-18	46			16-18	89	9.03	239.80	16-18	78	8.92	229.20
18-20	57	8.99	39.00	18-20	82	9.09	234.00	18-20	74	8.89	200.20
20-22	76			20-22	90	9.04	225.80	20-22	71	8.42	249.60
24-26	42	9.04	13.00	24-26	91	9.02	239.20	24-26	67	8.43	227.20
28-30	67	9.14	104.60	28-30	76	9.13	224.60	28-30	68	9.04	207.20
32-34	79			32-34	84	9.08	261.60	32-34	66	8.89	207.20
36-38	68	9.00	106.80	36-38	82	9.06	233.20	36-38	65	8.81	231.60
40-42	48	9.04	28.60	40-42	86	9.15	239.80	40-42	70	8.03	195.20
44-46	53	9.15	138.40	44-46	87	9.10	276.20	44-46	72	7.90	263.00
48-50	62			48-50	86	9.10	275.60	48-50	83	8.04	228.60
50-52	58	9.13	77.00	50-52	94	9.14	252.20	50-52	65	8.40	221.80
60-62	51	9.16	116.40	60-62	103	9.10	262.60	60-62	63	8.32	173.60

References

Allison, M.A., Bianchi, T.S., McKee, B.A., and Sampere, T.P., 2007. Carbon burial on river-dominated continental shelves: impact of historical changes in sediment loading adjacent to the Mississippi River. Geophysical Research Letters, 34 L01606.

Alongi, D.M., 1996. The dynamics of benthic nutrient pools and fluxes in tropical mangrove forests. Journal of Marine Research, 54, 123-148.

Alongi, D.M., 1998. Coastal Ecosystem Processes. CRC Press, New York, 399 pp.

Alongi, D.M., Sasekumar, A., Tirendi, F., and Dixon, P., 1998. The influence of stand age on benthic decomposition and recycling of organic matter in managed mangrove forests of Malaysia. Journal of Experimental Marine Biology and Ecology, 225, 197-218.

Alongi, D.M., Tirendi, F., and Clough, B.F., 2000. Below-ground decomposition of organic matter in forests of the mangroves *Rhizophora stylosa* and *Avicennia marina* along the arid coast of Western Australia. Aquatic Botany, 68, 97-122.

Andersen, F.O. and Kristensen, E., 1988. Oxygen microgradients in the rhizosphere of the mangrove *Avicennia marina*. Marine Ecology Progress Series, 44, 201-204.

Anderson, J.B., Rodriguez, A.B., Milliken, K.T., and Taviani, M., 2008. The Holocene evolution of the Galveston estuary complex, Texas: evidence for rapid change in estuarine environments. Geological Society of America Special Paper, 443, 89-104.

Ball, M.C., 1988. Ecophysiology of mangroves. Trees, 2, 129-142.

Barras, J., Beville, S., Britsch, D., Hartley, S., Hawes, S., Johnston, J., Kemp, P., Kinler, Q., Martucci, A., Porthouse, J., Reed, D., Roy, K., Sapkota, S., and Suhayda, J.,

2003. Historical and projected coastal Louisiana land changes: 1978-2050. U.S. Geological Survey Open File Report 03-334, 39pp. (revised January 2004).

Barras, J.A., 2006. Land area change in coastal Louisiana after the 2005 hurricanes—a series of three maps. U.S. Geological Survey Open File Report 06-1274.

Barras, J., 2009. Land area change and overview of major hurricane impacts in coastal Louisiana, 2004-08. U.S. Geological Survey, Scientific Investigations Map 3080, scale 1:250,000, 6p. pamphlet.

Bianchi, T.S., Pennock, J.R., and Twilley, R.R., 1999. Biogeochemistry of Gulf of Mexico Estuaries. John Wiley & Sons, Inc., New York, 423 pp.

Bianch, T.S., 2007. Biogeochemistry of Estuaries. Oxford University Press, New York, New York, 706.

Bindoff, N.L., Willebrand, J., Artale, V., Cazenave, A., Gregory, J., Gulev, S., Hanawa, K., Quéré, C.L., Levitus, S., Nojiri, Y., Shum, C.K., Talley, L.D., and Unnikrishnan, A., 2007. Observations: oceanic climate change and sea level. In: Solomon, S., Qin, D., Manning, M., Chen, Z., Marquis, M., Averyt, K.B., Tignor, M., and Miller, H.L. (Eds.), Climate change 2007: the physical science basis. Contribution of working group I to the fourth assessment report of the Intergovernmental Panel on Climate Change, Cambridge University Press, Cambridge, United Kingdom and New York, NY, USA, 386-432.

Blum, L.K., 1993. *Spartina alterniflora* root dynamics in a Virginia marsh. Marine Ecology Progress Series, 102, 169-178.

Boto, K.G., 1982. Nutrient and organic fluxes in mangroves. In: Clough, B.F. (Ed.), Mangrove Ecosystems in Australia. Australian National University Press, Canberra, Australia, pp. 239-257.

Brinkman, R.M., Massel, S.R., Ridd, P.V., and Furukawa, K., 1997. Surface wave attenuation in mangrove forests. Proceedings of 13th Australasian Coastal and Ocean Engineering Conference. Centre for Advanced Engineering, Canterbury, 2, pp. 941-946.

Buskey, E.J., Montagna, P.A., Amos, A.F., and Whitledge, T.E., 1997. Disruption of grazer populations as a contributing factor to the initiation of the Texas brown tide algal bloom. Limnology and Oceanography, 42 (5, part 2), 1215-1222.

Chen, R. and Twilley, R.R., 1999. A simulation model of organic matter and nutrient accumulation in mangrove wetland soils. Biogeochemistry, 44, 93-118.

Chmura, G.L. and Kosters, E.C., 1994. Storm deposition and ^{137}Cs accumulation in fine-grained Marsh Sediments of the Mississippi Delta Plain. Estuarine, Coastal and Shelf Science, 39, 33-44.

Clark, M.W., McConchie, D., Lewis, D.W., and Saenger, P., 1998. Redox stratification and heavy metal partitioning in *Avicennia*-dominated mangrove sediments: a geochemical model. Chemical Geology, 149, 147-171.

Coastal Wetlands Planning, Protection and Restoration Act Task Force, 2000. Brown marsh fact sheet: facts about the salt marsh dieback in Louisiana. http://brownmarsh.com/factSheets/brown%20marsh%20Fact%20sheet.pdf, 11 November 2010.

Coastal Wetlands Planning, Protection and Restoration Act Task Force, 2000. Brown marsh phenomenon: dieback of large expanses of Salt Marsh Grass in Coastal Louisiana. http://brownmarsh.com/factSheets/brown%20marsh%20flyer%202%20.pdf, 11 November 2010.

Coastal Wetlands Planning, Protection and Restoration Act Task Force, 2000. Brown marsh Q & A: questions and answers from the brown marsh scientific panel and other meetings, fact sheet No. 5. http://brownmarsh.com/factSheets/brown%20marsh%20Q%20and%20A.pdf, 11 November 2010.

Coastal Wetlands Planning, Protection and Restoration Act Task Force, 2000. Brown marsh severity: aerial surveys of salt marsh damage in the Barataria and Terrebonne basins. http://brownmarsh.com/factSheets/brown%20marsh%20damage.pdf, 11 November 2010.

Day, J., Hall, C.S., Kemp, W.M., and Yanez-Arancibia, A., 1989. Estuarine ecology. John Wiley, New York, 558 pp.

Dodd, R.S. and Rafii, Z.A., 2002. Evolutionary genetics of mangroves: continental drift to recent climate change. Trees, 16, 80-86.

Doran, K.S., Plant, N.G., Stockdon, H.F., Sallenger, A.H., and Serafin, K.A., 2009. Hurricane Ike: observations and analysis of coastal change. U.S. Geological Survey Open File Report, 2009-1061, 35 pp.

Ellison, A.M. and Farnsworth, E.J., 1997. Simulated sea level change alters anatomy, physiology, growth, and reproduction of red mangrove (*Rhizophora mangle* L.). Oecologia, 112, 435-446.

Emanuel, K., 2005. Increasing destructiveness of tropical cyclones over the past 30 years. Nature, 436, 686-688.

Everitt, J.H. and Judd, F.W., 1989. Using remote sensing techniques to distinguish and monitor black mangrove (*Avicennia germinans*). Journal of Coastal Research, 5 (4), 737-745.

Everitt, J.H., Judd, F.W., Escobar, D.E., and Davis, M.R., 1996. Integration of remote sensing and spatial information technologies for mapping black mangroves on the Texas Gulf Coast. Journal of Coastal Research, 12 (1), 64-69.

Feagin, R.A., Lozada-Bernard, S.M., Ravens, T.M., Möller, I., Yeager, K.M., and Baird, A.H., 2009. Does vegetation prevent wave erosion of salt marsh edges? PNAS, 106 (25), 10109-10113.

Folk, R.L., 1968. Petrology of Sedimentary Rocks. Hemphill's, Austin, TX, 170 pp.

Gilman, E.L., Ellison, J., Duke, N.C., and Field, C., 2008. Threats to mangroves from climate change and adaptation options: a review. Aquatic Botany, 89, 237-250.

123

Giurgevich, J.R. and Dunn, E.L., 1982. Seasonal patterns of daily net photosynthesis, transpiration, and net primary production of *Juncus roemerianus* and *Spartina alterniflora* in a Georgia salt marsh. Oecologia (Berl), 52, 404-410.

He, B., Lai, T., Fan, H., Wang, W., and Zheng, H., 2007. Comparison of flooding-tolerance in four mangrove species in a diurnal tidal zone in the Beibu Gulf. Estuarine, Coastal and Shelf Science, 74, 254-262.

Howes, B.L. and Goehringer, D.D., 1994. Porewater drainage and dissolved organic carbon and nutrient losses through the intertidal creekbanks of a New England salt marsh. Marine Ecology Progress Series, 114, 289-301.

Howes, B.L., Howarth, R.W., Teal, J.M., and Valiela, I., 1981. Oxidation-reduction potentials in a salt marsh: spatial patterns and interactions with primary production. Limnology and Oceanography, 26 (2), 350-360.

Kerr, R.A., 2005. Atlantic climate pacemaker for millennia past, decades hence? Science, 309, 41-42.

Knutson, T.R., McBride, J.L., Chan, J., Emanuel, K., Holland, G., Landsea, C., Held, I., Kossin, J.P., Srivastava, A.K., and Sugi, M., 2010. Tropical cyclones and climate change. Nature Geoscience, 3, 157-163.

Knutson, T.R. and Tuleya, R.E., 2004. Impact of CO_2-induced warming on simulated hurricane intensity and precipitation: sensitivity to the choice of climate model and convective parameterization. Journal of Climate, 17 (18), 3477-3495.

Krauss, K.W., Lovelock, C.E., McKee, K.L., López-Hoffman, L., Ewe, S.M.L., and Sousa, W.P., 2008. Environmental drivers in mangrove establishment and early development: a review. Aquatic Botany, 89, 105-127.

LeBlanc, R.J. and Hodgson, W.D., 1959. Origin and development of the Texas shoreline. Second Coastal Geography Conference. Louisiana State University, Coastal Studies Institute, Baton Rouge, Louisiana, pp. 197-220.

Maddox, J., Anderson, J.B., Milliken, K.T., Rodriguez, A.B., Dellapenna, T.M., and Giosan, L., 2008. The Holocene evolution of the Matagorda and Lavaca estuary complex, Texas, USA. Geological Society of America Special Paper, 443, 105-119.

Madrid, E.M., Armitage, A.R., Quigg, A., 2008. The evolution of wetland plant morphology in the Gulf of Mexico. Marine Science and Marine Biology Seminar Series. Texas A&M University at Galveston, Galveston, TX.

Marchand, C., Baltzer, F., Lallier-Vergès, E., and Albéric, P., 2004. Pore-water chemistry in mangrove sediments: relationship with species composition and developmental stages (French Guiana). Marine Geology, 208, 361-381.

Massel, S.R., Furukawa, K., and Brinkman, R.M., 1999. Surface wave propagation in mangrove forests. Fluid Dynamics Research, 24, 219-249.

Mazda, Y., Magi, M., Ikeda, Y., Kurokawa, T., and Asano, T., 2006. Wave reduction in a mangrove forest dominated by *Sonneratia* sp. Wetlands Ecology and Management, 14, 365-378.

Mazda, Y., Wolanski, E., King, B., Sase, A., Ohtsuka, D., and Magi, M., 1997. Drag force due to vegetation in mangrove swamps. Mangroves and Salt Marshes, 1, 193-199.

McCauley, A., Jones, C., and Jacobsen, J., 2003. Nutrient Management Module No. 8: soil pH and organic matter. Montana State University Extension, (Reprinted 2009), http://msuextension.org/publications/AgandNaturalResources/4449/4449_8.pdf, 2 November 2010.

McKee, K.L., Cahoon, D.R., and Feller, I.C., 2007. Caribbean mangroves adjust to rising sea level through biotic controls on change in soil elevation. Global Ecology and Biogeography, 16, 545-556.

McKee, K.L. and McGinnis II, T.E., 2002. Hurricane Mitch: effects on mangrove soil characteristics and root contribution to soil stabilization. U.S. Geological Survey Open File Report 03-178, 57 pp.

McKee, K.L., Mendelssohn, I.A., and Hester, M.W., 1988. Reexamination of pore water sulfide concentrations and redox potentials near the aerial roots of *Rhizophora mangle* and *Avicennia germinans*. American Journal of Botany, 75 (9), 1352-1359.

McMillan, C. and C.L. Sherrod, 1986. The chilling tolerance of black mangrove, *Avicennia germinans*, from the Gulf of Mexico coast of Texas, Louisiana and Florida. Contributions in Marine Science, Vol. 29, 9-16.

Meehl, G.A., Stocker, T.F., Collins, W.D., Friedlingstein, P., Gaye, A.T., Gregory, J.M., Kitoh, A., Knutti, R., Murphy, J.M., Noda, A., Raper, S.C.B., Watterson, I.G., Weaver, A.J., and Zhao, Z.C., 2007. Global Climate Projections. In: Solomon, S., Qin, D., Manning, M., Chen, Z., Marquis, M., Averyt, K.B., Tignor, M., and Miller, H.L. (Eds.), Climate Change 2007: the Physical Science Basis. Contribution of Working Group I to the Fourth Assessment Report of the Intergovernmental Panel on Climate Chang. Cambridge University Press, Cambridge, United Kingdom and New York, NY, USA, 748-845.

Middleton, B.A. and McKee, K.L., 2001. Degradation of mangrove tissues and implications for peat formation in Belizean island forests. Journal of Ecology, 89, 818-828.

National Oceanic and Atmospheric Administration (NOAA), 2006. Tides and Currents, Sea Levels Online. http://tidesandcurrents.noaa.gov/sltrends/sltrends.html, 3 November 2010.

Nittrouer, C.A. and Sternberg, R.W., 1981. The formation of sedimentary strata in an allochthonous shelf environment: the Washington Continental Shelf. Marine Geology, 42, 201-232.

Nordstrom, D.K. and Wilde, F.D., 1998. 6.5 Reduction-oxidation potential (electrode method). In: U.S. Geological Survey TWRI Book 9, pp. 1-20.

Passioura, J.B., Ball, M.C., and Knight, J.H., 1992. Mangroves may salinize the soil and in so doing limit their transpiration rate. Functional Ecology, 6 (4), 476-481.

Pendleton, E.A., Thieler, E.R., Williams, S.J., and Beavers, R.L., 2004. Coastal vulnerability assessment of Padre Island National Seashore (PAIS) to sea-level rise. U.S. Geological Survey Open File Report 2004-1090, 25 pp.

Penland, S., Roberts, H.H., Williams, S.J., Sallenger, Jr., A.H., Cahoon, D.R., Davis, D.W., and Groat, C.G., 1990. Coastal land loss in Louisiana. Transactions - Gulf Coast Association of Geological Societies, 40, 685-699.

Penland, S., Wayne, L., Britsch, L., Williams, S., Beall, A., and Butterworth, V., 2000. Geomorphic classification of coastal land loss between 1932 and 1990 in the Mississippi River Delta Plain, southeastern Louisiana. U.S. Geological Survey Open File Report 00-417.

Perry, C.L. and Mendelssohn, I.A., 2009. Ecosystem effects of expanding populations of *Avicennia germinans* in a Louisiana salt marsh. Wetlands, 29 (1), 396-406.

Pezeshki, S.R., 1997. Photosynthesis and root growth in *Spartina alterniflora* in relation to root zone aeration. Photosynthetica, 34 (1), 107-114.

Poore, R.Z., DeLong, K.L., Richey, J.N., and Quinn, T.M., 2009. Evidence of multidecadal climate variability and the Atlantic Multidecadal Oscillation from a Gulf of Mexico sea-surface temperature-proxy record. Geo-Marine Letters, 29, 477-484.

Quartel, S., Kroon, A., Augustinus, P.G.E.F., Van Santen, P., and Tri, N.H., 2007. Wave attenuation in coastal mangroves in the Red River Delta, Vietnam. Journal of Asian Earth Sciences, 29, 576-584.

Rabinowitz, D., 1978. Dispersal properties of mangrove propagules. Biotropica, 10 (1), 47-57.

Ravens, T.M., Thomas, R.C., Roberts, K.A., and Santschi, P.H., 2009. Causes of salt marsh erosion in Galveston Bay, Texas. Journal of Coastal Research, 25 (2), 265-272.

Ravit, B., Ehenfeld, J.G., and Häggblom, M.M., 2006. Effects of vegetation on root-associated microbial communities: a comparison of disturbed versus undisturbed estuarine sediments. Soil Biology and Biochemistry, 38, 2359-2371.

Richey, J.N., Poore, R.Z., Flower, B.P., and Quinn, T.M., 2007. 1400 yr multiproxy record of climate variability from the northern Gulf of Mexico. Geology, 35 (5), 423-426.

Saenger, P., 1998. Mangrove vegetation: an evolutionary perspective. Marine Freshwater Research, 49, 277-286.

Santschi, P.H., Li, Y.H., Adler, D.M., Amdurer, M., Bell, J., Nyffeler, U.P., 1983. The relative mobility of natural (Th, Pb, and Po) and fallout (Pu, Am, Cs) radionuclides in the coastal marine environment: results from model ecosystems (MERL) and Narragansett Bay. Geochimica et Cosmochimica Acta, 47, 201-210.

Scavia, D., Field, J.C., Boesch, D.F., Buddemeier, R.W., Burkett, V., Cayan, D.R., Fogarty, M., Harwell, M.A., Howarth, R.W., Mason, C., Reed, D.J., Royer, T.C., Sallenger, A.H., and Titus, J.G., 2002. Climate change impacts on U.S. coastal and marine ecosystems. Estuaries, 25 (2), 149-164.

Scholander, P.F., van Dam, L., and Scholander, S.I., 1955. Gas exchange in the roots of mangroves. American Journal of Botany, 42 (1), 92-98.

Scoffin, T.P., 1970. The trapping and binding of subtidal carbonate sediments by marine vegetation in Bimini Lagoon, Bahamas. Journal of Sedimentary Petrology, 40 (1), 249-273.

Sherrod, C.L. and McMillan, C., 1981. Black mangrove, *Avicennia germinans*, in Texas: past and present distribution. Contributions in Marine Science, 24, 115-131.

Sherrod, C. L. and McMillan, C., 1985. The distributional history and ecology of mangrove vegetation along the northern Gulf of Mexico coastal region. Contributions in Marine Science, 28, 129-140.

Singer, P.C. and Stumm, W., 1970. Acidic mine drainage: the rate-determining step. Science, 167, 1121-1123.

Smith III, T.J., 1987. Effects of seed predators and light level on the distribution of *Avicennia marina* (Forsk.) Vierh. in tropical, tidal forests. Estuarine, Coastal and Shelf Sciences, 25, 43-51.

Stevens, P.W., Fox, S.L., and Montague, C.L., 2006. The interplay between mangroves and saltmarshes at the transition between temperate and subtropical climate in Florida. Wetlands Ecology and Management, 14, 435-444.

Stuart, S.A., Choat, B., Martin, K.C., Holbrook, N.M., and Ball, M.C., 2007. The role of freezing in setting the latitudinal limits of mangrove forests. New Phytologist, 173 (3), 576-583.

Tanaka, N., Sasaki, Y., Mowjood, M.I.M., Jinadasa, K.B.S.N., and Homchuen, S., 2007. Coastal vegetation structures and their functions in tsunami protection: experience of the recent Indian Ocean tsunami. Landscape and Ecological Engineering, 3, 33-45.

TexaSoft, 2008. XLS Excel tutorials for statistical data analysis: two sample (independent group) t-test using Microsoft Excel. http://www.stattutorials.com/EXCEL/EXCEL_TTEST1.html, 5 October 2010.

Thibodeau, F.R. and Nickerson, N.H., 1986. Differential oxidation of mangrove substrate by *Avicennia germinans* and *Rhizophora mangle*. American Journal of Botany, 73 (4), 512-516.

Tomlinson, P.B., 1986. The botany of mangroves. Cambridge University Press, New York, New York, U.S.A., 399 pp.

Turner, R.E., 1976. Geographic variation in salt marsh macrophyte production: a review. Contributions in Marine Science, 20, 47-68.

Twilley, R.R., Chen, R.H., and Hargis, T., 1992. Carbon sinks in mangroves and their implications to carbon budget of tropical coastal ecosystems. Water, Air, and Soil Pollution, 64, 265-288.

Twilley, R.R. and Rivera-Monroy, V.H., 2009. CH. 23 Ecogeomorphic models of nutrient biogeochemistry for mangrove wetlands. In: Perillo, G.M.E., Wolanski, E., Cahoon, D.R., and Brinson, M.M. (Eds.), Coastal wetlands: an integrated ecosystem approach. Elsevier, Amsterdam, pp. 641-683.

Wallace, D.J. and Anderson, J.B., 2010. Evidence of similar probability of intense hurricane strikes for the Gulf of Mexico over the late Holocen. Geology, 38 (6), 511-514.

Ward, G.A., Smith III, T.J., Whelan, K.R.T., and Doyle, T.W., 2006. Regional processes in mangrove ecosystems: spatial scaling relationships, biomass, and turnover rates following catastrophic disturbance. Hydrobiologia, 569, 517-527.

Webster, P.J., Holland, G.J., Curry, J.A., and Chang, H.R., 2005. Changes in tropical cyclone number, duration, and intensity in a warming environment. Science, 309, 1844-1846.

Wells, J.T. and Coleman, J.M., 1981. Periodic mudflat progradation, northeastern coast of South America: a hypothesis. Journal of Sedimentary Petrology, 51 (4), 1069-1075.

White, W.A., Morton, R.A., and Holmes, C.W., 2002. A comparison of factors controlling sedimentation rates and wetland loss in fluvial-deltaic systems, Texas Gulf coast. Geomorphology, 44, 47-66.

White, W.A. and Tremblay, T.A., 1995. Submergence of wetlands as a result of human-induced subsidence and faulting along the upper Texas Gulf Coast. Journal of Coastal Research, 11 (3), 788-807.

Wiegert, R.G., Chalmers, A.G., and Randerson, P.F., 1983. Productivity gradients in salt marshes: the response of *Spartina alterniflora* to experimentally manipulated soil water movement. Oikos, 41 (1), 1-6.

Williams, K., Pinzon, Z.S., Stumpf, R.P., and Raabe, E.A., 1999. Sea-level rise and coastal forests on the Gulf of Mexico. U.S. Geological Survey Open File Report 99-441.

Wilson, C.A. and Allison, M.A., 2008. An equilibrium profile model for retreating marsh shorelines in southeast Louisiana. Estuarine, Coastal and Shelf Science, 80, 483-494.

Vita

Rebecca Suzanne Comeaux was born in San Antonio, TX and first became interested in geology during a mentorship in high school, where she worked with a geology professor to map cave formations and examine fault exposures. Rebecca entered the geology program at the University of Texas at Austin in the fall of 2003. She grew interested in paleontology and completed an undergraduate thesis entitled "A Detailed Morphological Analysis of the Uropeltid *Plecturus aureus* Incorporating X-Ray Computed Tomography" under the supervision of Chris Bell. Rebecca received a B.S. in Geological Sciences, General Geology from the Jackson School of Geosciences in 2007 and worked at the UT X-ray Computed Tomography Lab (UTCT) for one year before entering into the Jackson School graduate program. Rebecca started her Masters in the fall of 2008 and has been working on mangrove and marsh systems along the TX Gulf Coast since that time. She received awards from the American Federation Mineralogical Society (AFMS) and Devon Energy Corporation. In the spring of 2010 Rebecca presented her initial research findings at the American Geophysical Union (AGU) Ocean Sciences and International Conference on Sea Level Rise meetings and was awarded the Jackson School technical sessions Best Speaker (MS) presentation award. Rebecca will be pursuing environmental consulting or government agency work after graduation.

Email address: comeaux007@gmail.com

This thesis was typed and figures prepared by Rebecca Suzanne Comeaux